

University of Windsor

Scholarship at UWindor

Electronic Theses and Dissertations

Theses, Dissertations, and Major Papers

2010

Performance analysis of batteries used in electric and hybrid electric vehicles

Chitradeep Sen
University of Windsor

Follow this and additional works at: <https://scholar.uwindsor.ca/etd>

Recommended Citation

Sen, Chitradeep, "Performance analysis of batteries used in electric and hybrid electric vehicles" (2010). *Electronic Theses and Dissertations*. 8047.
<https://scholar.uwindsor.ca/etd/8047>

This online database contains the full-text of PhD dissertations and Masters' theses of University of Windsor students from 1954 forward. These documents are made available for personal study and research purposes only, in accordance with the Canadian Copyright Act and the Creative Commons license—CC BY-NC-ND (Attribution, Non-Commercial, No Derivative Works). Under this license, works must always be attributed to the copyright holder (original author), cannot be used for any commercial purposes, and may not be altered. Any other use would require the permission of the copyright holder. Students may inquire about withdrawing their dissertation and/or thesis from this database. For additional inquiries, please contact the repository administrator via email (scholarship@uwindsor.ca) or by telephone at 519-253-3000ext. 3208.

**PERFORMANCE ANALYSIS OF BATTERIES USED
IN ELECTRIC AND HYBRID ELECTRIC
VEHICLES**

By

Chitradeep Sen

A Thesis

Submitted to the Faculty of Graduate Studies
through the Department of Electrical and Computer Engineering
in Partial Fulfillment of the Requirements for
the Degree of Master of Applied Science at the
University of Windsor

Windsor, Ontario, Canada

2010

© 2010 Chitradeep Sen



Library and Archives
Canada

Bibliothèque et
Archives Canada

Published Heritage
Branch

Direction du
Patrimoine de l'édition

395 Wellington Street
Ottawa ON K1A 0N4
Canada

395, rue Wellington
Ottawa ON K1A 0N4
Canada

Your file *Votre référence*
ISBN: 978-0-494-62712-9
Our file *Notre référence*
ISBN: 978-0-494-62712-9

NOTICE:

The author has granted a non-exclusive license allowing Library and Archives Canada to reproduce, publish, archive, preserve, conserve, communicate to the public by telecommunication or on the Internet, loan, distribute and sell theses worldwide, for commercial or non-commercial purposes, in microform, paper, electronic and/or any other formats.

The author retains copyright ownership and moral rights in this thesis. Neither the thesis nor substantial extracts from it may be printed or otherwise reproduced without the author's permission.

AVIS:

L'auteur a accordé une licence non exclusive permettant à la Bibliothèque et Archives Canada de reproduire, publier, archiver, sauvegarder, conserver, transmettre au public par télécommunication ou par l'Internet, prêter, distribuer et vendre des thèses partout dans le monde, à des fins commerciales ou autres, sur support microforme, papier, électronique et/ou autres formats.

L'auteur conserve la propriété du droit d'auteur et des droits moraux qui protègent cette thèse. Ni la thèse ni des extraits substantiels de celle-ci ne doivent être imprimés ou autrement reproduits sans son autorisation.

In compliance with the Canadian Privacy Act some supporting forms may have been removed from this thesis.

Conformément à la loi canadienne sur la protection de la vie privée, quelques formulaires secondaires ont été enlevés de cette thèse.

While these forms may be included in the document page count, their removal does not represent any loss of content from the thesis.

Bien que ces formulaires aient inclus dans la pagination, il n'y aura aucun contenu manquant.


Canada

DECLARATION OF PREVIOUS PUBLICATION

This thesis includes three original papers that have been previously published and one submitted paper in peer reviewed proceedings, as follows:

Thesis Chapter	Publication Title	Publication Status
Chapter 3	Analysis of a Novel Battery Model to Illustrate the Instantaneous Voltage for Hybrid Electric Vehicle	Published
Chapter 3	Battery Pack Modeling for the Analysis of Battery Management System of a Hybrid Electric Vehicle	Published
Chapter 4	Analysis of the Battery Performance in Hybrid Electric Vehicle for Different Traction Motors	Published
Chapter 5	Electric Vehicle Multiple Source Optimization Using Wavelet Theory Transient Detection	Submitted

I certify that I have obtained a written permission from the copyright owners to include the above published materials in my thesis. I certify that the above material describes work completed during my registration as graduate student at the University of Windsor.

I declare that, to the best of my knowledge, my thesis does not infringe upon anyone's copyright nor violate any proprietary rights and that any ideas, techniques, quotations, or any other material from the work of other people included in my thesis, published or otherwise, are fully acknowledged in accordance with the standard referencing practices. Furthermore, to extent that I have included copyrighted material that surpasses the bounds of fair dealing within the meaning of the Canada Copyright Act, I certify that I have obtained a written permission from the copyright owners to include such materials in my thesis.

I declare that this is a true copy of my thesis, including any final revisions, as approved by my thesis committee and the Graduate Studies office, and that this thesis has not been submitted for a higher degree to any other University or Institution.

ABSTRACT

Hybrid electric vehicles (HEVs) and electric vehicles (EVs) are the most viable solutions to the undesirable high petroleum consumption by the present form of internal combustion engine driven vehicles. The varying requisites of HEVs and EVs have resulted in the advancement of battery technology in the area of chemical compositions such as electrode and electrolyte in addition to its electrical combination, control and protection schemes. The maximum utilization and protection of the battery is a challenge that needs to be tackled to improve its efficiency and reliability.

A comprehensive study of the present battery technology has been performed in this thesis. The research is focused on battery modeling and its applications taking the complete electric drive train into consideration. Novel models and research perspectives have been proposed and analyzed. The scopes of increasing the accuracy of the present day battery management system have also been discussed.

DEDICATION

To My Family

ACKNOWLEDGEMENT

I am grateful to my wonderful family whose love, encouragement and sacrifice has made me what I am today. I wish to express my sincere gratitude to my advisor Dr. Narayan Kar for his assistance at every step of the way. His valuable guidance has had an immense influence on my professional growth and without his technical expertise, reviews, and criticism it would not have been possible to shape this thesis. I would also like to thank my committee members Dr. Das and Dr. Wu for their valuable suggestions and guidance in the completion of this work.

I would also like to thank my colleagues in the Centre for Hybrid Automotive Research & Green Energy for their support and encouragement. Working in their friendly company was a memorable experience.

TABLE OF CONTENTS

DECLARATION OF PREVIOUS PUBLICATION.....	III
ABSTRACT.....	IV
DEDICATION.....	V
ACKNOWLEDGEMENT.....	VI
LIST OF TABLES.....	X
LIST OF FIGURES.....	XI
LIST OF APPENDICES.....	XIV
NOMENCLATURE.....	XV
1 INTRODUCTION.....	1
1.1 BACKGROUND.....	1
1.2 RESEARCH OBJECTIVES.....	4
1.3 THESIS OUTLINE.....	4
2 ENERGY STORAGE IN AUTOMOTIVE APPLICATIONS.....	6
2.1 BATTERY TECHNOLOGY.....	7
2.1.1 <i>Understanding battery operation</i>	7
2.1.2 <i>Battery selection parameters</i>	9
2.1.3 <i>Battery performance factors</i>	10
2.2 BATTERY TECHNOLOGY IN AUTOMOTIVE APPLICATIONS.....	12
2.2.1 <i>Lead-acid batteries</i>	12
2.2.2 <i>Nickel Metal Hydride batteries</i>	14
2.2.3 <i>Lithium-ion batteries</i>	17
2.3 ULTRACAPACITORS.....	18
2.4 COMPARATIVE STUDY OF THE ENERGY TO POWER DENSITIES OF RECHARGEABLE ENERGY STORAGE SYSTEMS.....	19
2.5 SUMMARY.....	20
3 DEVELOPMENT OF BATTERY MODELS FOR ILLUSTRATION OF ITS CHARACTERISTICS.....	21
3.1 BATTERY MODEL CLASSIFICATION.....	21
3.2 ELECTRIC CIRCUIT MODEL CLASSIFICATION.....	24

3.2.1	<i>Ideal Model</i>	25
3.2.2	<i>Linear Model</i>	26
3.2.3	<i>Thevenin Model</i>	27
3.2.4	<i>Impedance model</i>	28
3.2.5	<i>Run time based model</i>	28
3.3	NOVEL BATTERY MODEL DEVELOPMENT	29
3.3.1	<i>Research Objective</i>	29
3.3.2	<i>Proposed Model</i>	29
3.3.3	<i>Capacitive representation and illustration of the proposed model</i>	31
3.3.4	<i>Methodology</i>	33
3.4	RESULTS.....	37
3.4.1	<i>Simulation results for NiMH battery</i>	37
3.4.2	<i>Simulation results for Lead acid battery</i>	40
3.4.3	<i>Simulation results for Lithium ion battery</i>	41
3.5	SUMMARY	44
3.6	RESEARCH SIGNIFICANCE	45
4	APPLICATION OF BATTERY MODELING IN ELECTRIC DRIVETRAIN	46
4.1	HEV/EV BATTERY	47
4.1.1	<i>HEV/EV Battery Pack</i>	47
4.1.2	<i>HEV/EV Battery Management System</i>	48
4.2	TRACTION MOTORS IN HEV/EV	49
4.2.1	<i>Direct Current Motor</i>	51
4.2.2	<i>Induction motor</i>	52
4.2.3	<i>Permanent magnet synchronous motor</i>	54
4.3	REGENERATIVE BRAKING	54
4.4	APPLICATION OF BATTERY MODELING IN BATTERY MANAGEMENT SYSTEM	55
4.4.1	<i>Battery Pack Modeling</i>	55
4.4.2	<i>Electric Drivetrain Modeling</i>	56
4.4.3	<i>Methodology of Battery Modeling Application</i>	60
4.4.4	<i>Result and Analysis of Battery Modeling Application</i>	62
4.5	SUMMARY	66
4.6	RESEARCH SIGNIFICANCE	67

5	TRANSIENT PROTECTION OF BATTERY BY USING MULTIPLE SOURCES.....	68
5.1	WAVELET THEORY.....	68
5.1.1	<i>Continuous Wavelet Transform.....</i>	69
5.1.2	<i>Discrete wavelet transform</i>	69
5.2	ULTRA-CAPACITOR AND BATTERY COMBINATION.....	70
5.3	METHODOLOGY	71
5.3.1	<i>Transient detection using wavelet decomposition.....</i>	71
5.3.2	<i>Control Scheme for Source Optimization.....</i>	72
5.4	RESULTS.....	75
5.4.1	<i>Transient Detection Using Wavelet Decomposition.....</i>	76
5.4.2	<i>Power Optimization</i>	78
5.5	SUMMARY	80
5.6	RESEARCH SIGNIFICANCE	80
6	CONCLUSIONS AND FUTURE WORK	81
6.1	CONCLUSIONS	81
6.2	FUTURE WORK.....	82
	APPENDIX A LIST OF PUBLICATIONS	83
	APPENDIX B COPYRIGHT RELEASE	84
	REFERENCES.....	85
	VITA AUCTORIS.....	90

LIST OF TABLES

TABLE 2.1	SUMMARY OF BATTERY SYSTEMS FOR AUTOMOTIVE APPLICATION	15
TABLE 3.1	EV31A-A BATTERY PARAMETERS	34
TABLE 3.2	INDUCTION MACHINE PARAMETERS USED FOR MODEL VALIDATION	35
TABLE 4.1	3.7 kW DC MACHINE PARAMETERS.....	59
TABLE 4.2	2.5 kW INDUCTION MACHINE PARAMETERS	59
TABLE 5.1	HIGH PASS FIR COEFFICIENTS.	75
TABLE 5.2	INDUCTION MACHINE PARAMETERS.....	76

LIST OF FIGURES

Fig. 1.1. Worldwide petroleum consumption.....	1
Fig. 1.2. Effect of technology on global warming.....	2
Fig. 1.3. Ragone plot.....	3
Fig. 2.1. Electrochemical reaction in a cell during discharge.....	8
Fig. 2.2. Battery charge discharge operation.....	8
Fig. 2.3. Lead-acid battery.....	13
Fig. 2.4. Lead-acid battery used in ZENN electric vehicle.....	13
Fig. 2.5. NiMH Cylindrical battery construction.....	15
Fig. 2.6. Performance characteristics of Panasonic NiMH module. (a) Specific power for varying operating temperature. (b) Change in internal resistance over the cycle life.....	16
Fig. 2.7. Lithium ion battery pack used in Tesla electric vehicle.....	17
Fig. 3.1. Cyclic voltammetry.....	22
Fig. 3.2. Voltage-current behavior of electrochemical cells.....	24
Fig. 3.3. Ideal electric circuit model characteristics. (a) Ideal electric circuit model. (b) Battery terminal voltage (V_{ter}) as a function of internal generated voltage (V_m).....	25
Fig. 3.4. Linear electric circuit model.....	26
Fig. 3.5. Battery terminal voltage (V_{ter}) as a function of internal generated voltage (V_m) for a linear model.....	26
Fig. 3.6. Thevenin electric circuit model.....	27
Fig. 3.7. Impedance model.....	28
Fig. 3.8. Runtime based model.....	28
Fig. 3.9. Proposed model.....	30
Fig. 3.10. Capacitive representation of the battery model.....	32
Fig. 3.11. Battery model illustration.....	33
Fig. 3.12. Detailed view of the Matlab/Simulink model.....	35
Fig. 3.13. Matlab/Simulink representation of the proposed model.....	36
Fig. 3.14. EV31A-A battery in ZENN vehicle.....	37
Fig. 3.15. Battery terminal voltage (V_{ter}) as a function of internal resistance.....	38
Fig. 3.16. Internal resistance drop across SOC.....	38
Fig. 3.17. Battery terminal voltage (V_{ter}) as a function of battery current (I_{bat}).....	39
Fig. 3.18. Voltage drop with respect to internal resistance.....	39
Fig. 3.19. Charge-discharge of the lead-acid battery.....	40
Fig. 3.20. Battery discharge curve.....	41
Fig. 3.21. The change in resistance as a function of time.....	42
Fig. 3.22. Temperature gradient profile.....	42
Fig. 3.23. The loss across the temperature gradient.....	43

Fig. 3.24. Temperature profile across the complete simulation.	43
Fig. 4.1. Mitsubishi HEV battery pack.....	49
Fig. 4.2. Schematic representation of the battery pack.....	49
Fig. 4.3. Schematic representation of the battery management system.....	50
Fig. 4.4. HEV/EV traction motor requisites.....	51
Fig. 4.5. DC traction motor	52
Fig. 4.6. Induction motor used in HEV/EV.....	52
Fig. 4.7. Induction motor operational characterisitcs	53
Fig. 4.8. Permanent magnet synchronous motor used in HEV/EV.....	53
Fig. 4.9. Permanent magnet synchronous motor operational characteristics.....	53
Fig. 4.10. Battery pack model.	55
Fig. 4.11. Electric drivetrain using DC motor.....	56
Fig. 4.12. Electric drivetrain model using DC shunt motor	57
Fig. 4.13. Electric drivetrain model using DC series motor	57
Fig. 4.14. Electric drivetrain using induction motor.	59
Fig. 4.15. Modeling control scheme.....	60
Fig. 4.16. Circuit model used for EV drivetrain simulation	61
Fig. 4.17. Electromagnetic torque analysis of DC motor.....	62
Fig. 4.18. Battery charge-discharge across DC motor.....	63
Fig. 4.19. Result of torque on battery charge-discharge current.....	63
Fig. 4.20. Location of BMS voltage parameter for DC motor.....	64
Fig. 4.21. Electromagnetic torque analysis of induction motor.....	64
Fig. 4.22. Battery charge-discharge across induction motor.....	65
Fig. 4.23. Induction motor speed variation for motor and generator mode.....	65
Fig. 4.24. Motor to generator transition mode analysis for induction motor.....	66
Fig. 5.1. Transient detection using wavelet decomposition.....	69
Fig. 5.2. n -level asymmetric filter bank analysis.....	70
Fig. 5.3. Vehicular torque distribution corresponding to the power requirements.....	70
Fig. 5.4. Energy storage requisites.....	72
Fig. 5.5. Energy storage control acrhitecture.	72
Fig. 5.6. Parallel battery and ultracapacitor operation.....	73
Fig. 5.7. Flowchart of the power distribution control scheme.....	74
Fig. 5.8. Load current profile.	76
Fig. 5.9. High frequency details-level 1.....	77
Fig. 5.10. Normalised digital output.	77
Fig. 5.11 High frequency details-level 2.....	78
Fig. 5.12. Transient detector output	78

Fig. 5.13. Initial transients of the torque output of IM.	79
Fig. 5.14. Ultracapacitor current variation in accordance with the torque production.	79
Fig. 5.15 Ultracapacitor voltage profile..	80

LIST OF APPENDICES

Appendix A List of publications.....	83
Appendix B Copyright release.....	84

NOMENCLATURE

Generally symbols have been defined locally. The list of principle symbols is given below.

Ψ_{dr}, Ψ_{qr}	: d- and q-axis rotor flux respectively
Ψ_{ds}, Ψ_{qs}	: d- and q-axis stator flux respectively
i_{ds}, i_{qs}	: d- and q-axis stator current respectively
i_{dr}, i_{qr}	: d- and q-axis rotor current respectively
v_{dr}, v_{qr}	: d- and q-axis rotor voltage respectively
v_{ds}, v_{qs}	: d- and q-axis stator voltage respectively
L_m	: Mutual inductance
L_s, L_r	: Stator and rotor inductance respectively
L_{ss}, L_{rr}	: Stator and rotor leakage inductance respectively
R_s, R_r	: Stator and rotor resistance
ω_s, ω_r	: Synchronous speed and rotor speed respectively
T_m	: Mechanical load torque
T_e	: Electromagnetic torque
i_T	: Torque producing current
i_f	: Field producing current
H	: Combined inertia of rotor and load
V_{in}	: Battery internal voltage
V_{ter}	: Battery terminal voltage
I_{bat}	: Battery current
R_{in}	: Battery internal resistance
C_{cap}	: Battery capacitance
V	: Capacitor voltage

1 INTRODUCTION

1.1 Background

The apprehension of the economic and environmental impact of fossil fuel combustion has accelerated the popularization of alternative renewable sources of energy. The transportation sector which is one of the highest consumers of fossil fuel and largest contributor of greenhouse gas emissions; due to the rapid increase in population, advancement in technologies, urbanization and industrial development is increasing at a rate much more than anticipated. The petroleum consumption by transportation sector has increased from 16 million barrels per day in 1971 to 37 million barrels in 2002. According to an estimate by the International Energy Annual, the global oil demand will spike up to 121 million barrels per day by 2030, 54 percent of which will be consumed by transportation alone [1]. The worldwide petroleum consumption, according to the research conducted by US Energy Information Administration, is shown in Fig. 1.1. This increased and inefficient use of fossil fuels by on-road transportation has led to the development of alternative fuel vehicles. Alternative fuel vehicles refer to the class of vehicles that are partially or solely powered by sources of energy other than fossil fuels such as bio-fuels, electricity or hydrogen. The target of all such vehicles is to minimize vehicle emission, increase sustainability and reduce strain on the environment.

Battery electric vehicle (BEV) is one such form of alternative transportation that has

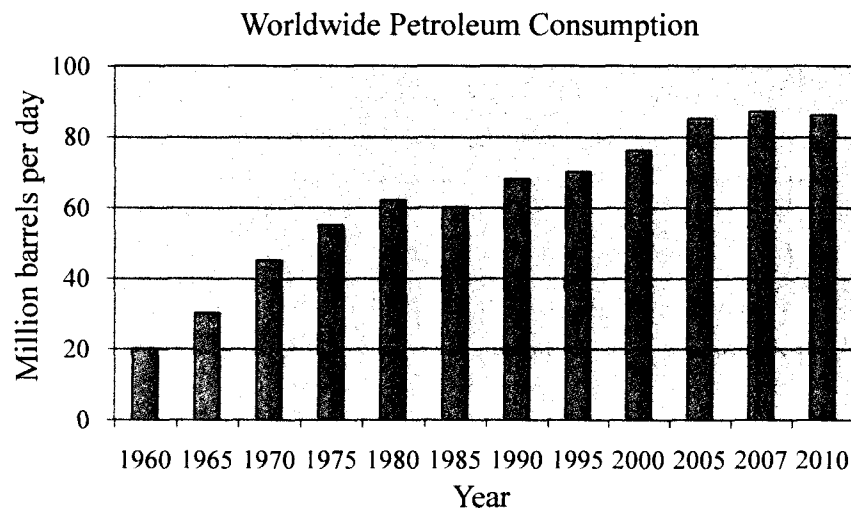


Fig. 1.1: Worldwide petroleum consumption.

the potential to become the most commercially successful technology amongst the numerous technologies proposed by researchers across the globe. BEVs use electric energy, stored in the form of chemical energy, to drive the vehicle, or share a considerable amount of power demand with the conventional internal combustion engine [2]-[4]. Depending upon the degree of power shared, the BEVs are classified into Hybrid Electric Vehicles (HEVs), which partly rely on the internal combustion engine, and Electric Vehicles (EVs) that are completely void of any form petroleum consumption [4]. Fig. 1.2 depict that the induction of these alterative vehicles and popularization of renewable energy will limit the steady rise in global temperature, preventing the dreadful ecological imbalance. However, past experiences with BEVs have often been poor and there are still a number of technological challenges in the area of battery technology that need to be addressed before a reasonable level of market success can be achieved. Currently, most of the batteries available in the market have serious constraints in delivering the desired driving performance, driving range and safety at a low initial cost. Therefore, the main objective of the proposed research is to analyze the performance of the batteries and push the envelope of the present battery technologies beyond what the automotive OEMs and suppliers are currently developing. The proposed research will address the inherent obstacles of batteries, which can result in significant improvements, facilitating the production of implementable solutions in the areas of efficiency, performance, and component volume and weight.

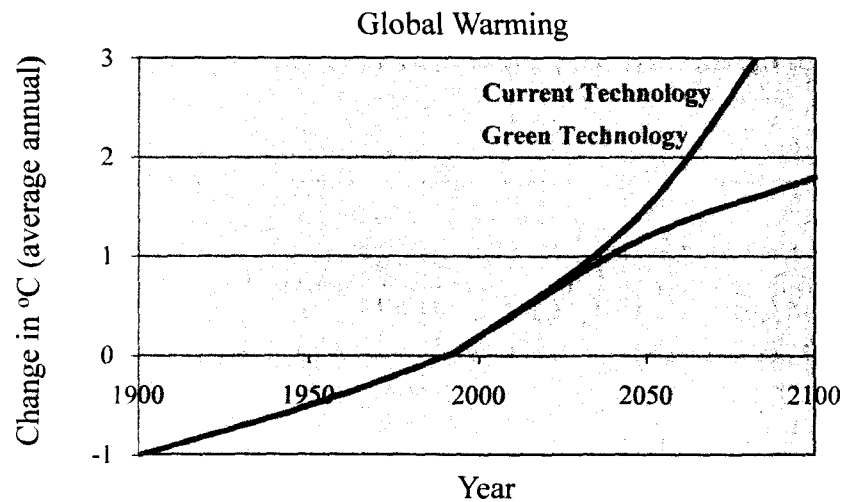


Fig. 1.2: Effect of technology on global warming.

The battery forms a very crucial component of the BEV drivetrain [3]. It provides the desired electric power to the traction motor in accordance with the driver's requirement. The battery properties widely vary with the chemistry as shown in Fig. 1.3. The battery should be capable of storing sufficient energy, offer high energy efficiency, high current discharge, good charge acceptance from regenerative braking, high cycle time and calendar life and abuse tolerant capability [3], [4]. It should also meet the necessary temperature and safety requisites. Although many different types of energy storage technologies are under development, batteries are currently used as the main source of electric power in all BEVs. The three main battery chemistries that find application in the automotive industry are:

- Lead-Acid Battery
- Nickel Metal Hydride Battery
- Lithium-ion Battery

The battery selection is primarily dependent upon its degree of dependence on the traction motors that drive the vehicle. For HEVs, where the power demand is shared between the motor and conventional internal combustion engine, the battery is sized by the peak power demand during vehicle acceleration [5]. Thus, the weight and volume of the battery for an HEV is determined primarily by its required pulse power density. In most cases, the corresponding energy density of an HEV battery is designed for a given power demand which is lower than EV batteries. For EVs, there has to be an optimum

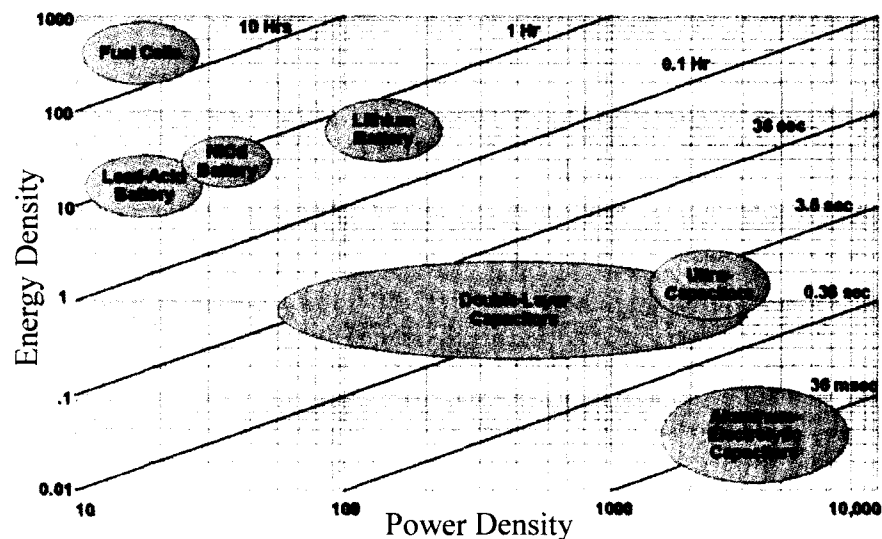


Fig. 1.3: Ragone plot.

compromise between the energy and power density in order to deliver the desired driving performance without sacrificing the driving range.

1.2 Research Objectives

Battery technology is one of most important areas of research pertaining to the reliability and commercial popularity of this alternative form of transportation. Since, the invention of rechargeable energy storage, the research had been limited to the field of electrochemistry. Its application in the conventional internal combustion vehicles had been concentrated to the initial cranking of engine and lighting. But, with the introduction of BEVs, the power demands from battery have increased significantly leading to complexity and constraints relating to the overall battery and vehicular performance. Thus these wide scopes of usage have resulted in an increased research on the electrical aspect of battery operation.

This research is focused on analyzing the battery operation and illustrating its characteristics, considering the variation in terms of chemical composition and power demands. The specific areas discussed in this thesis that contribute in the improvement of the overall battery performance are:

- Battery Modeling
- Battery Management System
- Energy Source Optimization

1.3 Thesis Outline

This thesis is organized as follows:

Chapter 2: This chapter discusses the present battery technology used in automotive applications. The different battery chemistries and the significance of their properties in relation to the application have been demonstrated. This chapter would give an understanding of the battery selection procedure for BEVs.

Chapter 3: This chapter is based on battery modeling, which is the representation of battery operation and illustration of its characteristics. Although, this chapter will illustrate the different conventional modeling methods, the focus will be on electric circuit models due to its wide applicability and degree of

accuracy. The novel electric model done as a part of the Master's Thesis is presented in this section. The advantages of the proposed model have also been demonstrated.

Chapter 4: This chapter is focused on the battery management system (BMS) that is responsible for battery safety by protecting the individual cells from surges, ensuring a better and improved performance in addition to a longer cycle and calendar life. The different battery management parameters that can enhance its performance have also been discussed.

Chapter 5: This chapter deals the cycle and calendar life enhancement of battery by protecting it against the undesired transients it experiences during normal vehicular operation. The vehicular power demand has been distributed between ultracapacitor and battery during the transient period. The obtained results have also been thoroughly discussed.

Chapter 6: The research findings of this detailed analysis have been presented in this section. The implications of this research have been discussed and the scopes of future improvements have been duly proposed.

2 ENERGY STORAGE IN AUTOMOTIVE APPLICATIONS

The rechargeable energy storage forms a very crucial component of the electric drive train. The hybrid and electric vehicles have different energy storage requisites in accordance to their drivetrain configuration. The required energy storage for hybrid vehicles is generally much smaller than that of electric vehicles. For hybrid vehicles, which are mostly intended for urban use, the energy storage systems have high power density as they are equipped with an internal combustion engine to substantiate the energy requirements [3]. The HEV energy storage is also subjected to more rigorous cycling as compared to EVs. Moreover, the energy storage unit for HEVs should be small and light weighted in order to maximize the efficiency by optimizing vehicular mass. In mild hybrids, the storage unit is primarily used to assist the prime mover during sudden acceleration and hill climbing, while absorbing the brake energy by regenerative braking [3]-[5]. The full hybrids, in addition to the mild hybrid characteristics, have excess energy to drive the vehicle on complete electric mode for a very limited time before converting into the engine assist mode. Electric vehicles on the other hand, are completely dependent on the rechargeable energy storage as their sole energy producing unit. Thus the power density and the energy density become equally important requisites of the storage unit. In addition to these specific features, the energy storage units of both HEVs and EVs should be capable of offering high energy efficiency, high current discharge, along with good charge acceptance from regenerative braking, and must meet the peak power demands of the vehicle. The storage unit must also meet appropriate cycle and calendar life requirements, exhibit abuse tolerance to ensure safety and provide a cost effective solution for market acceptability.

Battery is one such form of rechargeable storage unit that converts the electrochemical energy into usable electrical energy. In automotive application, batteries are the most commercially accepted reliable and mature technology as compared to its counterparts such as fuels cell and ultracapacitors [6], [7]. The recent advances in battery technology have fueled a surge in battery applications over a wide spectrum. With the increase in their operational diversity, the complexity and criticality have resulted in a vast scope of multidisciplinary research ranging from electrochemical design to electrical protection and thermal management. In this chapter, the battery operation and its important

parameters that are considered for automotive applicability are analyzed and discussed in detail. In addition, the different battery chemistries that find application in the present automotive industry have also been presented in this section.

2.1 Battery Technology

The battery is a collection of electro-chemical cells converting chemical energy directly into electrical energy via isothermal process having a fixed supply of reactants. It is broadly classified into ‘primary’ (that cannot be recharged due to irreversible chemical reactions) and ‘secondary’ (type rechargeable batteries) [6]. HEVs and EVs employ the latter; and several options, particularly lead-acid, nickel-metal hydride (NiMH) and lithium-ion (Li-ion) batteries, have been under consideration for this application. The detailed analysis of our research will be concentrated to the rechargeable battery technologies.

2.1.1 Understanding battery operation

The battery is an electrochemical device that converts chemical energy into electrical energy by means of electrochemical oxidation-reduction. Although, a battery is used to term a collection of individual electrolytic cells, a single cell unit is also referred to as battery. An electrolytic cell as shown in Fig. 2.1 is composed of a positive and negative electrode, called the cathode and anode respectively, immersed in an electrolyte that serves as a medium to permit ionic conduction between the electrodes. In addition, the cell has non-reactive components such as separators, collectors and container. Chemical oxidation and reduction take place at the electrodes releasing electrons. The maximum energy that is delivered by the chemicals is dependent on the change in free energy of the electrochemical couple [6].

During discharge, the active material is oxidized at the anode, giving up electrons to the external circuit as shown in Fig. 2.1. These electrons return via cathode where reduction takes place. When the cell is recharged, the electrons return via anode reconstituting the active materials. The voltage generation in the cell is due to oxidation that results in the displacement of charge. The theoretical voltage and capacity of the cell are functions of the anode and cathode materials.

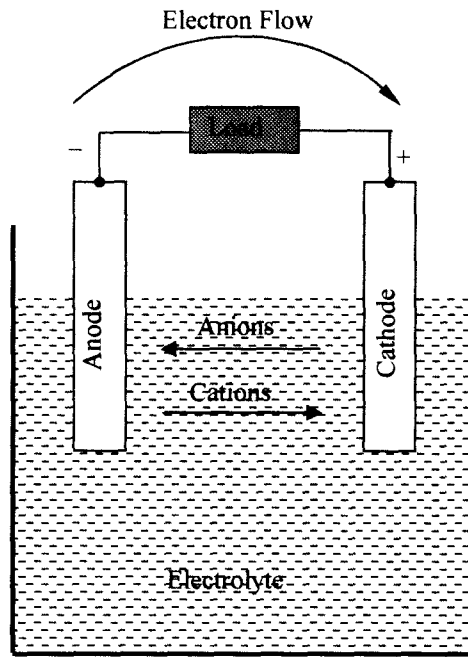


Fig. 2.1: Electrochemical reaction in a cell during discharge.

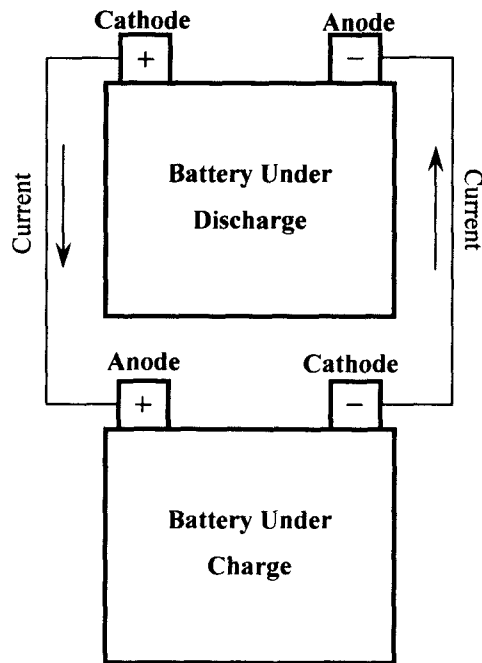


Fig. 2.2: Battery charge-discharge operation.

2.1.2 Battery selection parameters

The battery selection for any specific application is dictated by the consideration of performance, reliability and cost. The basic parameters that are used to determine the performance of a battery are given below [6]:

A. Energy and Power

- *Coulombic capacity*: It is expressed in ampere-hours and is the total quantity of electric charge involved in the electrochemical reaction. It can be calculated from the equivalent weight of the reactants.
- *Thermodynamic voltage*: The standard potential of a cell is determined by the type of active materials and can be calculated from oxidation and reduction potentials of the reactants. It is also dependent on concentration and temperature.
- *Theoretical energy*: This is the capacity per unit weight expressed in *Wh/kg*. The theoretical specific energy is the maximum energy that can be generated per unit total mass of the cell reactant and depends on the electrode materials. The actual specific energy, however, is only a fraction of the theoretical energy. This is mainly due to the additional weight and volume of inactive components. The theoretical energy of a cell is determined by

$$\text{Watt hour (Wh)} = V \times \text{Cap (Ahr)} \quad (2.1)$$

where *Cap* is the capacity of the cell.

The battery does not discharge at the theoretical voltage due to internal losses and cannot completely deliver the theoretical ampere-hours. The specific energy can be expressed in volumetric terms (*Wh/L*), where “*L*” is the volume.

- *Specific power*: This is the maximum power per unit weight that the cell (or battery) can produce in a short time period and is expressed in *W/kg*. It mainly depends on the internal resistance of the cell.

B. Energy Efficiency

The energy and power losses during battery discharge appear in the form of voltage loss. The efficiency at a given operating point during discharge is therefore defined as the ratio of the cell operating voltage to the theoretical thermodynamic voltage.

- *Columbic inefficiency*: This arises from the electric current wasted in non-productive side reactions such as corrosion of battery components.

- *Voltaic inefficiency*: The voltage required to charge a rechargeable battery is always greater than the discharge voltage. This difference is a measure of the voltaic inefficiency.

C. Life of the battery

- *Cycle life*: This is defined as the number of complete charge/discharge cycles a battery can perform before its capacity falls below 80% of its initial rated capacity.
- *Calendar life*. This is the elapsed time before a battery becomes entirely unusable. In addition to these criteria, the battery selection is also dependent on the range of ambient temperature over which it is expected to perform satisfactorily.

2.1.3 Battery performance factors

The parameters listed above are used to adjudicate the performance of the battery and select the most appropriate combination in accordance with a specific application. These parameters are influenced by many factors, thus varying the battery performance [6]. The interaction of these factors results in a much greater effect than anticipated. Furthermore, for every cell or battery, the performance will differ between manufacturers along with variation in the production lot. The extent of this variability is also dependent on the manufacturing process control precision, application and level of battery usage. The major performance affecting factors are listed below:

- *Current drain of discharge*: The battery performance is related to the rate of discharge current. With the increase in the current, the ohmic losses and polarization effect increase, thus reducing the discharge voltage and service life of the battery.
- *Mode of discharge*: The battery can be subjected to three modes of discharge namely the constant current, the constant load and the constant load mode. These variations in discharge have significant effect on the battery performance. Thus, the mode of discharge is applied after performing appropriate tests for a specific application.
- *Battery temperature*: The battery temperature during discharge has pronounced effect on its capacity and voltage characteristics. At lower temperatures, the

battery capacity decreases, the internal resistance increases, resulting in more losses and less efficiency. At higher temperatures, the resistance decreases, resulting in higher discharge voltage. But, after the optimum operating temperature of the battery, the chemical activity increases to an extent where it is rapid enough to cause a net loss in capacity.

- *Type of discharge:* The battery can be subjected to continuous or intermittent type of discharge. The types of discharge result in certain physical and chemical changes in the battery that are reflected in its performance. When a battery stands idle, after undergoing a deep discharge, the voltage will rise after a rest period, giving a saw tooth shaped discharge and enhancing the service life.
- *Duty cycles:* The variation in discharge current during a single duty cycle results in a significant variation in battery performance. Moreover, with the number of duty cycles, there results in permanent change in the chemical and physical property of the battery. These changes also affect the battery performance.
- *Charging mode:* Similar to the discharging procedure, the different charging modes such as constant current, constant current constant voltage, constant voltages affect the battery performance.
- *Battery age and storage design:* The physical and chemical properties change with the age and storage conditions of the battery. The self-discharge of the battery that varies with battery chemistry is generally low at lower temperatures. Some batteries tend to develop a passive film on the electrodes during prolonged storage, protecting the battery and increasing the service life.
- *Effect of battery design:* The performance of a multi-cell battery is much dependent on the efficient cell design. The accuracy level of thermal and cell management brings a substantial variation on the batter performance, life, safety and reliability.

Thus developing a battery technology with an acceptable combination of power, energy and life cycle for HEV and EV application continues to pose a constant challenge. Lead-acid batteries have been used in automotive applications since its day of existence. The present day HEV is equipped with a lead-acid battery to initiate the engine cranking in addition to a larger advanced battery pack. Lead-acid batteries due to their low

performance, do not find much use as the HEV or EV battery pack. NiMH batteries have been used in almost all commercial hybrids to date since they offer fairly good energy and power densities, long cycle life and abuse tolerance capability; however their cell efficiency is quite low with very high self discharge. Their life reduces with high depth-of-discharge cycling and heat production becomes a concern at high temperatures. Lithium ion batteries, on the other hand, although still in the developmental stage, are now seen as the long term solution for automotive application. But concerns of high cost, low cycle life and thermal runaways have to be addressed before they can be used in commercial hybrids.

2.2 Battery Technology in Automotive Applications

2.2.1 Lead-acid batteries

The automotive systems have been using lead-acid chemistry for the standard starting-lighting-ignition for decades. The basic constructional feature of a lead acid battery as presented in the encyclopedia of alternative energy and sustainable living is shown in Fig. 2.3. The typical lead acid battery has a cell potential of 2.1 V, gravimetric energy of 35-50 Wh/kg and volumetric energy of 100 Wh/L. The basic reaction of the lead acid batteries is:



The most important constraint of the lead acid battery is its need for regular maintenance. This occurs when the battery is stored for a long period of time. Recent developments have diminished this backlog to an extent where they now can be used for low power HEVs and EVs. A major reason for the shortened life in lead acid batteries is sulphation. The electrolyte had been immobilized by using absorbent glass mat of highly porous microfiber construction and gelled electrolyte [6].

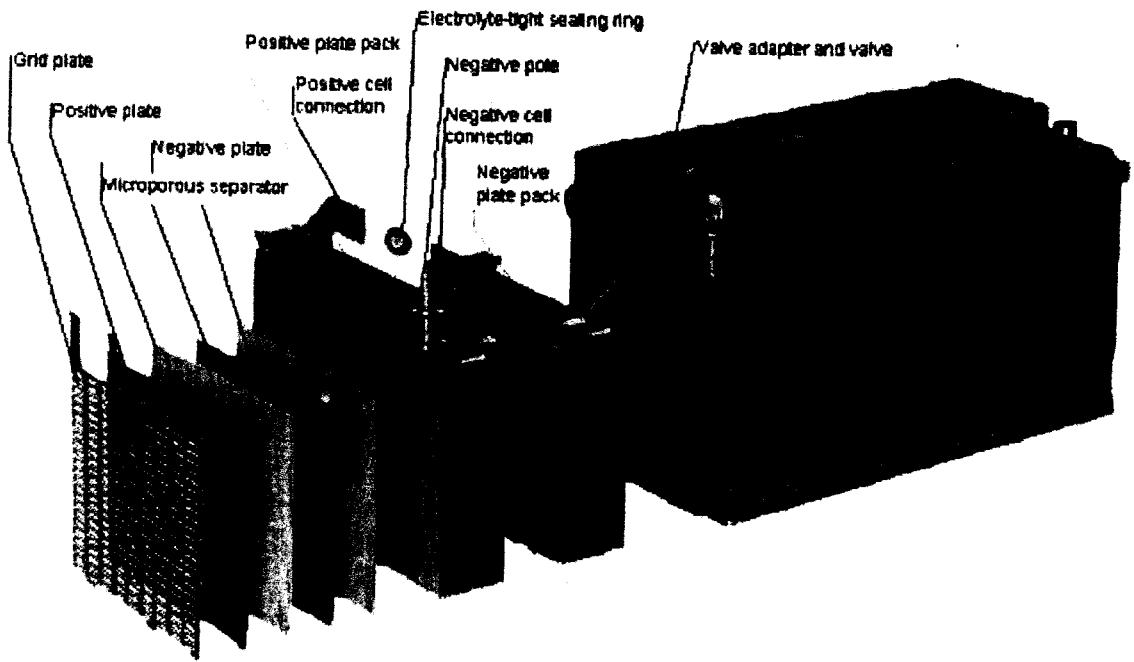


Fig. 2.3: Lead-acid battery.

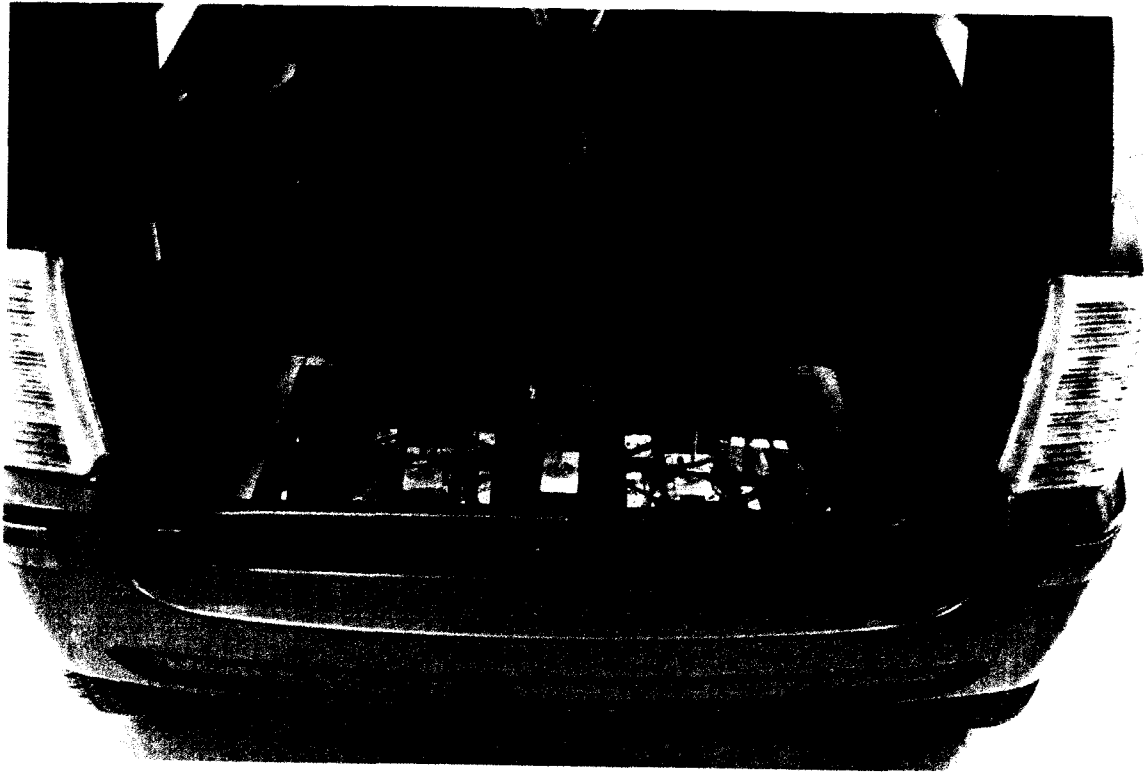


Fig. 2.4: Lead-acid battery used in ZENN electric vehicle.

Fig. 2.4 shows the use of advanced lead acid battery in electric vehicle operating a traction motor of 5 kW. The most noticeable feature of lead acid battery is its extremely low internal resistance, resulting in lower voltage drop for a specific current. They are the cheapest rechargeable batteries available in the market. The low specific energy prevents it from application in long range applications. The lead acid batteries are limited to around 700 cycles. The shorter life of the road vehicles is the result of greater battery load.

2.2.2 Nickel Metal Hydride batteries

Nickel metal hydride batteries have dominated the automotive application since 1990's due to their overall performance and best available combination of energy and power densities, thermal performance and cycle life. They do not need maintenance, require simple and inexpensive charging and electronic control and are made of environmentally acceptable recyclable materials. The basic NiMH reaction is:



The capacity of NiMH cell is relatively high but its cell potential is 1.35 V. The gravimetric energy density is about 95 Wh/kg and volumetric energy is about 350 Wh/L. NiMH batteries can have a cylindrical or prismatic construction. Fig. 2.5 shows a cylindrical NiMH battery. The low cost cylindrical construction can be manufactured faster and is used in application requiring less than 10 Ahr. Cylindrical batteries typically have a low to moderate discharge rate providing high discharge demand for vehicular traction. Cylindrical batteries are only developed in metal casing such that the casing itself serves as the negative terminal and is electrically connected to the metal hydride electrode. Prismatic construction is used for application requiring higher than 20 Ahr, whereas both cylindrical and prismatic configurations can be used for 10 Ahr to 20 Ahr range. Prismatic batteries consist of electrode stacks of alternating positive and negative electrode with immediate separators. HEV prismatic NiMH batteries are expected to deliver specific power of 500 W/kg or higher, for which the thickness of the electrode is kept small. Unlike cylindrical construction, prismatic design has both a positive and negative terminal at the top cover plate. Both metal and plastic cell cases are common in prismatic batteries used for vehicular applications. The concerns for NiMH are the low

specific power and energy as compared to lithium batteries. Due to the low cell potential, the number of cells increases, resulting in higher weight of the vehicle. Charge acceptance of NiMH is also a concern for the hybrid propulsion systems in addition to its high self-discharge. These batteries have serious limitations at cold temperatures, thus needing precise climate control system. Table 2.1 shows the summary of specifications of various batteries used in vehicles. However, Panasonic, the battery supplier for leading hybrid manufacturers such as Toyota, now offers metal case prismatic NiMH batteries for HEVs with specific power up to 1300 W/kg and specific energy of 46 Wh/kg. The Toyota Prius is equipped

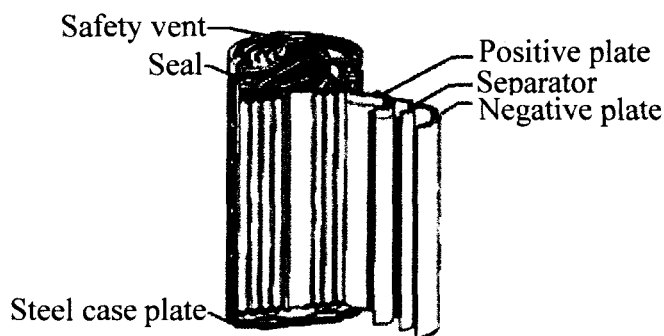


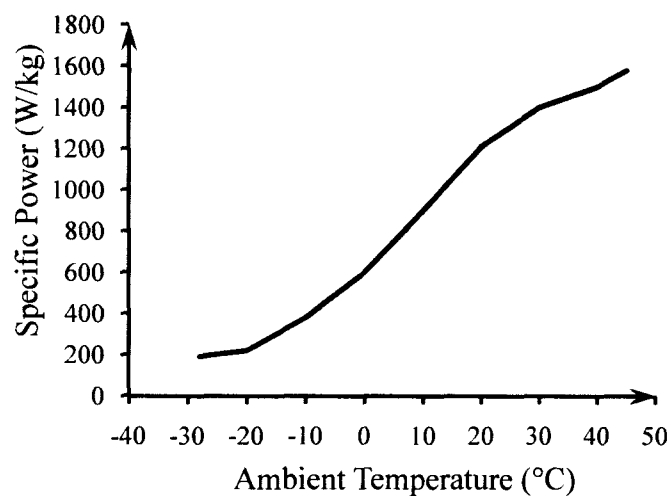
Fig. 2.5: NiMH Cylindrical battery construction.

TABLE 2.1

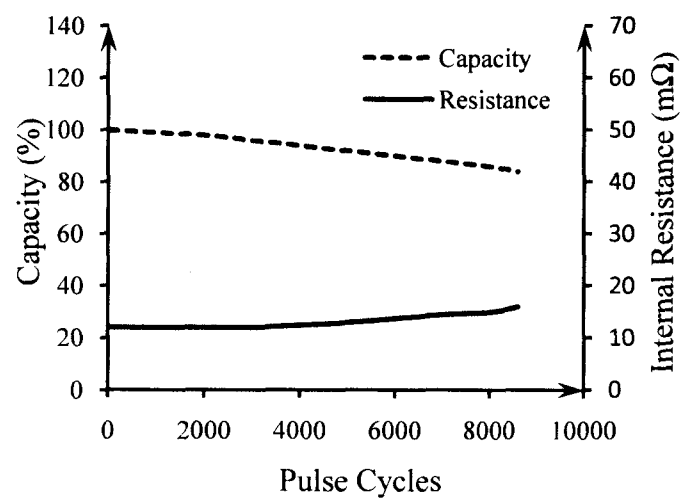
SUMMARY OF BATTERY SYSTEMS FOR AUTOMOTIVE APPLICATION

Battery Type	Specific Energy (Wh/kg)	Peak Specific Power (W/kg)	Efficiency (%)	Cycle Life	Self Discharge (% per 48 h)	Cost (Cdn\$/kWh)
Lead acid	35-50	150-400	>80	500-1000	0.6	144-180
Nickel-cadmium	50-60	80-150	75	800	1	300-420
Nickel-zinc	55-75	170-260	65	300	1.6	120-360
NiMH	70-95	200-300	70	750-1200+	6	240-420
Lithium-iron sulfide	100-130	150-250	80	1000+	n/a	130
Lithium-ion	80-130	200-300	>95	1000+	0.7	240

with a 201.6 V battery pack of prismatic NiMH. Each module consisting of six 1.2 V cells connected in series, having a capacity of 6.5 Ahr. The specific power by Panasonic's NiMH module under varying operating temperatures can be seen in Fig. 2.6(a). The specific power of the module increases at higher temperature due to increase in chemical activity and the battery can deliver up to 1500 W/kg at 40°C. The cycle life of the battery, shown in Fig 2.6(b), is close to 9,000 pulse cycles after which the battery's capacity reduces to 80% of its initial capacity.



(a)

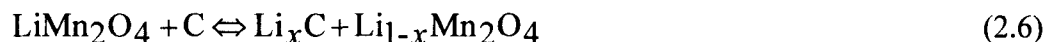
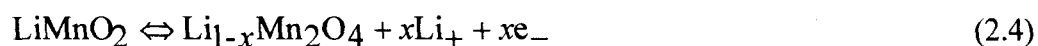


(b)

Fig. 2.6: Performance characteristics of Panasonic NiMH module. (a) Specific power for varying operating temperature. (b) Change in internal resistance over the cycle life.

2.2.3 Lithium-ion batteries

Lithium-ion batteries are the current promising alternative to the NiMH batteries due to their relatively higher specific power and energy density, low self-discharge, reduced volume and light weight [6], [7]. Their efficiency and single cell voltages are higher than any other battery technology available on the market. With a cell potential of 3.7 V to 4.1 V, they are undoubtedly the market leaders in terms of deliverables. Lithium ion batteries use lithiated transition metal oxides as the cathode and graphite as anode. The lithium ion chemical reactions are:



Lithium batteries only allow the passage of lithium ions across the separator, filling into the pores of the anode lattice. These batteries have a nearly reciprocal charge-discharge characteristic.

Many manufacturers including SAFT, Panasonic, EnerDel Inc. and Sony are involved in extensive research to develop commercially viable high performance lithium-ion batteries for hybrid vehicles with higher calendar life and reduced cost. A123 Systems have developed lithium-ion batteries for HEVs that exhibit drastic reduction in



Fig. 2.7: Lithium ion battery pack used in Tesla electric vehicle.

impedance change even after 250,000 pulse cycles. The battery pack used in Tesla electric vehicle is shown in Fig. 2.7. Li-ion batteries tend to heat when overcharged which may cause failure with shortened life or melting of the battery.

This property of lithium ion is termed as thermal runaway. Lithium-ion batteries need to be made tolerant to such electrical abuse before they can be used commercially in vehicular applications. The proper thermal management of these batteries is reflected in the high cost of the battery pack. General Motors is targeting a 100 L, 16 kWh Li-ion battery for its upcoming plug-in series hybrid Chevy Volt while BMW is launching Li-ion powered 7-series hybrid. The development of high performance batteries will play a crucial role in the effective usage of the electric drivetrain in a hybrid traction system. This will, in turn, translate into a drastic reduction in fuel consumption due to the removal or minimized operation of the IC engine. Thus, the primary consideration while designing an electric drivetrain configuration, developing its supervisory control unit and improving the performance of battery packs is to maximize the utilization of the electric motor in the vehicle. The endeavor in the advancement of these technologies is to replace the gasoline powered mechanical propulsion with electric propulsion where electric motor is the only source of traction. Moreover, the increase in battery life, safety, reliability and charging easiness at low initial cost will render market success.

2.3 Ultracapacitors

In addition to the batteries, the scopes of ultracapacitors are also being looked into by researchers and automotive engineers due to its high power density and prolonged life. An ultracapacitor discharges in seconds delivering very high instantaneous power. Its high charge acceptance capability also makes it highly suitable for the regenerative operation of traction motors, a special feature of the electric drivetrain [4]-[6]. The Nissan Condor capacitor hybrid truck relies on a 583 Wh, 346 V ultra-capacitor modules. According to the current developments and research trends, ultracapacitors are also being used in conjunction with batteries to improve the battery performance and overall drivetrain efficiency. Unlike normal capacitors, which offers capacitance by winding great lengths of metal foil plates separated by dielectric film, ultracapacitors achieve charge separation in the order of ion dimensions ($\sim 10\text{\AA}$) [6].

The energy stored in capacitors is:

$$Energy_{stored} = \frac{1}{2} \times C \times V^2 \quad (2.7)$$

where C is the capacitance and V is the voltage.

However, the constraints of high price and low specific energy have to be met in order to attain commercial stability.

2.4 Comparative Study of the Energy to Power Densities of Rechargeable Energy Storage Systems

The energy to power densities comparative study is the most important consideration for battery selection. These trends have been characterized in the laboratory and derived from constant power test data. The energy density is represented by γ_E and the power density is represented by γ_P [5]. The terms k_1 is achieved from the high power rate discharge test and k_2 from the slope derived from high minus low power rate test data. The relation is given by:

$$\gamma_E = k_1 - k_2 \gamma_P \quad (2.8)$$

- Lithium ion battery

$$\gamma_E = 75 - 0.025 \gamma_P \quad (2.9)$$

Nickel metal hydride battery

$$\gamma_E = 50 - 0.035 \gamma_P \quad (2.10)$$

- Lead acid battery

$$\gamma_E = 50 - 0.2 \gamma_P \quad (2.11)$$

- Ultracapacitor system

$$\gamma_E = 3 - 0.00127 \gamma_P \quad (2.12)$$

These equations are reflected in the Ragone plot shown in Fig. 1.3. It is evident from the equations that the energy density and power density of lithium batteries are much superior as compared to the other chemistries making it a forerunner in the automotive industry.

2.5 Summary

This section discusses the different battery parameters that are taken into consideration for determining its characteristics. It also analyses the factors that determine the battery performance with respect to the battery parameters. This chapter provides substantial information on the present energy storage developments occurring in the automotive industry and justifies its future trends and requirements.

3 DEVELOPMENT OF BATTERY MODELS FOR ILLUSTRATION OF ITS CHARACTERISTICS

As discussed in the previous section, battery is an electrochemical device that stores electrical energy in the form of chemical energy. The rate of consumption and behavioral characteristics of this energy varies unpredictably in accordance with the drivers need. Thus, the reliability of HEV/EV, which is highly dependent on the accurate knowledge of the battery's usable state-of-charge, becomes questionable, hindering its commercial popularity. Battery modeling is thus essential for the analysis of battery's dynamic behavior and predicting its state-of-charge for a given driving schedule [9]. The correct modeling of the battery will determine and describe its operational efficiency. Moreover, it will also increase its cycle time and calendar life, leading to higher economic pay back and increased consumer satisfaction.

3.1 Battery Model Classification

The battery is a very critical part of the electric drive train. It can ideally be represented as a simple voltage source with zero internal resistance. However, in reality, the battery internal parameters such as conductivity, resistance, rate of reactivity, active material decomposition etc affect its real-time characteristics. These internal parameters change along the charge-discharge cycle. Temperature, ageing, level of charge and discharge affect these internal parameters. The different battery chemical compositions also render variations in the internal parameters leading to a considerable dissimilarity in their charge-discharge characteristics. This charge-discharge characteristic of a battery can broadly be represented and explained by electrochemical models, mathematical models and electric circuit models [9], [10]. The mathematical models are capable of predicting the efficiency and capacity of a battery but their accuracy is questionable [10]-[13]. Thus, this modeling method is least preferred. Electrochemical models are complicated and time consuming although they explain the basic physical characteristics of the battery [10]. There are many steady-state and impulse electro analytical techniques that determine the electrochemical parameters and assist in improving the battery

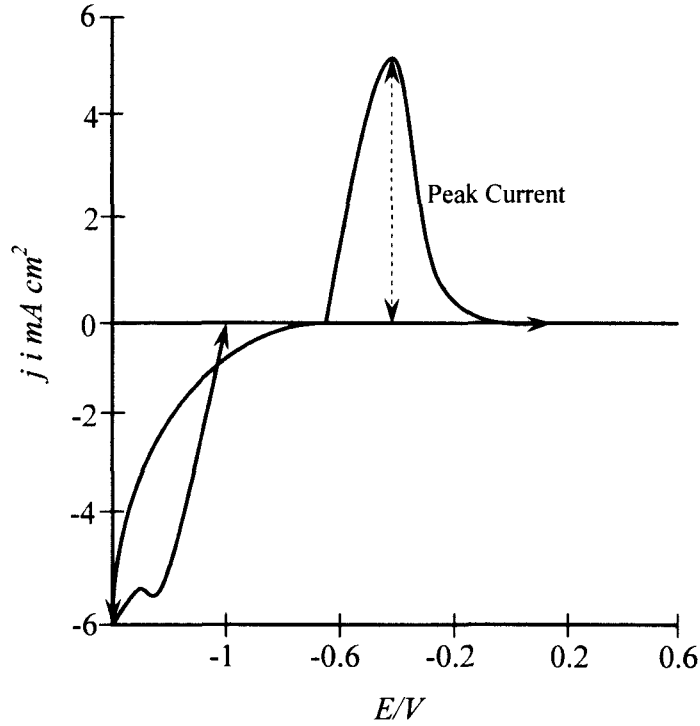


Fig. 3.1: Cyclic voltammetry.

performance. Cyclic voltammetry is one of the most preferred electro analytical techniques as shown in Fig. 3.1. This method in spite of some ingenuity is able to identify reversible couples, transfer coefficient of an electrode process and provide tool to analyze complex electrochemical systems. The initial potential sweep is represented by [6]:

$$E = E_i - vt \quad (3.1)$$

where E_i = initial potential

t = time

v = rate of potential change

The reverse sweep is given by:

$$E = E_i + v't \quad (3.2)$$

where $v' = v$

The peak current shown in Fig. 3.1 is given by:

$$i_p = \frac{\left[0.447 \sqrt[3]{F} \sqrt[3]{A_n C_o} \sqrt{Dv} \right]}{\sqrt{RT}} \quad (3.3)$$

where i_p = peak current

F = Faradays constant

A_n = electrode area

R = gas constant

T = absolute temperature

D = diffusion coefficient

C = concentration

Chronopotentiometry is another process that involves the study of voltage transients at electrodes upon which is imposed a constant current. It is also termed as galvanostatic voltammetry. Unlike the above mentioned methods, electrochemical impedance spectroscopy is a more direct method for studying the electrode process. It measures the change in the electrical impedance of the electrode. Polarography is one of the most old and widely employed methods [6]. The expression derived using this methodology is given below:

$$I_m = 607n\sqrt{DC}m^{0.66667}t_d^{0.16667} \quad (3.4)$$

where I_m = mean diffusion current

n = number of electrons involved in the overall electrode process

D = diffusion coefficient of electroactive species

C = concentration of electroactive species in nmol/L

m = mercury flow rate, mg/sec

t_d = mercury drop time,sec

It can be evident from the above process that the electrochemical models render detailed information of the battery operation illustrating its characteristics. But the high time makes it unsuitable for real time application. Moreover, it analyses the battery operation as a single entity with no scope of test across the other electrical drivetrain components. Unlike mathematical models, electric circuit models are more accurate and can also explain the V-I characteristics in relation to the internal parameters. Thus electric representation is necessary in order to substantiate the electrochemical changes in batteries, increase their life span and facilitate the designing of efficient battery management systems and electric drive trains.

3.2 Electric Circuit Model Classification

The electric circuit representation of a battery is composed of the basic electrical elements such as resistance and capacitance. These electrical elements are arranged in an order that illustrates the losses occurring in the battery, reflected by the terminal voltage, and matches the obtained charge-discharge characteristics. Literature depicts the proposal of various electric models that consider certain real-time operating constraints into account while explaining the battery characteristics [10]-[15]. The different basic electric circuit models have been discussed in the following section. The battery voltage to current relationship is shown in Fig. 3.2.

At real time operation, the voltage of the battery is measured on loaded condition. Thus, it is obviously lower than the open circuit voltage due to the presence of internal losses. These losses are broadly classified as

- *Polarization losses*: The losses that take place at the electrodes. During battery operation, there is a shift in potential of an electrode away from the reversible value termed as electrode over potential [6]. This electrode over-potential is composed of active and concentration over potential. These over potentials result in voltage drop at the electrode. Batteries use depolarization substances like manganese di-oxide to minimize these losses.

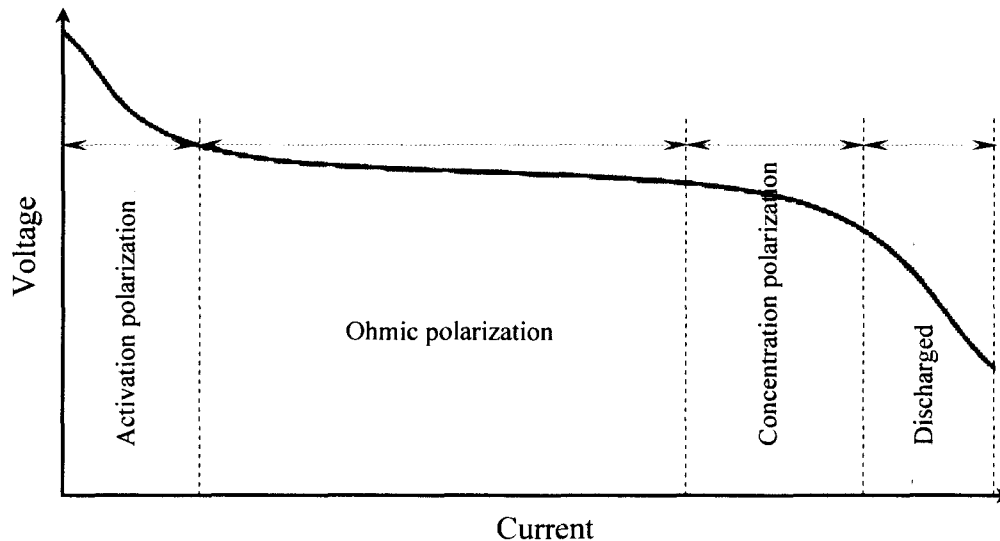


Fig. 3.2: Voltage-current behavior of electrochemical cells.

- *Ohmic (resistive) losses*: the losses due to the current flowing, recorded mainly in the current collectors, electrolyte and active masses.

The resultant voltage during charge and discharge is given by:

$$V_d = V_r - n_+ - n_- - IR \quad (3.5)$$

$$V_{cd} = V_r + n_+ + n_- + IR \quad (3.6)$$

where V_d and V_{cd} are charging and discharging voltage, V_r is the potential between the electrodes and I and R represents the battery current and internal resistance respectively.

3.2.1 Ideal Model

According to the ideal electric circuit representation of a battery as shown in Fig. 3.3(a), it is a simple voltage source with zero resistance. Here, V_{in} , which signifies the theoretical generated voltage, is received across the terminals. The V_{in} vs V_{ter} graph corresponding to this model, shown in Fig. 3.3 (b), is highly unrealistic. Thus, this model is discarded for any practical application.

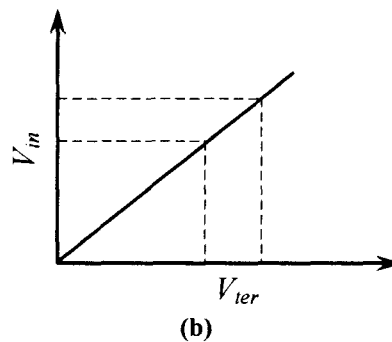
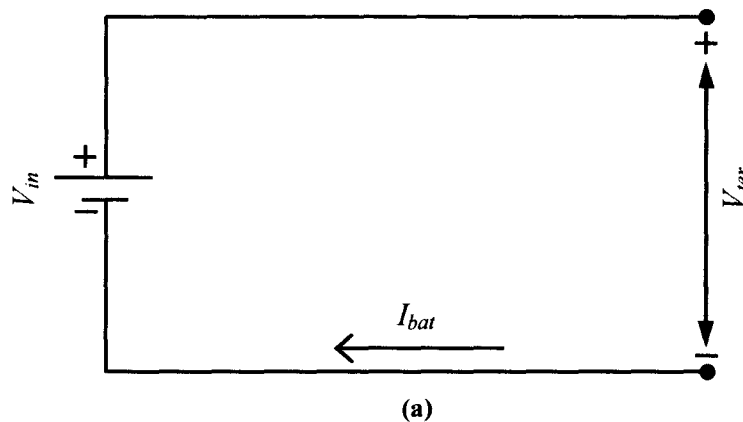


Fig. 3.3: (a) Ideal electric circuit model (b) Battery terminal voltage (V_{ter}) as a function of internal generated voltage (V_{in}).

The theoretical voltage is the difference between the potentials of the positive and negative electrodes. This is also termed as the standard cell voltage. It can be obvious from Fig. 3.2 that the internal parameters of the cell that result in the real time characteristics are absent. Here the theoretical voltage is proportional to the terminal voltage with no internal drop and losses.

3.2.2 Linear Model

In the linear model, as shown in Fig. 3.4, an internal resistance is added to the circuit in order to justify the real-time characteristics [12]. The resistance represents the total internal losses that take place in a battery. This resistance, which is assumed to be fixed, is independent of the level of charge and temperature. The green dotted line shown in Fig. 3.5 represents the V_{in} vs V_{ter} characteristics of the linear model. The red line is considered as a reference, representing the ideal battery operation. We can conclude from the graph that due to the fixed internal resistance, the V_{in} vs V_{ter} variation is linear but there is a constant variation between the two voltages, substantiating the losses occurring in the battery. It is represented as:

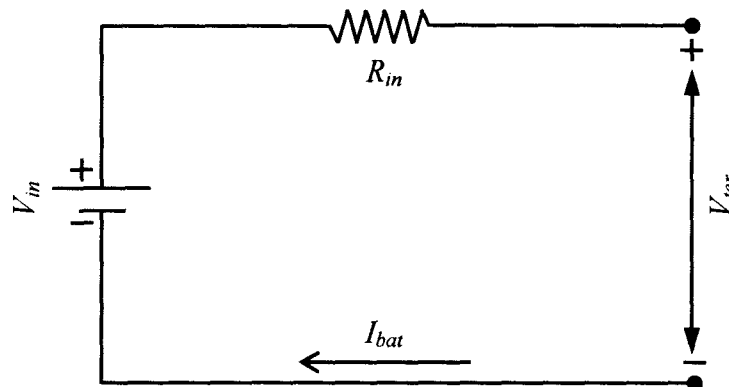


Fig. 3.4: Linear electric circuit model.

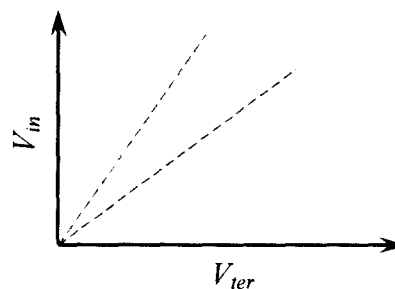


Fig. 3.5: Battery terminal voltage (V_{ter}) as a function of internal voltage (V_{in}) for a linear model.

$$V_{ter} = V_{in} - R_{in} \times I_{bat} \quad (3.7)$$

This model is a simple representation of the real battery operational characteristics. It is unable to predict any transient occurring in the battery [10], [12]. This model fails to consider many important real-time constraints as discussed in Chapter 2 that have ample influence on the battery performance and its charge-discharge characteristics.

3.2.3 Thevenin Model

The Thevenin model shown in Fig. 3.6 has an overvoltage protection incorporated in addition to the linear model. The Thevenin model is applicable for a fixed state-of-charge and constant open circuit voltage [10], [12]. Unlike linear models, it can predict the transient responses. The Thevenin model consists of an ideal no-load battery voltage (V_{in}), internal resistance (R_{in}), capacitance (C_{th}) and overvoltage resistance (R_{th}). C_{th} represents the capacitance of the parallel plates and R_{th} represents the non-linear resistance contributed by the contact resistance of plate to electrolyte. An increase in the number of parallel RC networks can increase the accuracy of the predicted battery response. However, as the SOC and time-constant are dependent on cycle number and temperature, prediction errors for estimating run time and SOC tend to be high. Thus the main disadvantage of the Thevenin battery model is that all the elements are assumed to be constant although in reality all the values are functions of battery conditions.

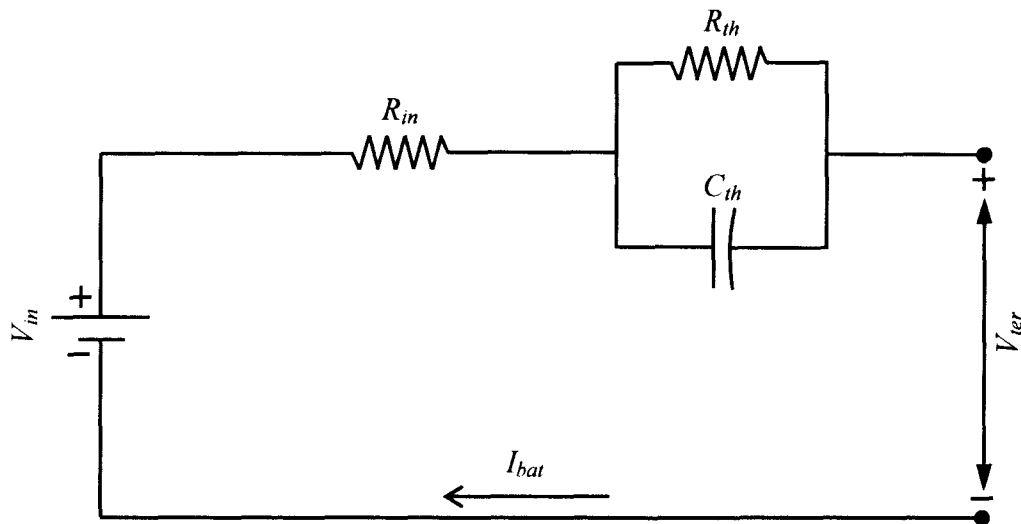


Fig. 3.6: Thevenin electric circuit model.

3.2.4 Impedance model

The impedance-based model shown in Fig. 3.7, employ the method of electrochemical impedance spectroscopy to obtain ac-equivalent impedance model in the frequency domain [6], [10]. It then uses a complicated equivalent network (Z_{ac}) to fit the impedance spectra. The fitting process is difficult, complex, and non-intuitive. In addition, impedance-based models only work for a fixed SOC and temperature setting, and therefore they cannot predict dc response or battery runtime.

3.2.5 Run time based model

The runtime model as shown in Fig. 3.8 is one of the most practical models that have been improvised by researchers for predicting the runtime of the battery under real time conditions [12]-[15]. Runtime-based models use a complex circuit network to simulate battery runtime and dc voltage response for a constant discharge current.

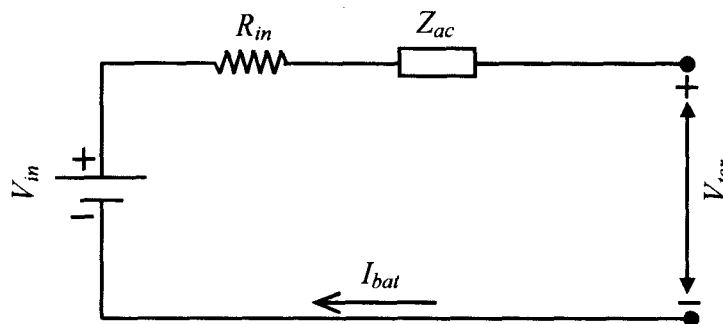


Fig. 3.7: Impedance model.

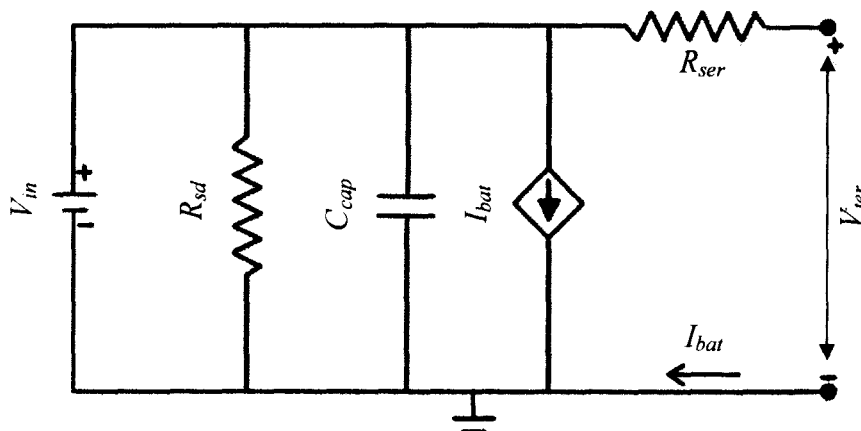


Fig. 3.8: Runtime based model.

3.3 Novel Battery Model Development

The models discussed in the previous section have been developed by taking certain battery chemistry into account, matching their charge-discharge characteristics. The proposed model is based on the positive attributes of these basic conventional electric circuit models.

3.3.1 Research Objective

As mentioned in Chapter 2, the automotive industry uses a variety of battery chemistries for HEV/EV applications. Each chemical composition has its own unique properties that are reflected in their respective charge-discharge characteristics. Furthermore, the electric circuit models discussed in the previous section varies with the real-time constraints that have been taken into consideration. These deviations have lead to the proposition of numerous models, increasing the complexity and ambiguity in terms of reliability and effectiveness. In order to address this concern, the proposed model is developed on the basis of the research objectives mentioned below:

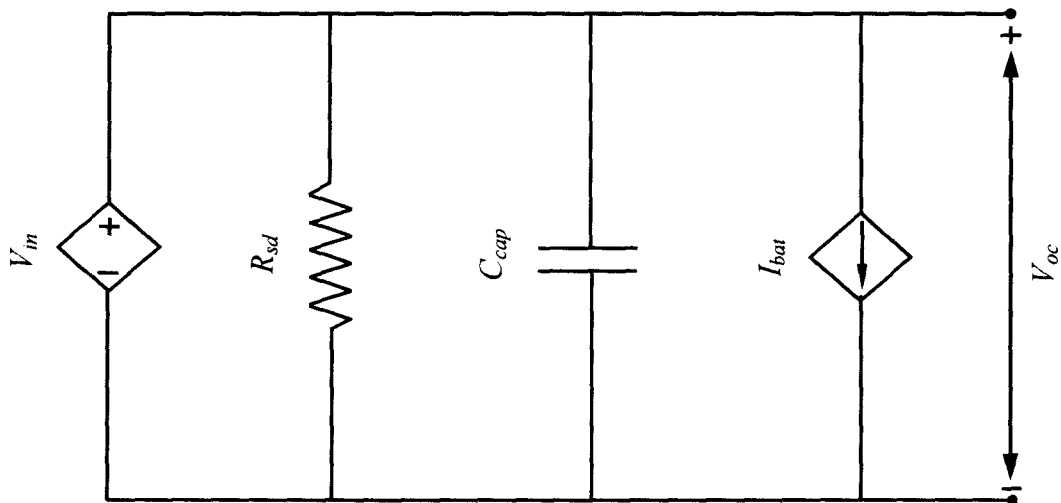
- Development of an electric circuit model that is applicable for different chemistries with minor modifications
- Scope of simplification of the model in order to apply it in conjunction with other electric drive train components
- Charge-discharge characteristics illustration under real-time operating conditions

3.3.2 Proposed Model

The proposed model as shown in Fig. 3.9 is focused on illustrating the terminal voltage and V-I characteristics of the battery. The battery model takes into consideration the open-circuit voltage, the current and the cycle number for a steady charge-discharge cycle. The runtime model of the battery is shown in Fig. 3.9 (a) and the model to analyze its charge-discharge characteristics is shown in Fig. 3.9 (b). The voltage drop across the battery is explained with the help of internal resistances. The effect of heat, generated due to the in-vehicle and external attributes, on the internal resistance has been neglected. V_{in} is a current controlled voltage source used to represent the battery voltage variation with the charge and discharge current. R_{sd} is used to characterize the losses that occur in a

battery stored for a long time. Although the effect of R_{sd} is negligible when the battery is connected across the load, it differs widely with the chemical compositions of the battery. The self discharges for NiMH batteries are 15%, while the lithium ion batteries have rates as low as 3% under room temperature.

The capacitor C_{cap} represents the charge of the battery. It charges and discharges with the charge and discharge current thus representing the instantaneous state of charge V_{oc} . I_{bat} is the current flowing through the circuit during charge or discharge of the battery. The amount of charge stored in the capacitor is a function of I_{bat} . The resistance R_{ser} in series with the parallel RC networks (R_1, C_1 and R_2, C_2) as shown in Fig. 3.9(b) has been incorporated from the Thevenin electric circuit model. This RC network is used to predict the battery response to transient loads for a fixed SOC. Increase in the number of RC networks would increase the accuracy of the transient response but for ease of calculation only two RC networks have been considered [10]. R_c and R_d are the charging and discharging resistances respectively while R_{co} and R_{do} are overcharge and over discharge resistances. The considerations of the charge-discharge resistance and the overcharge, over discharge resistance have been discussed in [10]. The diodes ensure that the resistances corresponding to the charging and discharging of the battery act separately. V_{oc} is a voltage controlled voltage source that signifies the state-of-charge of the battery.



(a)

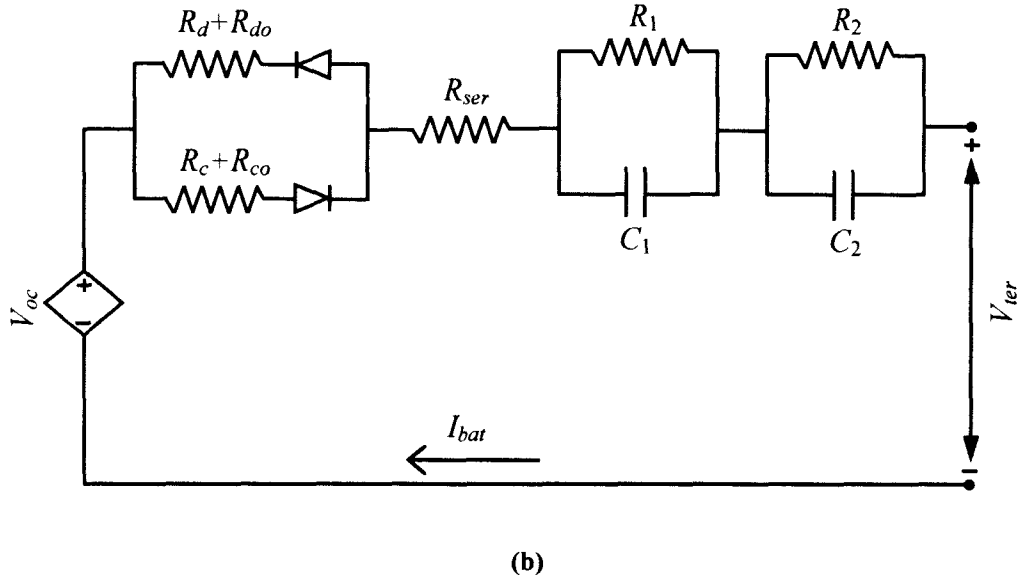


Fig. 3.9: Proposed model. (a)Run-time determination (b) V-I characteristics determination.

3.3.3 Capacitive representation and illustration of the proposed model

The discharging capacity of the battery is represented by the capacitor C_{cap} . The model to illustrate the V- I characteristics as shown in Fig. 3.9 (b) is further improved as shown in Fig 3.10. This time-constant for the battery is derived from the charge-discharge characteristics. The permissible operating range of the battery varies with the chemistry, battery management system design and energy management system precision. The voltage ratings and capacity of the battery are provided by the manufacturer's data sheet. The capacitor has been calculated on the basis of this provided information.

We know

$$1 \text{ Ah} = 3600 \text{ Columbs} \quad (3.8)$$

$$Q = CV \quad (3.9)$$

where Ahr is the charge of the battery, Q is the charge stored in the battery and V is the cell voltage, similar to the cell being used in HEV/EV. The value of the resistance changes along the charge-discharge cycle, according to the charge present and the current flowing through it. The internal resistances are a function of the state-of-charge for the given proposed model. The state of charge is calculated by

$$SOC = Q - \int_0^t i(t)dt \quad (3.10)$$

The initial voltage across the capacitor is that of the battery at full charge. The capacitor charges or discharges according to the direction of battery current.

The proposed model thus can be used to accurately validate batteries of different chemistries of different ratings by modifying the time constant, and the value of the capacitance. It can similarly be used to model the working of an ultracapacitor. The electric circuit models are developed to justify the charge-discharge characteristics of a battery. A generic discharge graph of a battery is shown in Fig. 3.11. The significance of the electrical components considered for the proposed model is justified in this figure. The curve has been separated into seven zones each identifying a certain stage. Zones 1 and 5 represent the linear drop of the voltage represented by R_{ser} and R_{dc} & R_c . The zones 2 and 4 are the transients, which have been represented by the two RC components. Zone 3 is the steady stage, which forms the most optimum operating region of NiMH and li-ion batteries. It is the normal HEV operating region. Moreover, zone 6, represents the capacity of the battery which is represented in the electric circuit as C_{cap} .

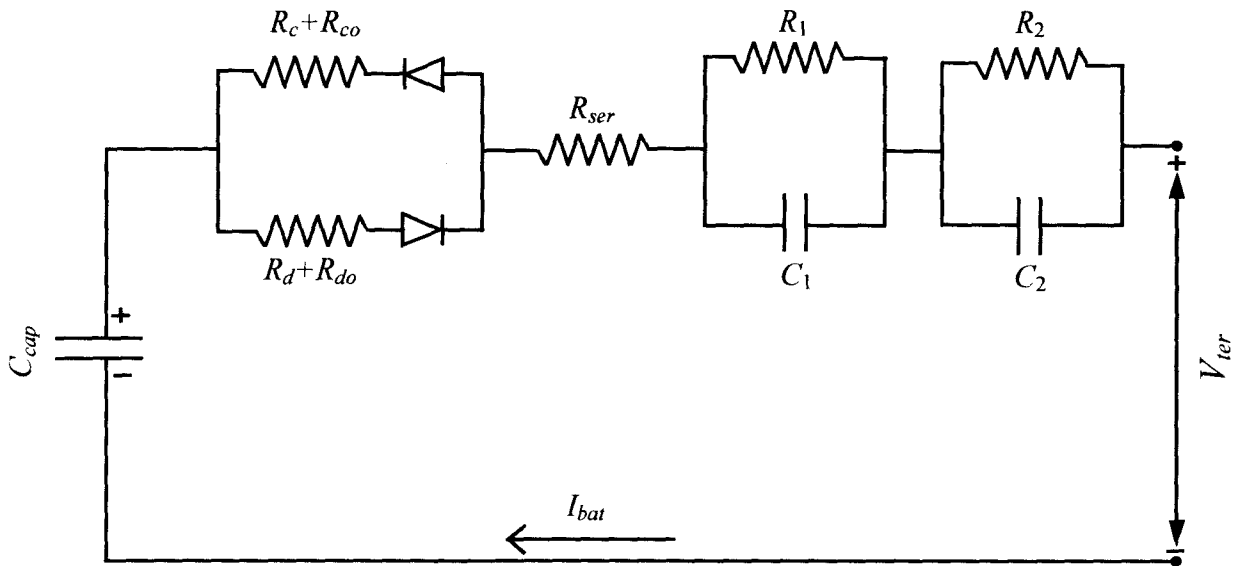


Fig. 3.10: Capacitive representation of the battery model.

3.3.4 Methodology

The proposed model has been simulated in a Matlab/Simulink environment as shown in Fig.3.12. The assumptions for this model are:

1. The self discharge resistance is negligible at loaded operation.
2. The internal resistance varies along the charge-discharge cycle.
3. No Peukert effect.
4. The charging and the discharging characteristics are assumed to be identical.

The model is initially simulated against a DC machine that works both as a generator and motor depending upon the power demand and state-of-charge of the battery. The battery terminal voltage is operated in an optimum region within the full charge voltage and permissible discharge voltage for real time operation of the vehicle. It has been assumed that initially the battery is completely charged. The battery is discharged by providing power to an external load (similar to the operation used in [8], in order to validate the model under similar conditions, with some more precise improvements as per recent developments) until it maximum discharge. The battery is never completely discharged under real operating conditions, but in order to analyze the voltage drop across the complete state-of-charge range, it is pushed to its limits. The generated current provides power for both the external load and the battery. The changing of the DC machine from the generator and motor modes need to be precise in order to prevent overcharging or over-discharging of the battery.

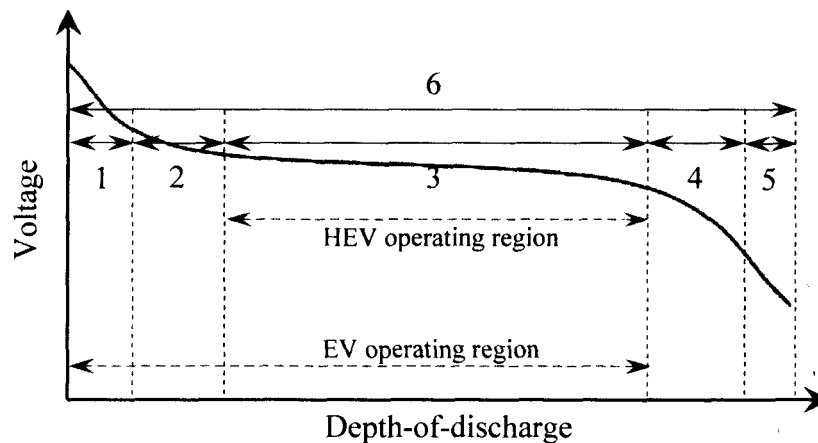


Fig. 3.11: Battery model illustration.

The internal generated cell voltage is always constant, but the terminal voltage varies with the varying resistance at different state-of-charge. The terminal voltage is also dependent upon the direction of the current. The rate of charge acceptance by regenerative braking is neglected while validating the proposed model. The capacitive nature of the battery also has a dependence on the machine parameters which needs to be precisely optimized in order to improve the overall efficiency.

The proposed model is then validated against an absorbed glass Mat VRLA industrial battery block, EV31A-A, shown in Fig. 3.14, manufactured by Discover Energy Corp. This battery has an extended temperature range of -40°C to 60°C and is used in electric vehicles. The battery supplies power to a constant load of 110 A. The load current represents the 7 hp induction motor present in the electric drivetrain of the ZENN electric vehicle that houses the battery pack. When the battery terminal voltage drops below a pre-determined permissible level, the 7 hp, 210 V induction machine connected across it instigates the charging. The battery pack parameters are shown in Table 3.1. The parameters of the induction machine connected to the battery are given in Table 3.2. The capacitive representation of the battery has been modified according to the battery parameters. The proposed model is also tested against the lithium batteries considering their thermal effects in order to justify its validity.

TABLE 3.1

EV31A-A BATTERY PARAMETERS

Parameters	Value
Rated Voltage	12 Volts
Internal Resistance @ 20°C	3.9 mOhms at full charge
Self discharge @ 20°C	<3% of capacity per month
Optimum Operating Temperature	-20°C to 60°C
Short Circuit Current	3100 Amps
Minutes of Discharge @ 75 A	60 minutes
End Point Cell Voltage	1.65 Volts
Temperature Compensation	$-30\text{ mV}/^{\circ}\text{C}$ for cyclic use

TABLE 3.2

INDUCTION MACHINE PARAMETERS USED FOR MODEL VALIDATION

Parameters	Value
Rated Power	5,222 W
Rated Speed	4,000 rpm
Rated Voltage	210 V
Mechanical Torque	20 N.m
Stator Resistance	0.435 Ω
Stator Inductance	2.2 mH
Rotor Resistance	0.816 Ω
Rotor Inductance	2 mH
Mutual Inductance	69.31 mH
Total Inertia	0.089 kg.m ²

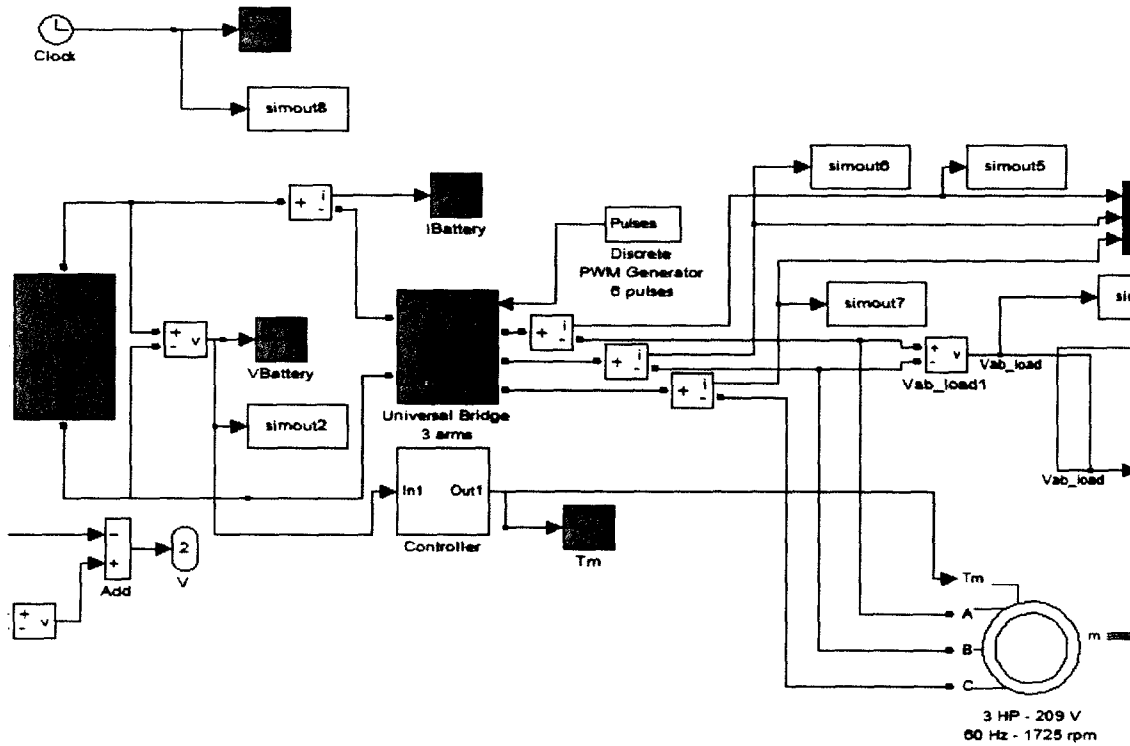


Fig. 3.12: Detailed view of the Matlab/Simulink model.

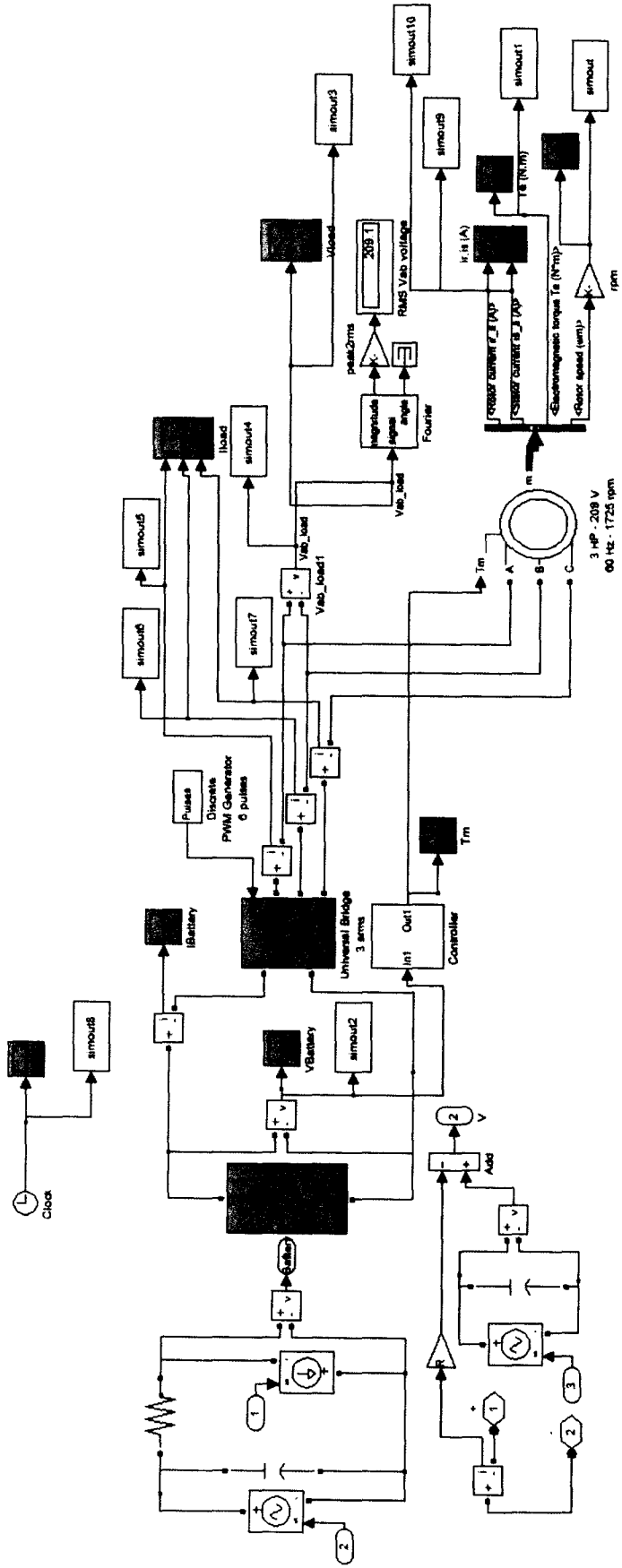


Fig. 3.13: Matlab/Simulink representation of the proposed model.



Fig.3.14: EV31A-A battery used in ZENN vehicle.

3.4 Results

3.4.1 Simulation results for NiMH battery

The results are obtained by simulating the proposed model to analyze a 6.5AHrr NiMH battery. The battery is initially allowed to discharge completely under a constant load, i.e. the state-of-charge is allowed to be reduced to zero by inhibiting the generator operation. It is performed for the analysis of the change in internal resistance across the complete SOC range. It is observed that a steady gain in the battery internal resistance takes place along with the discharge. The terminal voltage with respect to the internal resistance is shown in Fig. 3.15.

Fig. 3.16 shows the variation in internal resistance till the discharge capacity reaches 85% of its rated value. The rate of increase of the internal resistance accelerates after attaining a 15% degree of discharge. This rate of increase is dependent on the rate of charge and discharge. In Fig. 3.17, the variation of the terminal voltage with respect to the battery current is shown. Here, the terminal voltage is allowed to operate within a calculated range with a certain degree of overdischarging. This is due to the reaction time

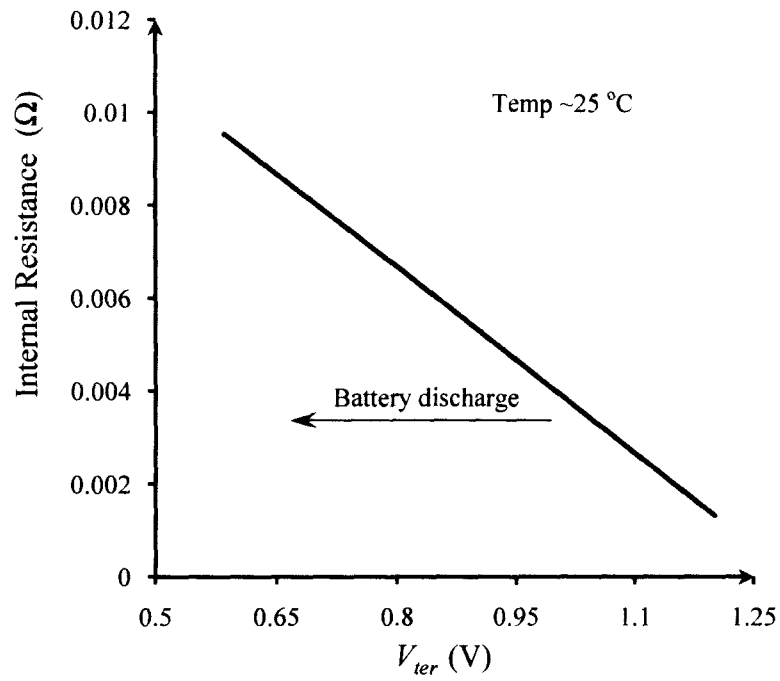


Fig. 3.15: Battery terminal voltage (V_{ter}) as a function of internal resistance.

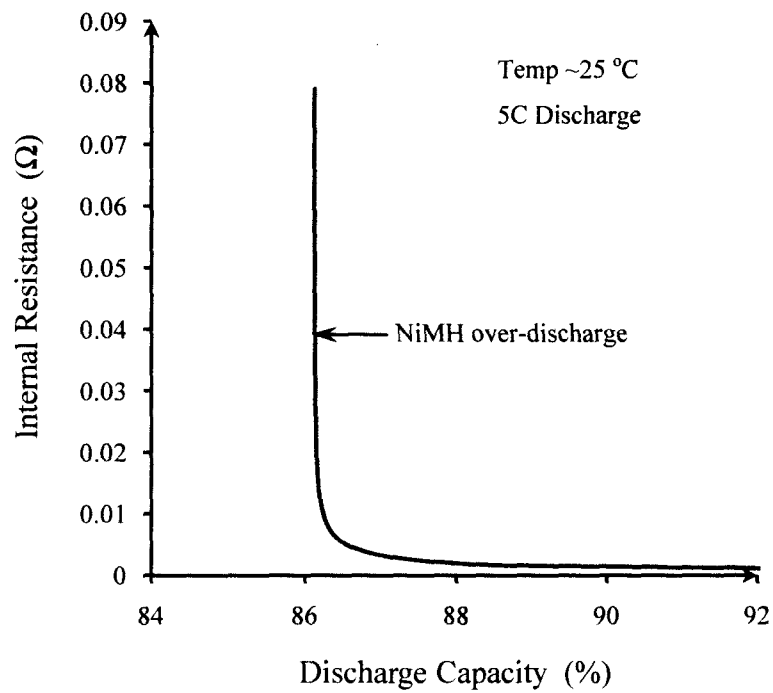


Fig.3.16: Internal resistance drop as a function of SOC.

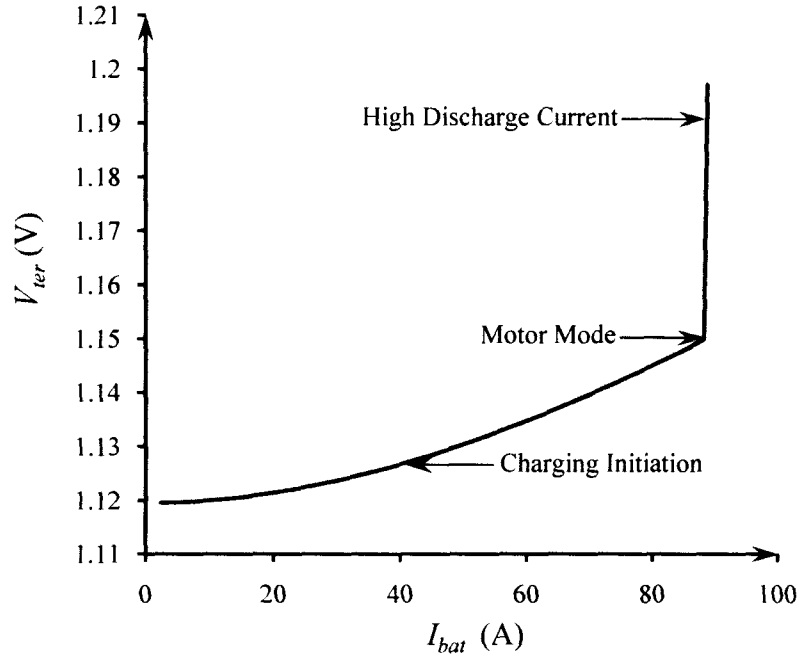


Fig.3.17: Battery terminal voltage (V_{ter}) as a function of battery current (I_{bat}).

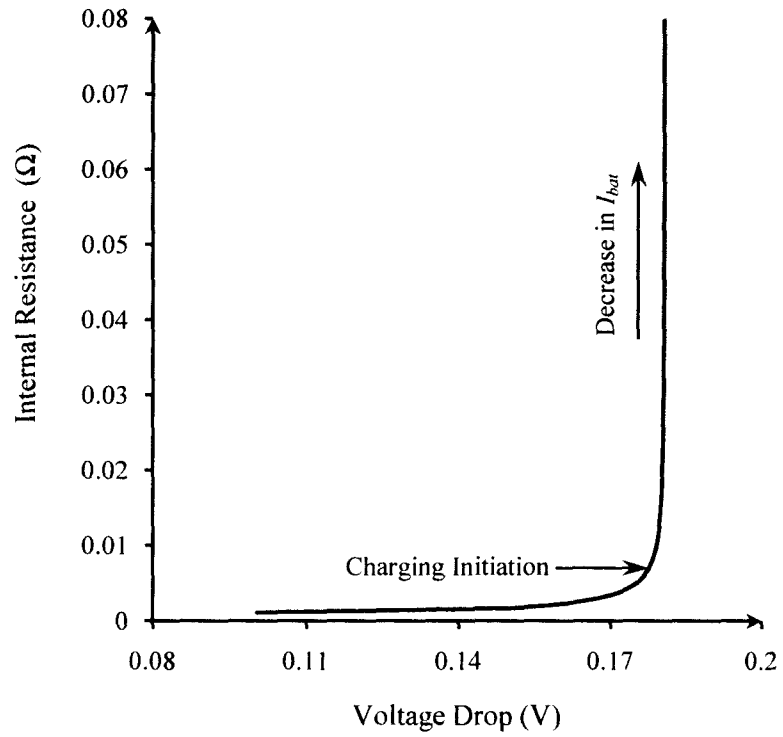


Fig.3.18: Voltage drop with respect to internal resistance.

between the motor to generator transition. The generator pick-up time that is required to produce enough power to meet the load demand and to charge the battery is dependent on the external applied torque and machine parameters. It should be noted that I_{bat} becomes zero when V_{ter} reaches 1.12 V as the DC machine shifts from motor mode to the generator mode. The internal resistance variation that is resulting the loss is shown in Fig. 3.18.

3.4.2 Simulation results for Lead-acid battery

The maximum permissible discharge voltage of the 400 V battery, in accordance with the end point cell voltage of 1.65 V, is limited to 330 V. According to the manufacturer's data sheet, the battery will be completely drained off in a time span of 40 minutes when connected across a constant load of 100 A. In order to precisely analyse the variation in resistance, the voltage drop has been limited to a range of 6 V. Fig. 3.19 shows the charge-discharge pattern of the battery, which is almost linear. The capacity of the battery has been reduced considerably in order to attain the requisite voltage drop for the analysis of the internal resistance. The voltage loss is analogous to the lead acid battery discharge curve Fig. 3.20. The difference in the rate of voltage drop is justified on the account of different machine parameters.

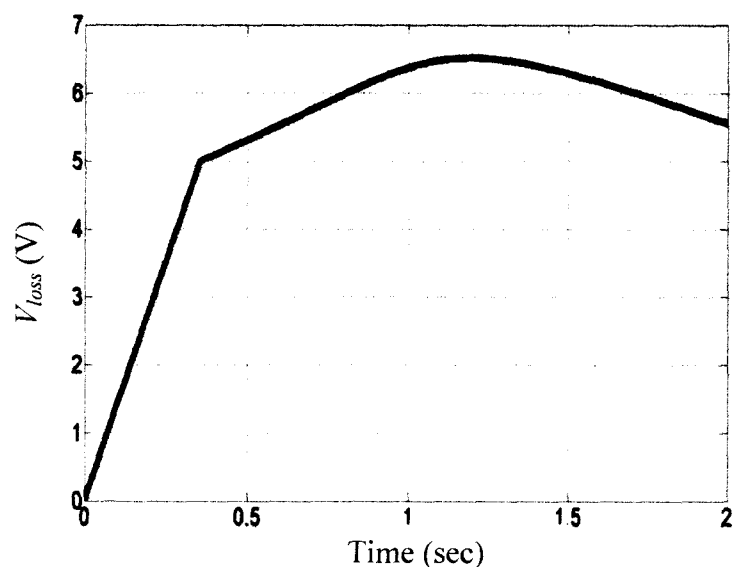


Fig.3.19: Charge-discharge of the lead-acid battery.

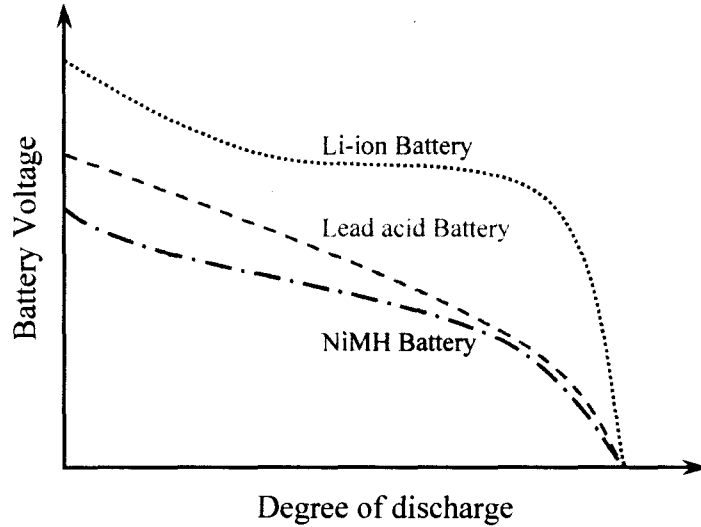


Fig.3.20: Battery discharge curve.

3.4.3 Simulation results for Lithium ion battery

The simulation has been limited to a region of optimum operation of 201.6 V and 198 V for a constant voltage DC machine. The initial loss across the resistance is in accordance with the temperature and charge-discharge cycle.

The variation of the overall internal resistance with time is shown in Fig. 3.21. This overall resistance is a result of the combined effect of the individual cell resistance (R_c , R_{co} and R_d , R_{do}) and the battery pack resistance. It has been observed that the resistance decreases due to the proliferation of the cell reaction with the increasing temperature. The variation of temperature along the charge-discharge cycle is shown in Fig. 3.22. It is the overall battery pack temperature as incorporated by the combination of negative temperature and positive temperature coefficient thermostats. The control algorithm takes into account the cumulative effect of the increase in temperature and rate of cell reactions. The result shows an increase in the rate of temperature along with the time of operation.

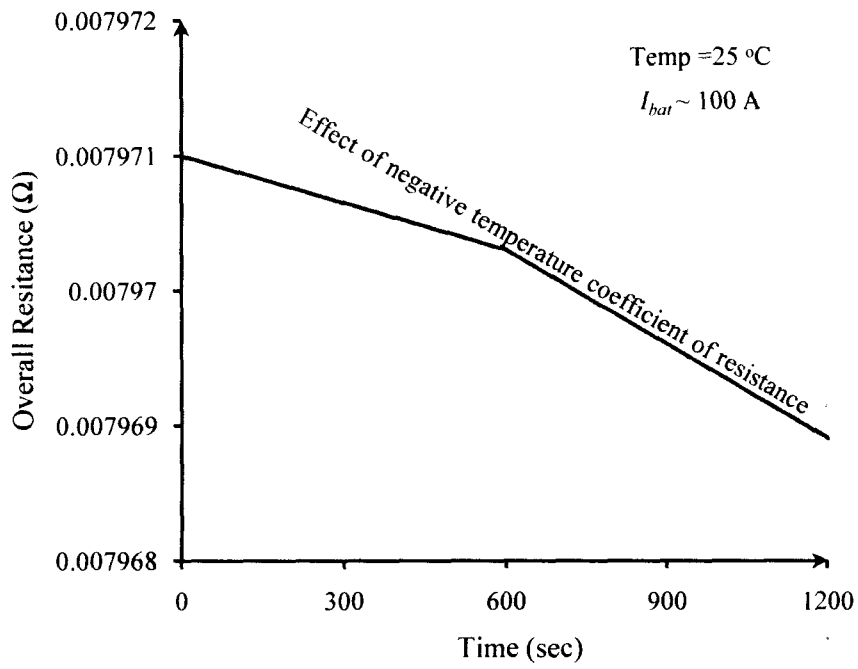


Fig.3.21: The change in resistance as a function of time.

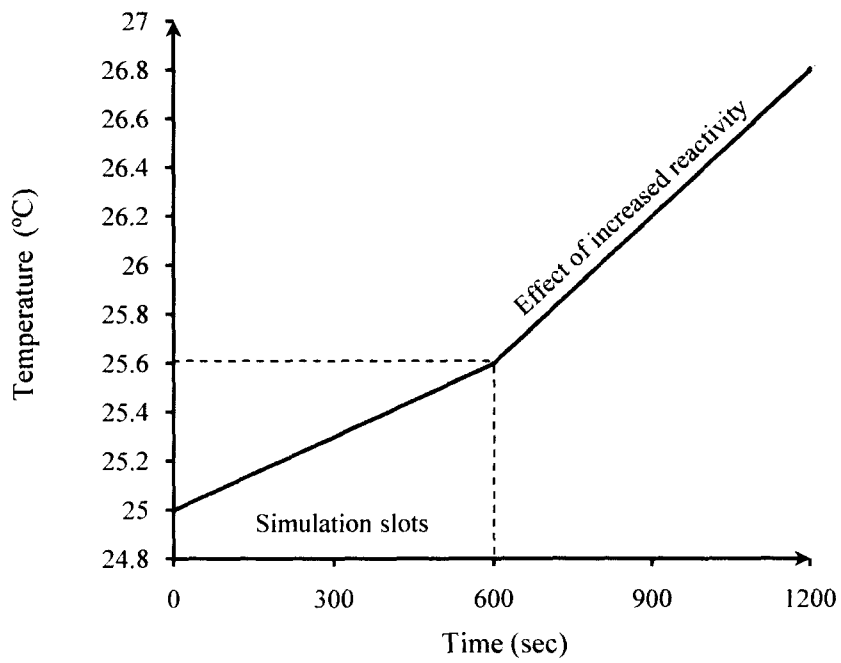


Fig.3.22: Temperature gradient profile.

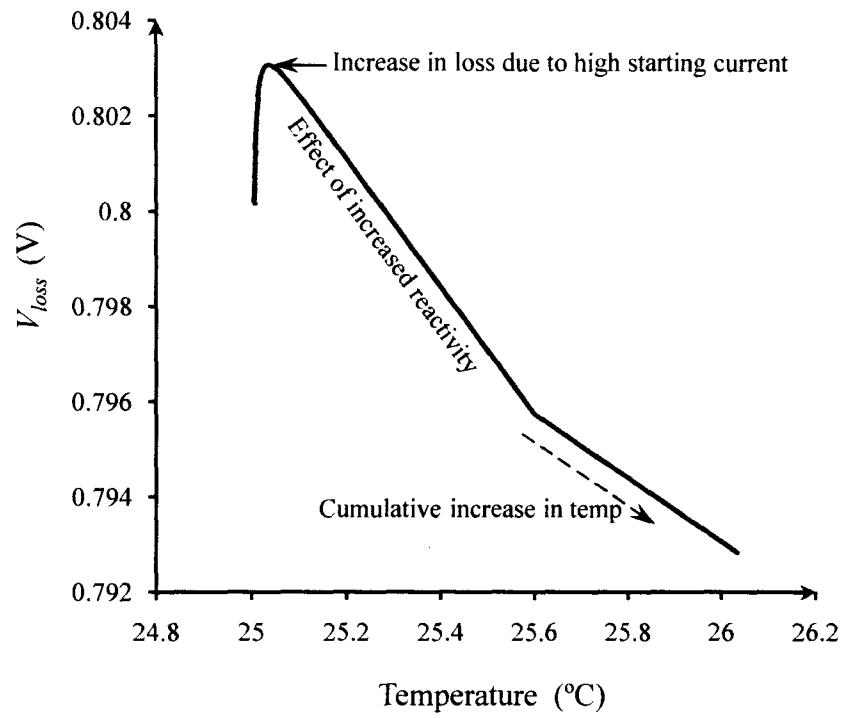


Fig.3.23: The loss across the temperature gradient.

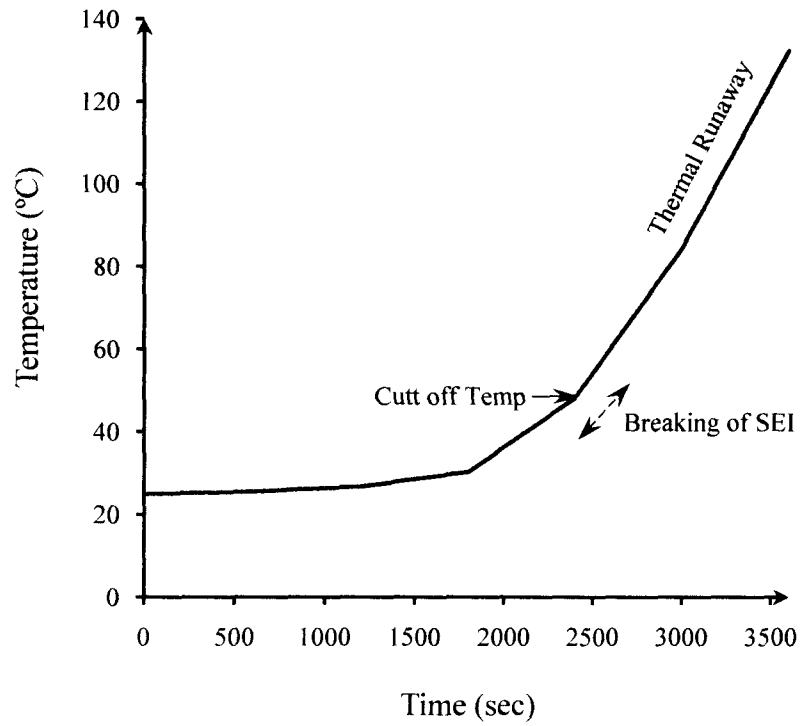


Fig.3.24: Temperature profile across the complete simulation.

Due to this decreasing resistance, the voltage drop, as shown in Fig. 3.24, is reducing with time and temperature signifying an increase in battery performance. The initial sudden increase in voltage drop is a result of the cell reaction initiation. It should be noted that the simulations had been initiated for battery operation at room temperature i. e. 25 °C.

The temperature gradient increases with the charge-discharge cycle as shown in Fig. 3.25. As the safe operating range of Li-ion batteries are limited to 45°C, the rate of cell reactions decreases with further increase in temperature. With no effective cooling, the temperature increases linearly with time after attaining 45°C as shown in Fig. 3.24. The battery pack, which has been modeled with a positive temperature coefficient of resistance, now limits its performance and safety. It can be inferred that the positive affect of cell reactions on the overall performance is limited to 45°C. The ageing effect, signifying the irreversible change in the active material composition of the battery and leading to a decrease in the internal voltage can be justified. Ageing is more prominent with the increase in number of charge-discharge cycles. This phenomenon is also aggravated by the rapid rise in temperature. The model thus can predict the life-time of the battery for a given operating temperature range.

3.5 Summary

The proposed model can analyze the variation in the internal resistance of the battery which accounts for the terminal voltage pertaining to the real time operation of the electric drivetrain. The proposed model can be also used for different battery ratings and chemistries used in the HEVs/EVs with minor modifications, according to their respective charge-discharge characteristics. The capacitive representation of the battery renders a better understanding of the battery operation. The variation of internal resistance in accordance with the state-of-charge and discharge rate of the battery has been verified. The variation in load also affects the internal resistance. It has been observed that the internal resistance increases almost proportionally at lower SOC, thus allowing for a faster discharge. It is hence recommended to maintain an optimum range of SOC depending upon the load connected across the battery, in order to prevent abuse. Temperature has immense effect on the internal resistance of the battery which in turn

accounts for its performance. The proposed model incorporates this temperature dependency and illustrates the battery performance based on the derived results. The terminal voltage has been justified with the variation in resistance of the cell and battery pack with time, number of charge-discharge cycles and temperature gradient. The discrepancy between the obtained overall resistance across the battery pack and accumulation of individual cell resistance is justified by the proposed model. The efficient operating range of the Li-ion cells which is limited to 45° C is explained with the help of the proposed model. The cell reaction acts as the determining factor for the overall internal resistance. After 45° C, the internal cell resistance increases drastically, resulting in rapid increase of temperature. In absence of proper protection, this thermal abuse can result in thermal runaway, leading to self destruction. Thus the BMS, which is essential for proper monitoring and protection of the battery, will be discussed in the forthcoming chapter.

3.6 Research Significance

The proposed research provides an improved understanding of the battery characteristics. It is also designed for application with variable battery chemistries with minor modification. The model can be successfully used illustrate the lead acid, NiMH and Lithium-ion battery properties shown in Fig. 3.20. The model is flexible in order to simulate the different battery characteristics, explaining their individual characteristics. The model simplification facilitates an improved and easy application of the battery models discussed in Chapter 4. The broaden scopes of application helps in better understanding of the battery operation and the electric drivetrain.

4 APPLICATION OF BATTERY MODELING IN ELECTRIC DRIVETRAIN

As discussed, HEVs/EVs are the most efficient solutions to meet this emerging fuel crisis. It has two power sources, namely the internal combustion engine (ICE) and battery that meets the drivers varying demand. Moreover, regenerative braking used to charge the onboard battery system also reduces the loss of brake power in the form of heat. These developments lead to a cheap and low emitting means of transportation. The electric propulsion system requires energy storage systems having turn around efficiency of about 90% [3]-[5]. In cases where this efficiency is less than 90%, hybridization would be completely wasted. The main challenges in this path of development are battery and battery management system (BMS) [16]. The overall efficiency of battery and battery management system accounts for the success of the vehicle. Thus the increase in charge retention, utilization and life of the battery would boost the reliability of the HEV/EV.

The distribution of the required power demand among the two power sources is dependent on the capacity of the battery and the power rating of the traction motor attached to the transmission. The effective reduction in the size of ICE, which in turn accounts for the amount of fuel consumed, is thus dependent on the capacity of the battery. The battery and motor thus forms a very critical part of the HEV/EV drivetrain [17].

HEVs/EVs have been using variety of traction motors such as DC motor, induction motor (IM) and permanent magnet synchronous motor (PMSM) [18]. In recent times, the commercial feasibility of switched reluctance motor (SRM) in HEV/EV application is also being tested [19]-[22]. All the above mentioned motors are selected on the basis of their efficiency in accordance with the vehicular payload and degree of hybridization. The battery performance, which is a crucial factor in determining the reliability of HEV/EV, is subjected to an unpredictable power demand variation at every instant [23]. The battery discharges by providing the necessary power to the motor which in turn charges it by the means of regenerative braking. This charging-discharging rate is dependent on the motor type and its power rating. These characteristics are also dependent on many factors such as chemical composition of the active materials, the operating temperature and the number of charge-discharge cycles. In order to prevent

damage and maintain an optimum performance, the HEV battery has to have a very precise battery management system. Thus, the analysis of minor variations is essential to determine the control parameters of the battery management system (BMS) [23]-[30].

Battery modeling plays an important role in the determination of these battery parameters. The model can be connected across the conventional motor models in order to anticipate and analyze the variation it will be subjected to, leading to a considerable rise in BMS accuracy and battery performance enhancement in terms of cycle life, calendar life and efficiency.

4.1 HEV/EV Battery

4.1.1 HEV/EV Battery Pack

The HEV battery pack shown in Fig. 4.1 consists of cells that are arranged in small groups termed as modules. These modules are then grouped together to form the battery pack. Fig. 4.2 represents a schematic diagram of a generalized battery pack composed of m modules having n cells in each module. Battery management system controls these cells to attain maximum efficiency.

The capacity (AHr) of the battery pack remain constant as the cells are connected in series. The voltage adds up according to the number of cells. The number of cells is normally determined by:

$$CN = \frac{Rt \times I_{avg_bat}}{AHr} \quad (4.1)$$

Where CN is the number of cells, Rt is the runtime, I_{avg_bat} is the average battery current and AHr is the battery capacity

The open-circuit voltage across the terminals of the battery pack shown in Fig. 4.1 would be the summation of all the cell voltages and can be expressed as:

$$V_b = m \times n \times E \quad (4.2)$$

where E is the open-circuit voltage across each cell and n is the number of cells in each module in the battery pack. For example, Toyota Prius Generation III uses prismatic NiMH modules from Panasonic each of which consists of six 1.2 V cells connected in series. Each of these modules has a nominal voltage of 7.2 V and capacity of 6.5 AHr.

The Prius III battery pack consists of 28 such modules connected in series resulting in a nominal voltage of 201.6 V.

In reality, there are significant internal losses during the real-time operation of HEV battery pack. Along with the charge-discharge cycle, the pack construction (i.e. the arrangement of cells along with the insulation and ventilation) and manufacturing dissimilarities have considerable impact on the cell internal parameters such as self-discharge resistance, polarization resistance and charging-discharging resistance.

The overall internal resistance of the battery pack is more than the accumulation of individual cell resistances. The study of this variation is necessary for accurate terminal voltage justification and state-of-charge prediction. The terminal voltage of the battery pack is dependent on the interaction between the cell and battery pack construction. This interdependent phenomenon is explained with the help of the proposed model.

4.1.2 HEV/EV Battery Management System

Battery management system is the control and optimization of the function of cells and battery pack, protecting it from electrical and thermal abuse when subjected to an unpredictable varying load and driving conditions. Its control strategy is based on the information fed to it by the sensors as shown in Fig. 4.3 and the power demand from the energy management controller [27]-[34].

The important features of the BMS are as follow:

- a) SOC maintenance in accordance with the energy management system algorithm.
- b) Individual cell voltage and temperature.
- c) Cell balancing, and over-charge and over-discharge protection.
- d) State-of-Health (SOH) monitoring.
- e) Battery packs temperature monitoring.
- f) Internal fault analysis.

Fig. 4.3 is the block diagram of the basic operation of a BMS consisting of an array of n cells. The output of cell voltage, temperature and current sensor namely the CVS, CTS and CCS are fed to battery management controller for its optimum performance and protection. The resistance R across each cell is used for resistive cell balancing. The precise determination of this voltage, temperature and current would in turn render an

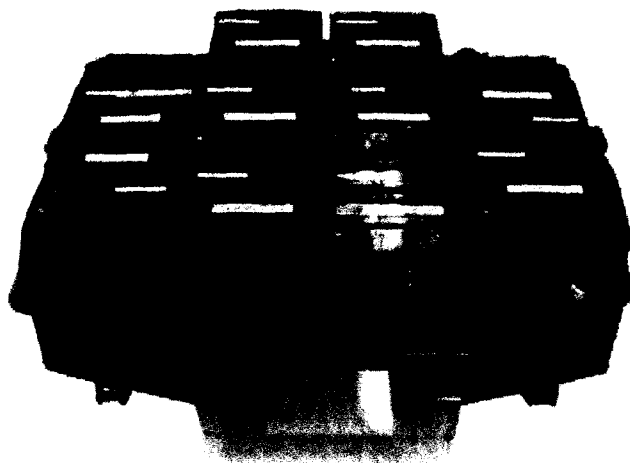


Fig. 4.1: Mitsubishi HEV battery pack.

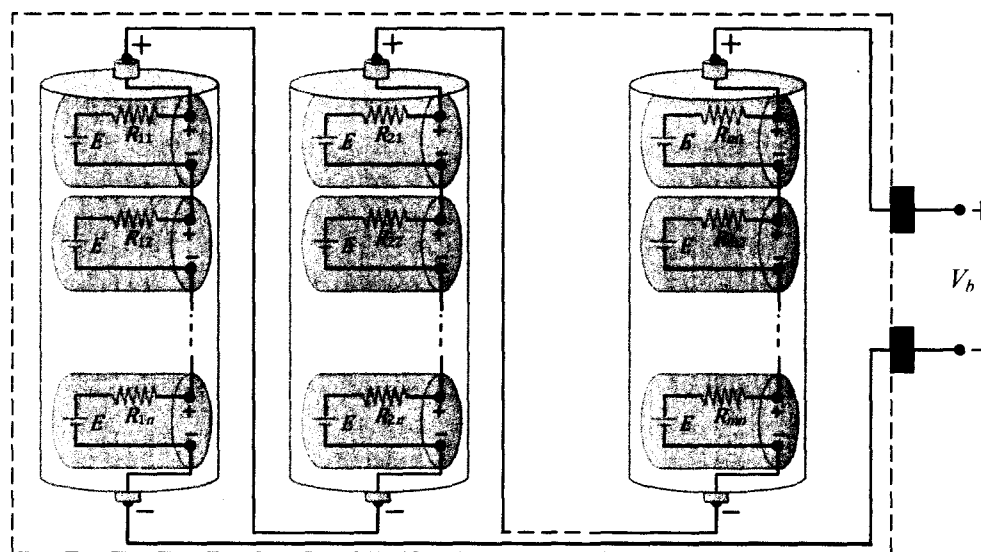
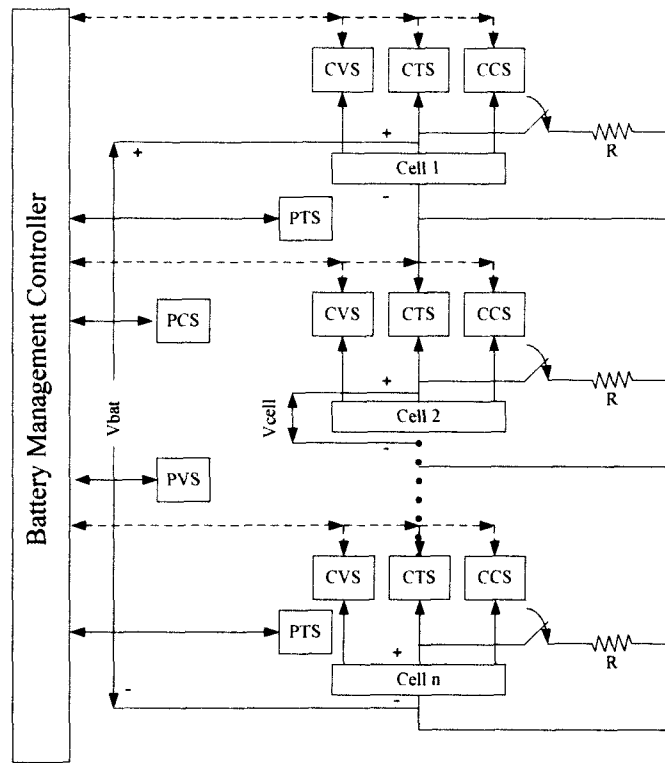


Fig. 4.2: Schematic representation of the battery pack.

accurate battery management system, with efficient cell balancing. The developed battery models can be used for these parameters detection justifying the need of battery models and its applicability.

4.2 Traction Motors in HEV/EV

In case of HEV series architecture, motor is the only power sink, directly connected to the transmission. For parallel and complex architectures, the power is shared between the ICE and the motor. Thus, the motor performance is a major issue while determining the efficiency of the vehicle. HEV traction motor ideally needs to have a high torque density



- CVS- Cell Voltage Sensor
- CTS- Cell Temperature Sensor
- CCS- Cell Current Sensor
- PVS- Pack Voltage Sensor
- PTS- Pack Temperature Sensor

Fig. 4.3: Schematic representation of the battery management system.

and power density to render efficient start ups, hill climbing and high-speed operation respectively. The unpredictable frequent start-stops, sudden accelerations and decelerations in HEV also require the efficient operation of the motor over wide speed and torque ranges [3]-[5]. The most popular motors that are in use for HEV application are the DC motor, induction motor (IM) and permanent magnet AC synchronous motor [18] . The choice of the electric motor is dependent on factors such as driver expectations, vehicular constraints and available energy sources. Thus, acceleration, speed, braking, type of the vehicle, HEV architecture, payload, battery capacity, generator and ICE ratings are considered during this selection procedure.

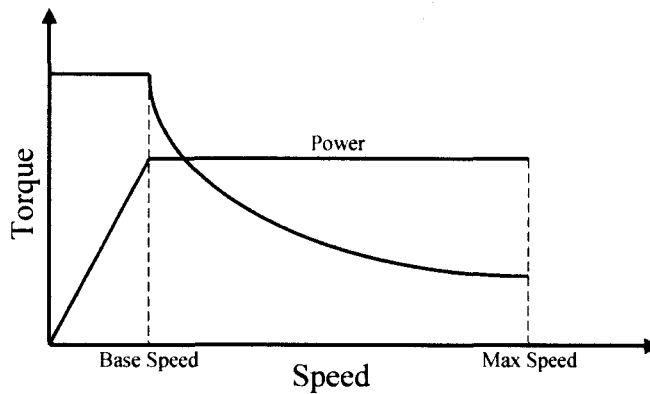


Fig. 4.4: HEV/EV traction motor requisites.

The main features that are essential from the HEV traction motor are: a) high power density b) very wide speed range c) high efficiency over the stipulated wide speed range for a fixed torque d) efficient regenerative braking capability e) optimized cost, size, and weight in accordance to the power capability f) robustness [18], [32].

Fig. 4.4 shows the desired operating condition of the HEV traction motor. It can be inferred that the vehicular power demand stabilizes with constant power. A constant torque is maintained below the base speed by setting both the armature and field current to their rated values. In order to increase the speed further, the torque is decreased by weakening the flux at constant armature current.

4.2.1 Direct Current Motor

DC motors are used in a wide range of applications. Its torque-speed characteristics, especially at low speed suits the HEV traction requirements. Among the different types of motors commercially available, DC motor in spite of its poor controllability is used for traction purposes mainly due to its high starting torque. PSA Peugeot uses DC motor in its electric drivetrain as shown in Fig. 4.5 .Although DC motors have simple control mechanism, they are currently being replaced by the commutatorless induction motors or permanent magnet motors due to its low specific power density, low efficiency, large size, high maintenance cost and need for commutation [18].

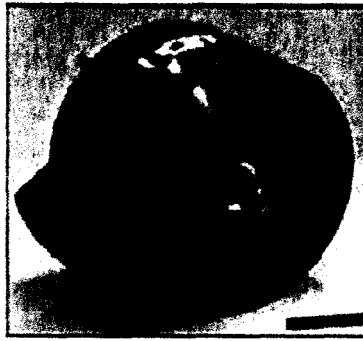


Fig. 4.5: DC traction motor.

4.2.2 Induction motor

Induction motor as shown in Fig. 4.6 is a mature technology, popular for its robust construction, low maintenance cost, light weight, small volume, and reliable operation. Among the two types of induction motor: 1) wound rotor and 2) squirrel-cage; the latter is used in the vehicular drivetrain. The operational characteristic of IM is shown in Fig. 4.7. During the constant torque range, the vehicle overcomes the inertia of rest with the rotor accelerating from zero to base speed. In case of the constant power, the base speed further increases to maximum speed. At this instant the electromagnetic torque becomes inversely proportional to the speed. It can attain an efficiency of 90% approximately when operating at its full load condition. The main disadvantages of IMs that are posing threat to its popularity are the low-inverter usage factor and low efficiency. The efficiency during light load can be as low as 20-30% [35]-[37].

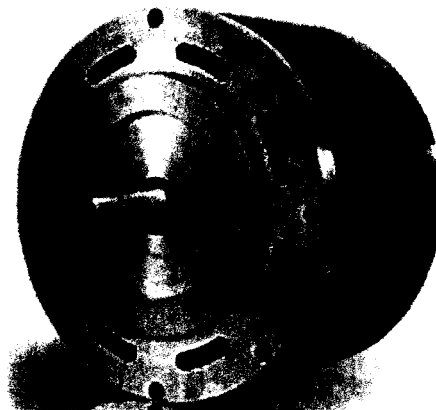


Fig. 4.6: Induction motor used in HEV/EV.

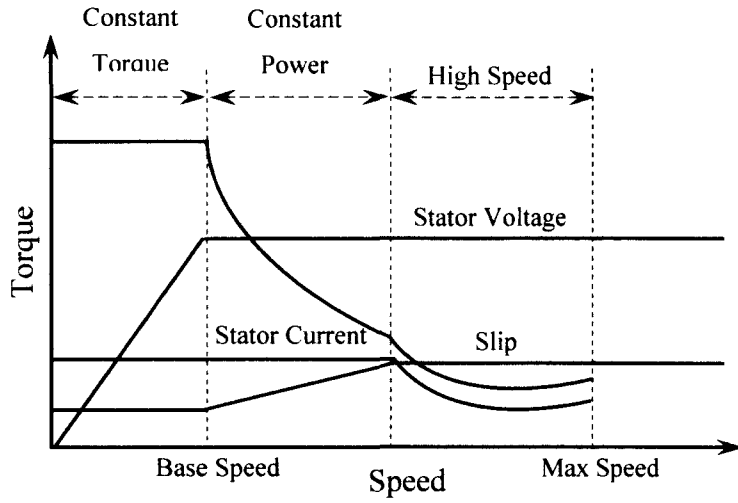


Fig. 4.7: Induction motor operation characteristics.



Fig. 4.8: Permanent magnet synchronous motor used in HEV/EV.

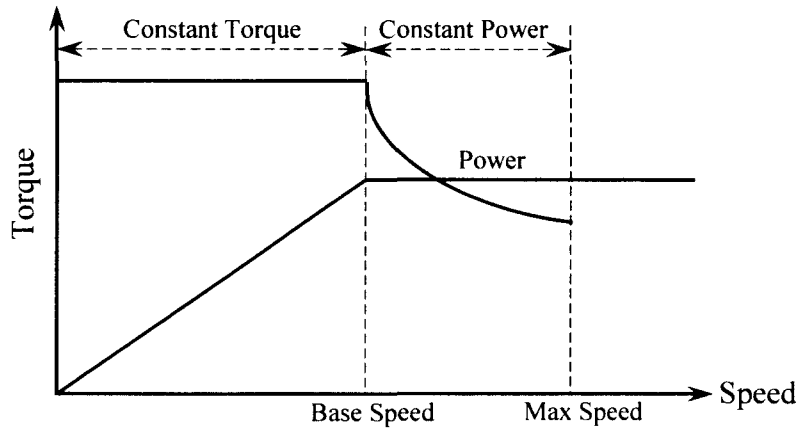


Fig. 4.9: Permanent magnet synchronous motor operation characteristics.

4.2.3 Permanent magnet synchronous motor

Currently, permanent magnet synchronous motors as shown in Fig. 4.8 are being used commercially in hybrid vehicles like Toyota Prius and Honda Insight. This is mainly due their higher power density and efficiency as compared to the induction motors. Absence of rotor windings gives PMSMs an edge over induction motors in terms of efficiency. In addition, these motors also have much lower weight and volume with efficient heat dissipations. The high power density, fast torque response and comparatively lighter weight, makes them the primary choice of leading automakers for most hybrid cars available commercially today [38], [39].

Unlike other motors, PMSMs are capable of producing three times over its base speed. The absence of field windings makes the flux weakening capability of PMSMs rather constrained, limiting their speed ranges in the constant power region. The torque-speed characteristic of PMSMs is shown in Fig. 4.9. The basic configurations of PMSM commercially available are surface mounted and inset. The major disadvantages of PMSMs are its high material cost and lack of mechanical strength to withstand large torques [18], [38], [39].

4.3 Regenerative Braking

The braking performance is one of the key features that determine the safety of the vehicle. In urban driving a significant amount of energy is lost during driving due to frequent braking, resulting in high fuel consumption. The integration of an electric drivetrain in an HEV/EV that enables the vehicle to recapture this energy during braking is one of its most significant characteristics. The electric motor serves as a generator during braking to convert kinetic energy of the vehicle into electrical energy that can be stored in the battery through a bidirectional converter. Braking energy in a typical urban driving pattern may reach up to 25% of the total traction energy [40]. Thus, the effective recovery of this energy and its conversion to electrical power by the motor has a significant impact on the fuel economy of automobiles.

Regenerative braking adds complexity to the design of braking system in the vehicle. The main concern is to distribute the total braking forces between regenerative brake and mechanical brake with maximum possible recovery of kinetic energy. At the same time,

the braking forces have to be distributed between the front and rear axles to ensure steady braking. The electric drivetrain consisting of a battery powered electric motor drive is, thus, primarily responsible in improving fuel efficiency of HEVs/EVs as compared to conventional vehicles by allowing the engine to run in its optimum efficiency region and recovering part of the braking energy. The primary objective in the development of the electric drivetrain of HEV is to select the drivetrain topology and design, size and control its drivetrain components to maximize the utilization of electric motor in the vehicle while sustaining sufficient reserves of electrical energy and maintaining the vehicle performance.

4.4 Application of Battery Modeling in Battery Management System

4.4.1 Battery Pack Modeling

There is a high probability of manufacturing variation between cells within the battery pack. This variation leads to a difference in charge and discharge characteristics of each cell. Temperature difference is a major consequence of this charge-discharge cycle variation that cumulates with time which is also influenced by ageing, number of continuous charge-discharge cycles, load demand, type of discharge and the external temperature.

This has a great impact on the state-of-health of the battery and in turn its performance. The proposed model takes into account individual cell operation along with

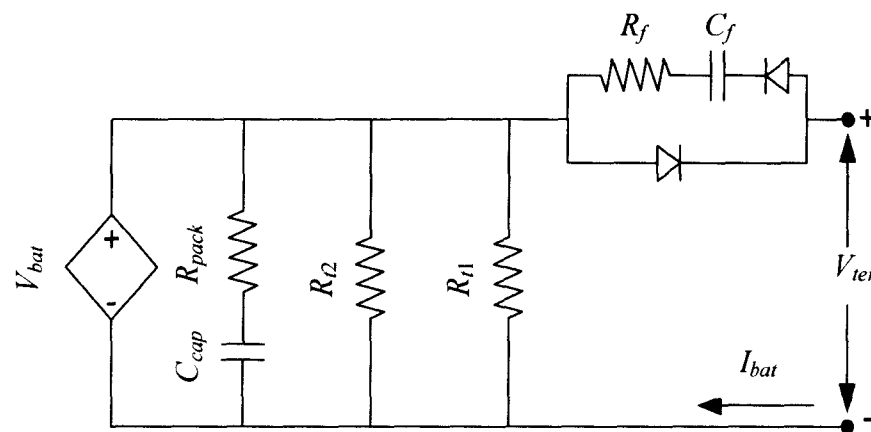


Fig. 4.10: Battery pack model.

their integration, representing the battery pack. The battery pack model is shown in Fig. 4.10. V_{bat} is the internal generated voltage of the cell. The capacitor C_{cap} and resistance R_{pack} represent the capacity and the pack internal resistance respectively. R_{t1} and R_{t2} denote resistances with positive and negative temperature coefficient respectively. R_f and C_f are filter resistance and capacitance to the incoming disturbances.

The model has been designed for Li-ion battery used in HEVs and EVs. It can also be applicable for NiMH batteries with minor modifications. It is a capacitive representation of the battery, connected across a traction motor whose applied torque determines the direction of the current. R_{ser} is the overall battery pack resistance.

4.4.2 Electric Drivetrain Modeling

DC Motor drivetrain

The HEV/EV electric drive train using a DC motor is shown in Fig. 4.11. The electric circuit model of the battery is connected across the DC machine which operates both as a motor and generator depending upon the battery terminal voltage. The battery is directly connected across the machine, as represented by the equivalent circuit shown in Figs.4.12 and 4.13 for both shunt and series configuration respectively.

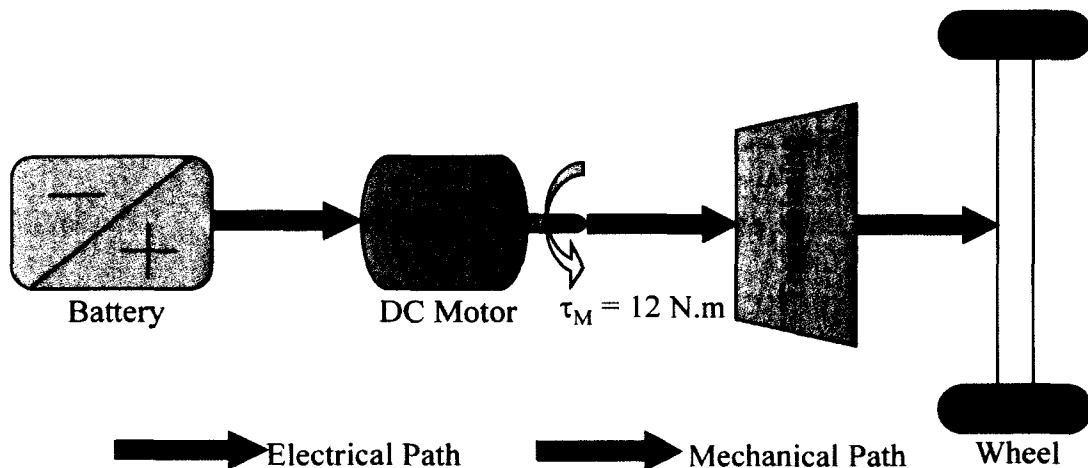


Fig. 4.11: Electric drivetrain using DC motor.

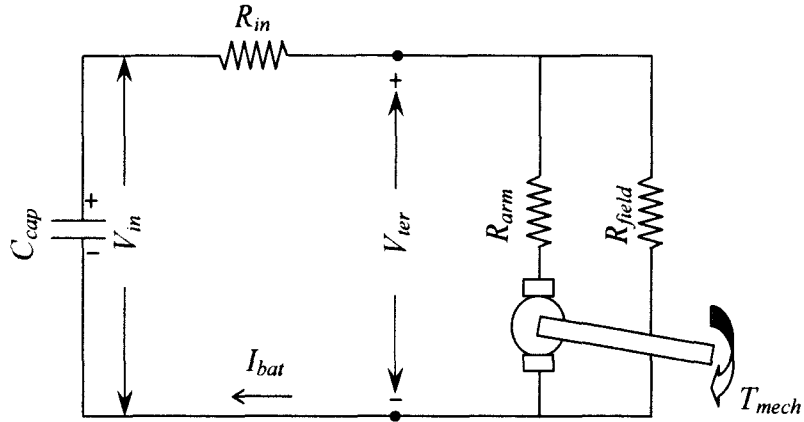


Fig. 4.12: Electric drivetrain model using DC shunt motor.

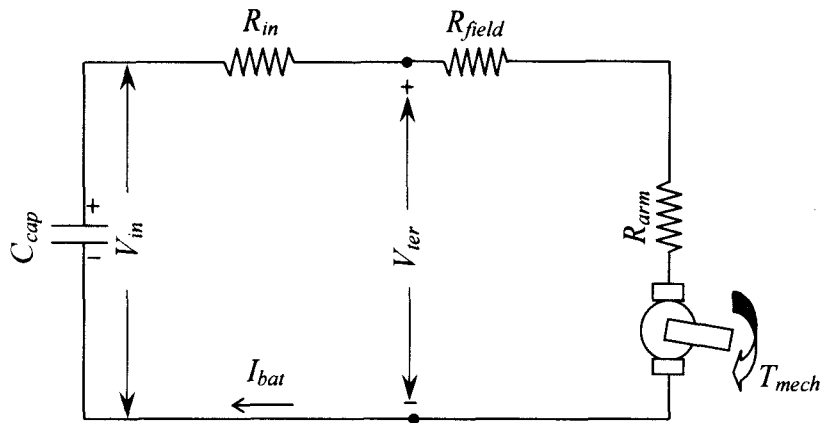


Fig. 4.13: Electric drivetrain model using DC series motor.

The mechanical torque externally applied is maintained at 12 N.m. The terminal battery voltage range is limited to a small region of 239 V in order to measure the transition time in continuous mode; as discrete mode simulation results in loss of precise information. The detail of the DC motor is shown in Table 4.1.

The equations that determine the battery SOC corresponding to the DC motor performance is given below:

$$SOC[I_{bat}, Temperature, Cycle] = SOC_0 \pm \int I_{bat} dt \quad (4.3)$$

$$V_{ter} = V_{in}[SOC, Temperature] \pm I_{bat} \times R_{in} \quad (4.4)$$

$$V_{ter} = E_a \pm I_{bat} \times R_{mac} \quad (4.5)$$

where R_{mac} is the total internal resistance of the DC machine

The electromagnetic torque developed is given by:

$$T_e = K_a \times I_{bat} \times \Phi_d \quad (4.6)$$

where K_a is the design constant and Φ_d is the flux

The power delivered is given by:

$$P_e = E_a \times I_{bat} \quad (4.7)$$

Induction Motor drivetrain

Similarly, the d-q induction motor machine equations have been used in the simulation.

The d- and q-axis stator voltage equations of the induction motor in the synchronous frame are given in (4.8) and (4.9).

$$v_{ds} = R_s i_{ds} - \omega_s \psi_{qs} + \frac{d\psi_{ds}}{dt} \quad (4.8)$$

$$v_{qs} = R_s i_{qs} - \omega_s \psi_{ds} + \frac{d\psi_{qs}}{dt} \quad (4.9)$$

And the d- and q-axis components of rotor voltage are:

$$v_{dr} = R_r i_{dr} - (\omega_s - \omega_r) \psi_{qr} + \frac{d\psi_{dr}}{dt} \quad (4.10)$$

$$v_{qr} = R_r i_{qr} + (\omega_s - \omega_r) \psi_{dr} + \frac{d\psi_{qr}}{dt} \quad (4.11)$$

The mechanical equation representing rotor speed and electromagnetic torque are given as:

$$\frac{d\omega_r}{dt} = \frac{1}{2H} (T_e - T_m) \quad (4.12)$$

$$T_e = \frac{3}{2} \frac{P}{2} L_m (i_{qs} i_{dr} - i_{ds} i_{qr}) \quad (4.13)$$

The details of squirrel cage induction machine used are shown in Table 4.2. The mechanical torque is fixed to 12 N.m at rated speed. The battery voltage is fixed to 400 V

TABLE 4.1
3.7 kW DC MACHINE PARAMETERS

Parameters	Value
Rated Power	3,730 W
Rated Speed	1,750 rpm
Rated Voltage	240V DC
Mechanical Torque	12 N.m
Armature Resistance	2.51 Ω
Armature Inductance	0.028 H
Field Resistance	281.3 Ω
Field Inductance	156 H
Total Inertia	0.002953 kg.m ²

TABLE 4.2
2.5 kW INDUCTION MACHINE PARAMETERS

Parameters	Value
Rated Power	2,238 W
Rated Speed	1,725 rpm
Rated Voltage	209 V
Mechanical Torque	12 N.m
Stator Resistance	0.435 Ω
Stator Inductance	2.2 mH
Rotor Resistance	0.816 Ω
Rotor Inductance	2 mH
Mutual Inductance	69.31 mH
Total Inertia	0.089 kg.m ²

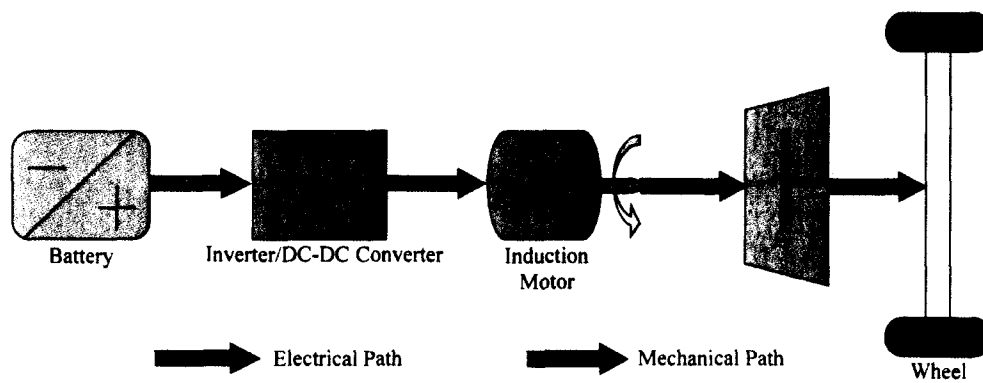


Fig. 4.14: Electric drivetrain using induction motor.

and the range of operation is limited to 399 V in order to increase the precision of transition time analysis.

4.4.3 Methodology of Battery Modeling Application

The variation in performance and characteristics of different traction motors affect the battery performance. The block diagram for the analysis of charge-discharge characteristic of the battery is shown in Fig. 4.14. The battery represents the electric circuit model shown in Fig. 3.9. The motor represents the vehicular load. The BMS represents the battery management system that controls the selection of the operating mode, depending upon the state-of-charge of the battery. The different modes of operation considered for the simulation are the motor mode and the generator mode. In motor mode, which occurs between 80% and 95% state-of-charge, the battery is supplying power to the motor, which is directly connected to the transmission. It is assumed that the battery has the capacity to meet the motor's full power demand. In generator mode, as represented by Gen Mode in Fig. 4.15 either the motor that behaves like a generator during regenerative braking or the generator connected to the ICE, charges the battery once its state-of-charge goes below 80%.

The internal resistance of the battery is considered constant along the charge-discharge cycles. The initial state-of-charge of the battery is assumed to be 100%, and the effect of temperature on the internal resistance is neglected.

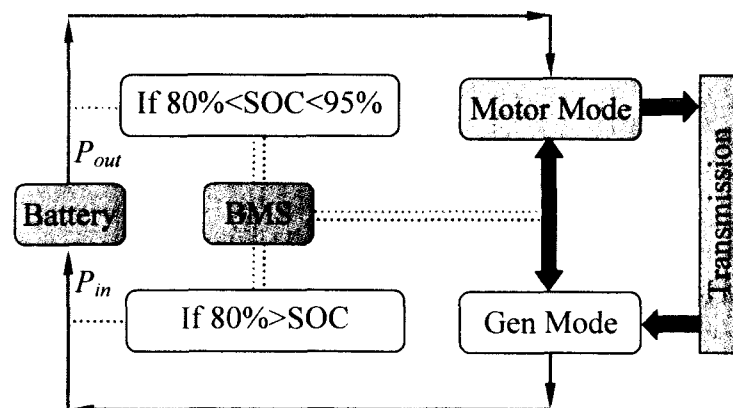


Fig. 4. 15: Modeling control scheme.

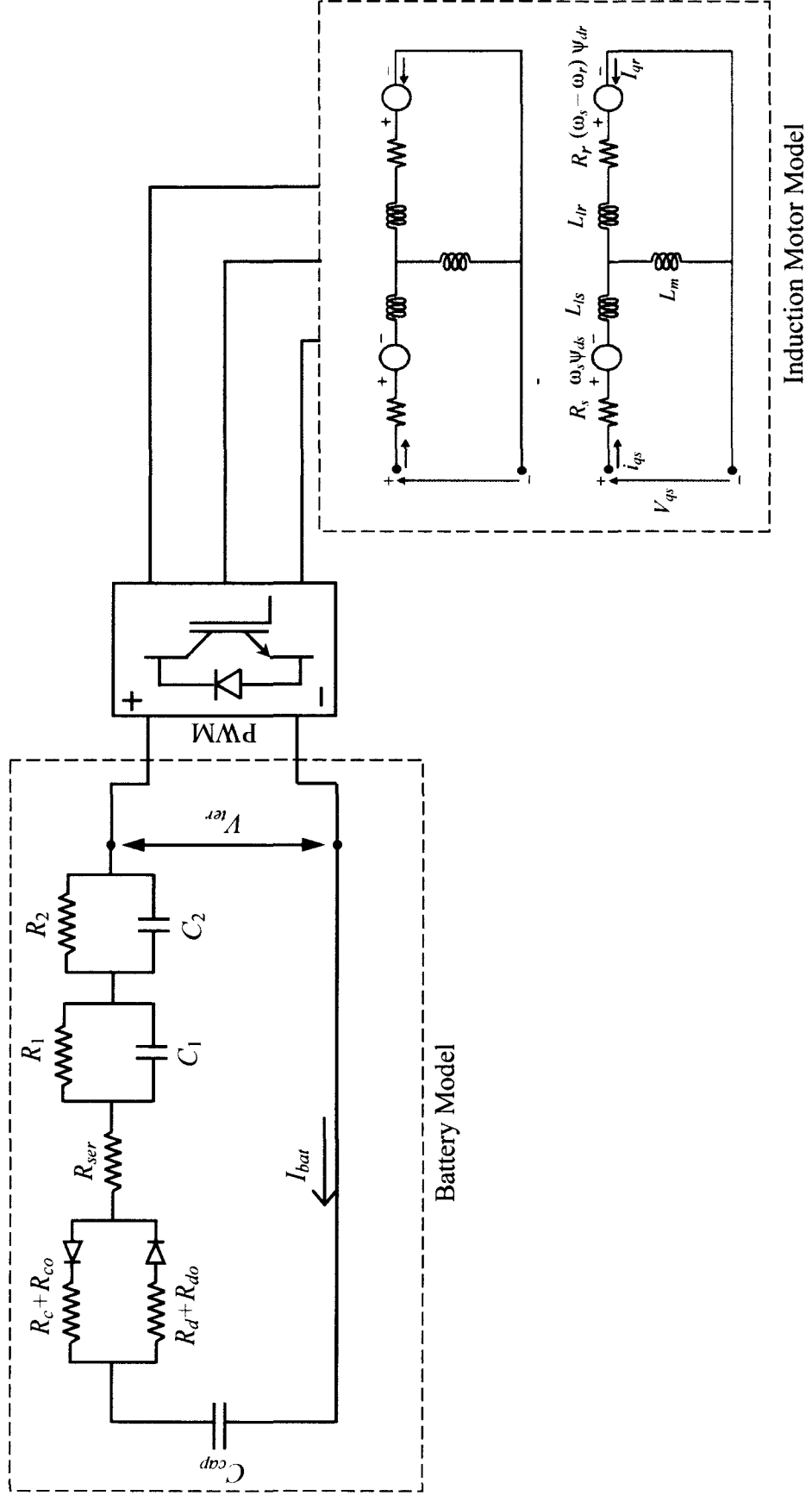


Fig. 4. 16: Circuit model used for EV drivetrain simulation.

The influence of different starting characteristics and efficient operating regions of every motor as reflected in the corresponding battery discharge curves is analyzed in addition to the variation in transition time of the motor to generator mode interchange.

4.4.4 Result and Analysis of Battery Modeling Application

The mechanical torque externally applied is maintained at 12 N.m. Fig. 4.17 shows the change in DC electromagnetic torque. Fig 4.18 depicts the corresponding battery charge-discharge. The extent of this decrease is dependent on the property of the DC machine. It is after 0.07 seconds that the armature current effectively starts the charging of battery, although the rated charge is achieved after 0.3 seconds as shown in Fig. 4.19. It shows that the effective charging of the battery initiates when the battery voltage reaches 238.993 V as shown in Fig. 4.20. The starting electromagnetic torque for IM is higher as shown in Fig. 4.21, thus meeting the HEV traction requisites. The higher initial torque results in increased voltage loss as shown in Fig. 4.22. The voltage drop for 12 N.m torque is less than that of DC machine, indicating higher efficiency. Figs. 4.23 and 4.24 correlate the charging and discharging profile of the battery. It takes 0.12 seconds to initiate the effective charging of battery.

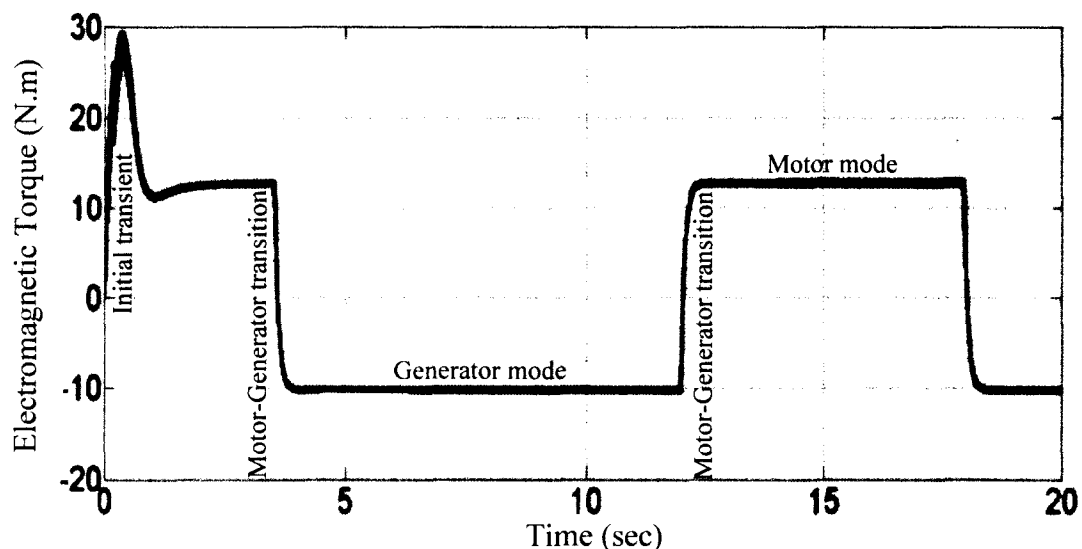


Fig. 4. 17: Electromagnetic torque analysis of DC motor.

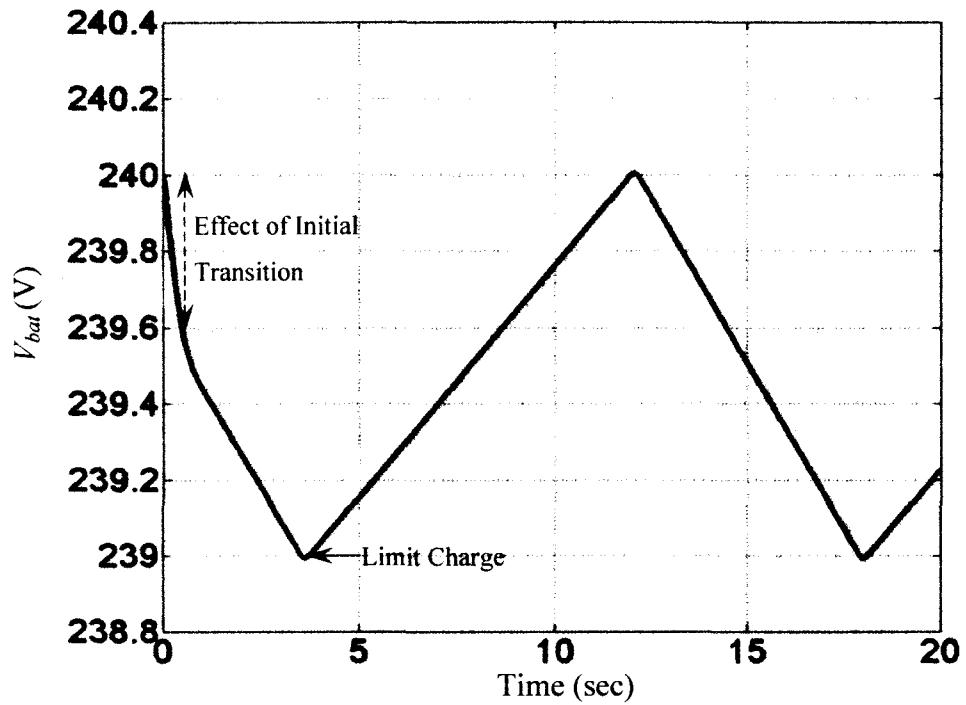


Fig. 4. 18: Battery charge-discharge across DC motor.

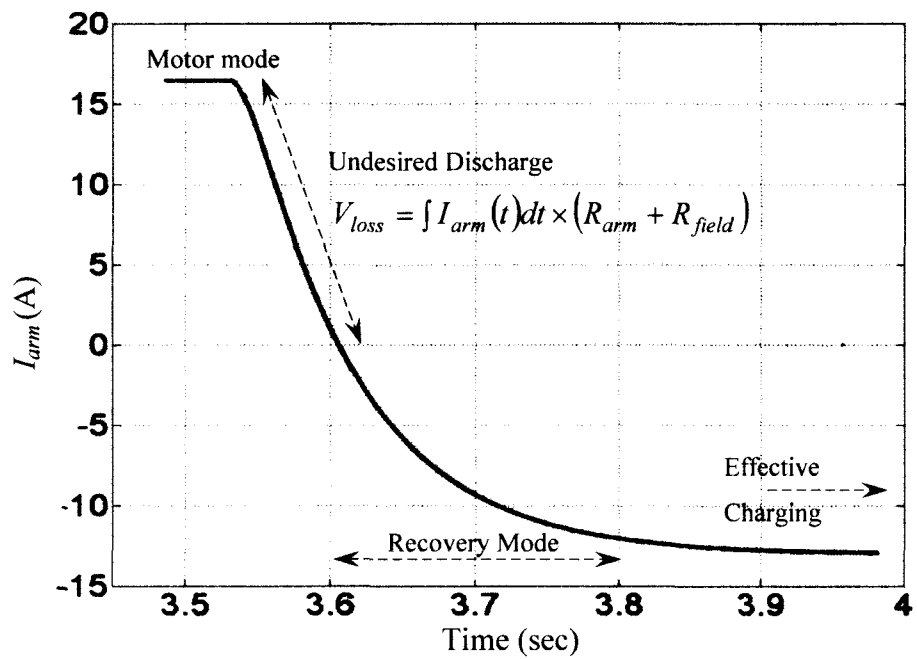


Fig. 4. 19: Result of torque on the battery charge-discharge current.

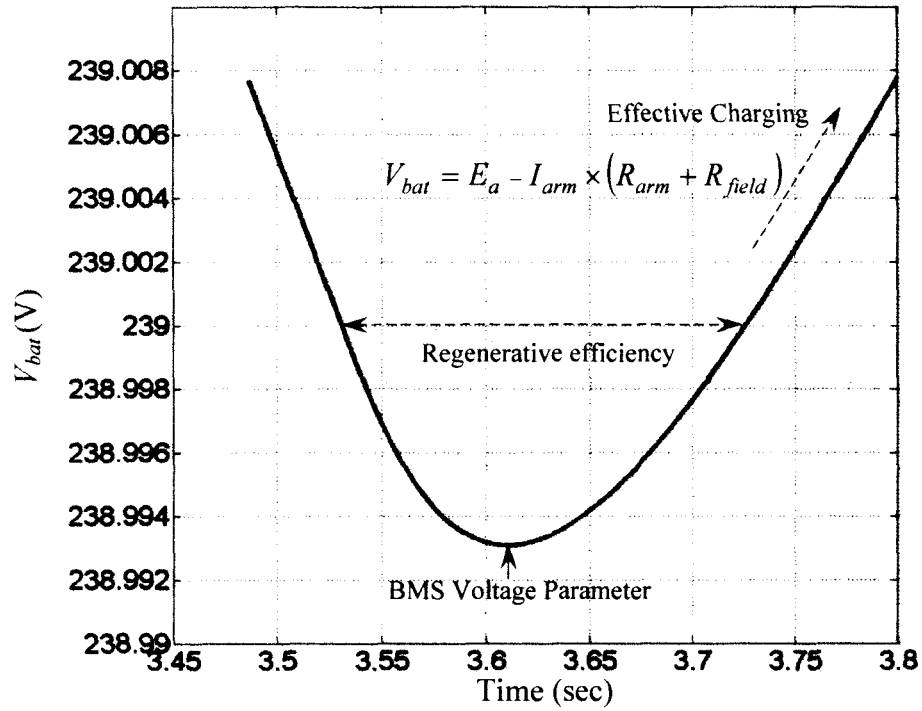


Fig. 4. 20: Location of BMS voltage parameter for DC motor.

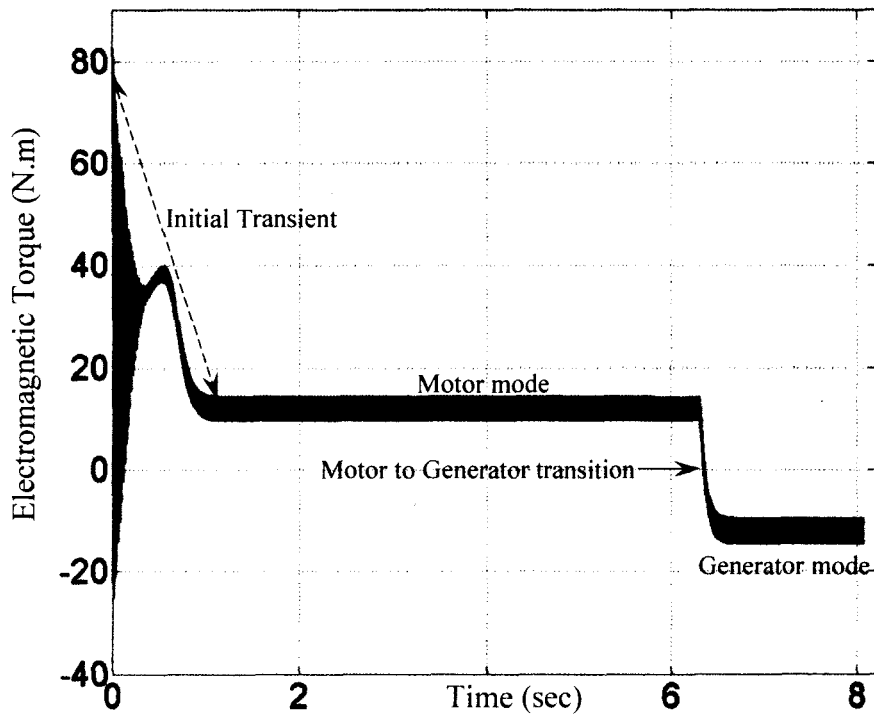


Fig. 4. 21: Electromagnetic torque of induction motor.

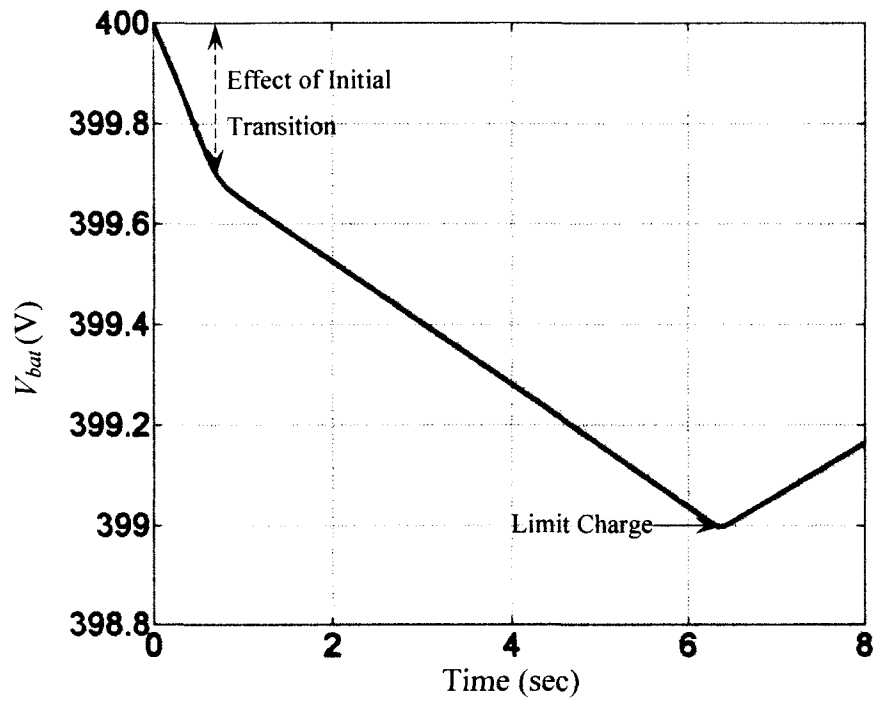


Fig. 4. 22: Battery charge-discharge characteristics across induction motor.

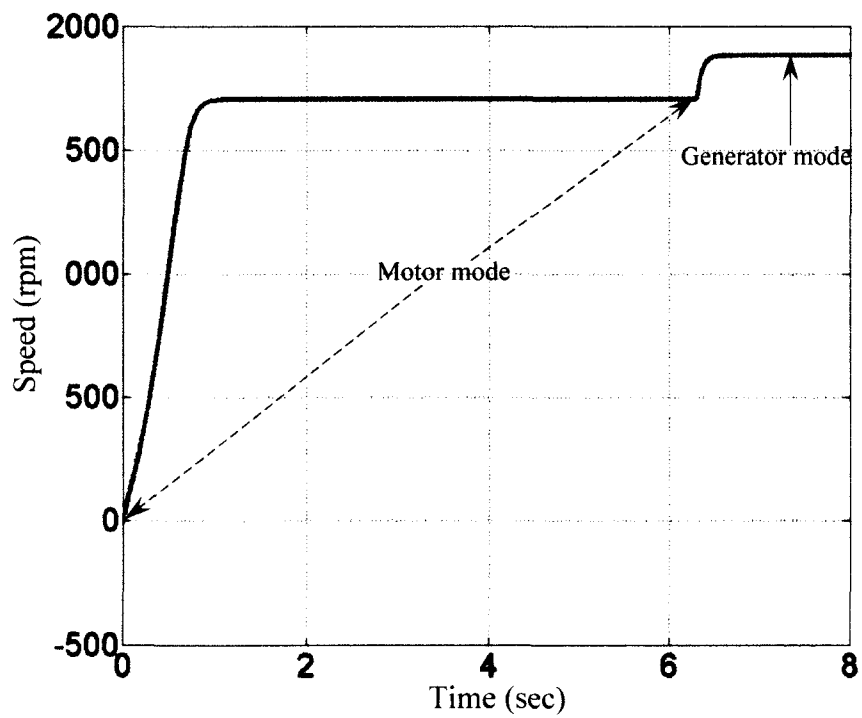


Fig. 4. 23: Induction motor speed variation for motor and generator mode.

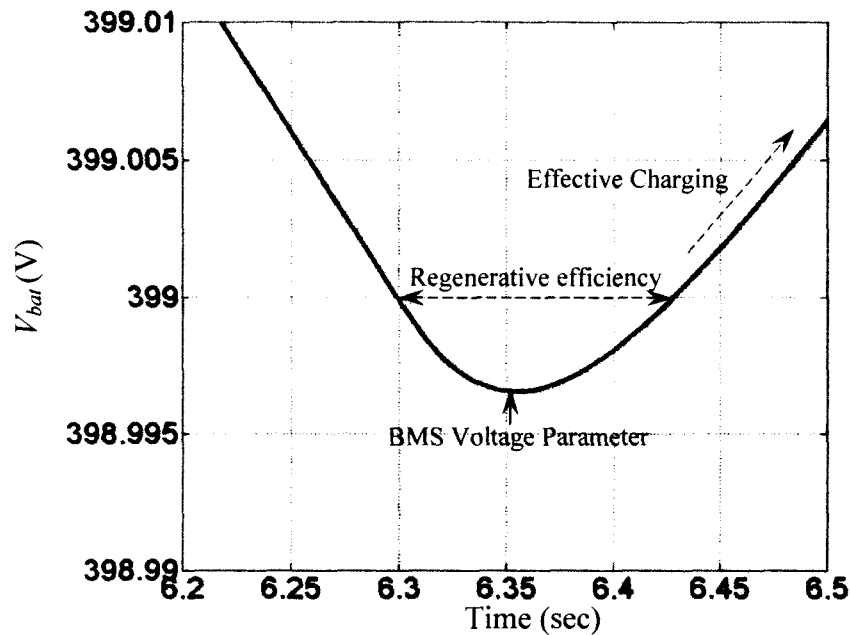


Fig. 4. 24: Motor-generator transition mode analysis for induction motor.

4.5 Summary

This research has a twofold motivation. It is the real-time implementation of the battery electric circuit model which tests the performance of other electrical equipment connected across it. The starting characteristics and operation of every motor is different which has a considerable effect on the battery performance. The simulations infer that the battery continues to remain in its state of charge or discharge even after introducing change in the operating mode. For battery chemistries like Li-ion, which are extremely sensitive to overcharge and over-discharge, this simulation will render accurate limiting values for BMS operation, increasing its sensitivity and precision. The study is performed on the two most mature and widely used motor technologies. During HEV or EV operation, regenerative braking is an essential phenomenon that conserves a considerable amount of energy. This phenomenon lasts for a fraction of second and the efficiency of the motor accounts for the amount of energy saved. This analysis of battery charge-discharge variation with respect to the traction motor determines the efficiency of the motor-generator transition. The lower transition time indicates higher conservation of energy, accounting for a higher fuel efficiency of the vehicle.

4.6 Research Significance

As mentioned, this chapter focuses on analyzing the application of battery modeling for the improvement of battery performance and efficiency. It can be applied to find the precise battery management parameters. For conventional vehicles, braking results in the loss of 40% of the developed power. Thus, a considerable improvement in fuel efficiency can be attained by efficient regenerative braking. The battery models which had been limited to state-of-charge determination can be widely applied for electric drivetrain simulation and component analysis. The design of electric drivetrain components can also be optimized by the developed models. This simulation and modeling can be used by the present automotive industry to developing efficient electric drivetrains.

5 TRANSIENT PROTECTION OF BATTERY BY USING MULTIPLE SOURCES

The automotive sector is currently focused on developing electric vehicles that completely replace the internal combustion engine with a series of high charge sustaining batteries as the sole power source. The battery has an optimum energy and power density and experiences transients when subjected to varying drivers need. These undesirable stresses have a considerable affect on its performance and life. This leads to the initiation of research on the design and implementation of ultracapacitors in conjunction with batteries, distributing the vehicular power demand. Unlike batteries, ultracapacitors have very high power density, low energy density and the ability to undergo over a million duty cycles [5], [41], [42].

Moreover, it has a very high rate of charge acceptance making it ideal for short transition high loads and regenerative braking [43]-[45]. Thus, the optimal distribution of vehicular power demand between the battery and ultra-capacitor can prevent the undesired current surges, prolonging the life and enhancing its performance. It is a twofold research, initiated by the precise location of transients followed by the power distribution scheme and control. The determination of transient is an important criterion that accounts for the drivetrain efficiency. Wavelet based analysis have gained popularity due to its accurate transients tracking ability [46]-[50]. This paper presents an optimal power distribution between the battery and super-capacitor using discrete wavelet transformation theory. The super-capacitor provides power during sudden transients, thus protecting the battery.

5.1 Wavelet Theory

A wavelet is a mathematical function used to divide a given function or continuous-time signal into different scale components, assigning a frequency range to each scale component. Wavelets not only dissect signals into their component frequencies but also vary the scale at which the component frequencies are analyzed. Therefore wavelets, as component pieces used to analyze a signal, are limited in space [46], [47].

A wavelet transform (WT) is the representation of a function by wavelets. The wavelets are scaled and translated copies (known as "daughter wavelets") of a finite-

length or fast-decaying oscillating waveform (known as the "mother wavelet") [43], [44]. It can be broadly classified into continuous and discrete wavelets.

5.1.1 Continuous Wavelet Transform

The continuous wavelets, represented on a frequency band of the form $[f, 2f]$ for all positive frequencies $[f > 0]$ are scaled by factor 1. The subspace is generally obtained by shifting the mother wavelet. The subspace of scale 'a' or frequency band $[1/a, 2/a]$ is generated by the functions:

$$\Psi_{a,b}(t) = \frac{1}{\sqrt{a}} \Psi\left(\frac{t-b}{a}\right) \quad (5.1)$$

where 'a' is the scale factor, 'b' denotes the shift factor and $\Psi_{a,b}(t)$ is defined as the mother wavelet.

5.1.2 Discrete wavelet transform

The continuous wavelets are converted into discrete domain for real-time implementation. One such system is the affine system for real parameters $a > 1, b > 0$. The corresponding discrete subset of the half-plane consists all the points $(a^m, na^m b)$ with integers $m, n \in \mathbb{Z}$. Here, \mathbb{Z} represents a set of integer numbers. The corresponding *mother wavelet* is given as:

$$\Psi_{m,n}(t) = a^{-m/2} \Psi(a^{-m}t - nb) \quad (5.2)$$

A sufficient condition for the reconstruction of any signal x of finite energy is given by:

$$x(t) = \sum \sum (x, \Psi_{m,n}) \Psi_{m,n}(t) \quad (5.3)$$

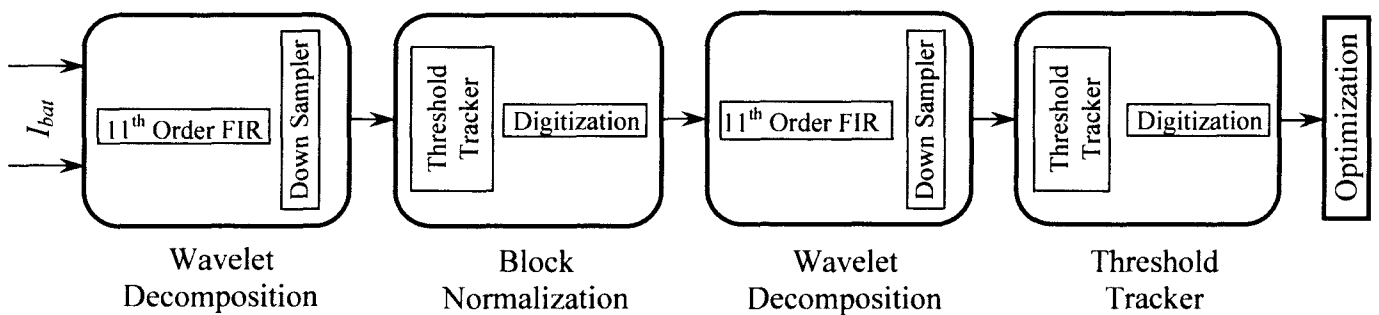


Fig. 5.1: Transient detection using wavelet decomposition.

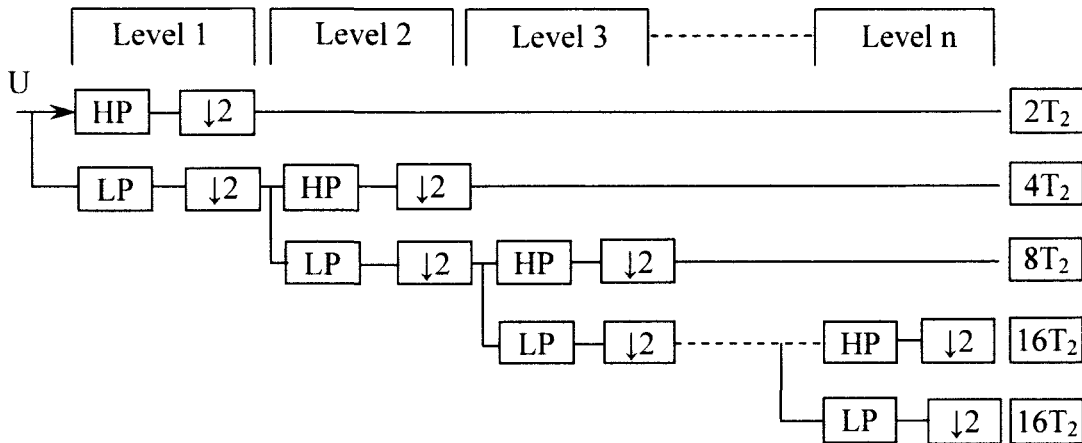


Fig. 5.2: n -level asymmetric filter bank analysis.

where $m, n \in \mathbb{Z}$ and $\Psi_{m,n}$ is the discrete mother wavelet respectively. The discrete wavelet transform (DWT) is defined as:

$$DWT(m,n) = 2^{-m/2} \sum \sum x(n) \psi \frac{t - n2^m}{2^m} \quad (5.4)$$

5.2 Ultracapacitor and Battery Combination

The high power density and charge acceptance capability of the ultracapacitor can be used as an energy delivery and recovery device (as shown in Fig. 5.3) in order to maximize the battery and overall efficiency. The most common architectures for the capacitor and battery combination are: (a) parallel battery and capacitor and (b) capacitor with independent power processor [5].

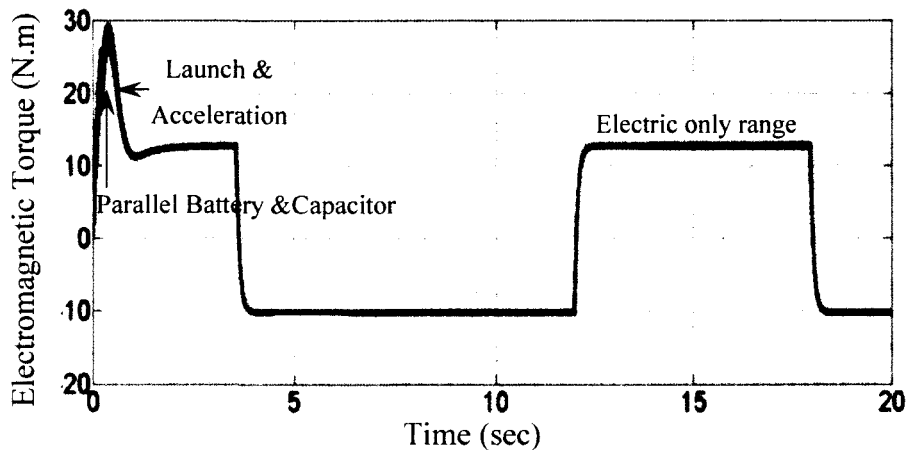


Fig. 5.3: Vehicular power distribution with time.

5.3 Methodology

5.3.1 Transient detection using wavelet decomposition

This methodology implements two level of wavelet decomposition in order to extract transient in formation. Wavelet analysis is efficient in tracking transients occurring in any signal or data. I_{bat} signal is passed through an 11th order low pass filter in order to localize transients of specific frequency. Current study implemented 10 kHz stop band and 8 kHz cutoff frequency. The filter output is passed through the transient tracker to produce a control signal for Power Optimization Unit. Filtered signal is decomposed with a Wavelet Decomposition Block which consists of a filter-bank.

A filter-bank is an array of band-pass filters that separates the input signal into several components, each one carrying a single frequency sub-band of the original signal. It also is desirable to design the filter bank in such a way that sub-bands can be recombined to recover the original signal. The first process is called analysis, while the second is called synthesis. The output of analysis is referred to as a sub-band signal with as many sub-bands as there are filters in the filter bank. The filter-bank serves to isolate different frequency components in a signal. Using filter-bank, an input signal (discrete) $x[n]$ is decomposed as

$$y_{high}[k] = \sum_n x[n] \times g[2k - n] \quad (5.5)$$

where $y_{high}[k]$ is the output of the high-pass filter at a given level after sub-sampling by 2. There are mainly two ways to implement this array of filters. One is called asymmetric and the other is symmetric.

Both ideas can be used to decompose (analyze) and reconstruct (synthesize) the original signal. The asymmetric structure decomposes only the low-frequency output from each level, while the symmetric structure decomposes the high- and low-frequency sub-bands output from each level [45]. Daubechies wavelets are widely used in solving a broad range of problems. In general, the Daubechies wavelets are chosen to have the highest number A of vanishing moments, (this does not imply the best smoothness) for given support width $N=2A$, and among the 2^{A-1} possible solutions the one is chosen whose scaling filter has external phase [44]. Db 6 mother wavelet was used for this study. Level 1 filter was used and high frequency details were utilized for the analysis.

Table 5.1 shows high frequency finite impulse response filter coefficients. High frequency details were checked for a specified threshold which produces digital high once detected and digital low otherwise. Digital normalized signal is obtained from the high frequency details to isolate the dominant details in order to analyze signal. The normalized signal produced from the Normalization Block is passed through another Wavelet Decomposition Block to identify the high frequency details from the normalized signal. High frequency details were then passed through a Threshold Tracker to identify transient zone. A digital output is produced to provide signal to the Power Optimization Unit.

5.3.2 Control Scheme for Source Optimization

The transient detection is followed by source optimization method. The optimization unit provides digitized information to the power control unit as shown in Fig. 5.5. This power control unit then distributes the vehicular power demand between the battery and super-capacitor in accordance with their individual state-of charge and operating condition. The battery maintains a constant discharge rate as long as the super-capacitor has sufficient charge to meet the transient power demand.

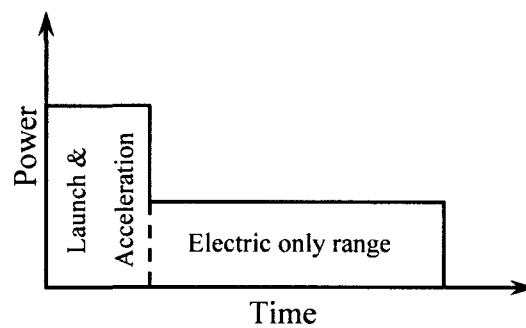


Fig. 5.4: Energy storage requirements.

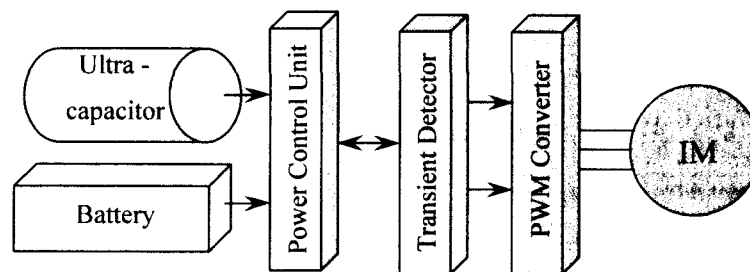


Fig. 5.5: Energy storage control architecture.

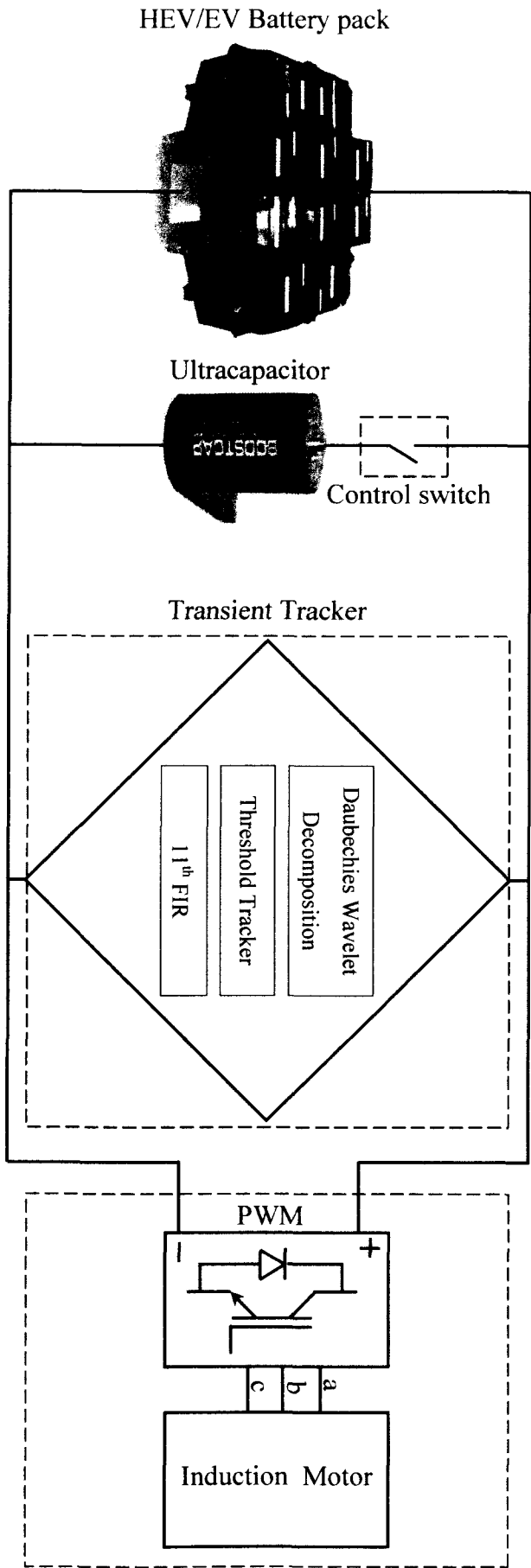


Fig. 5.6: Parallel battery and ultracapacitor operation.

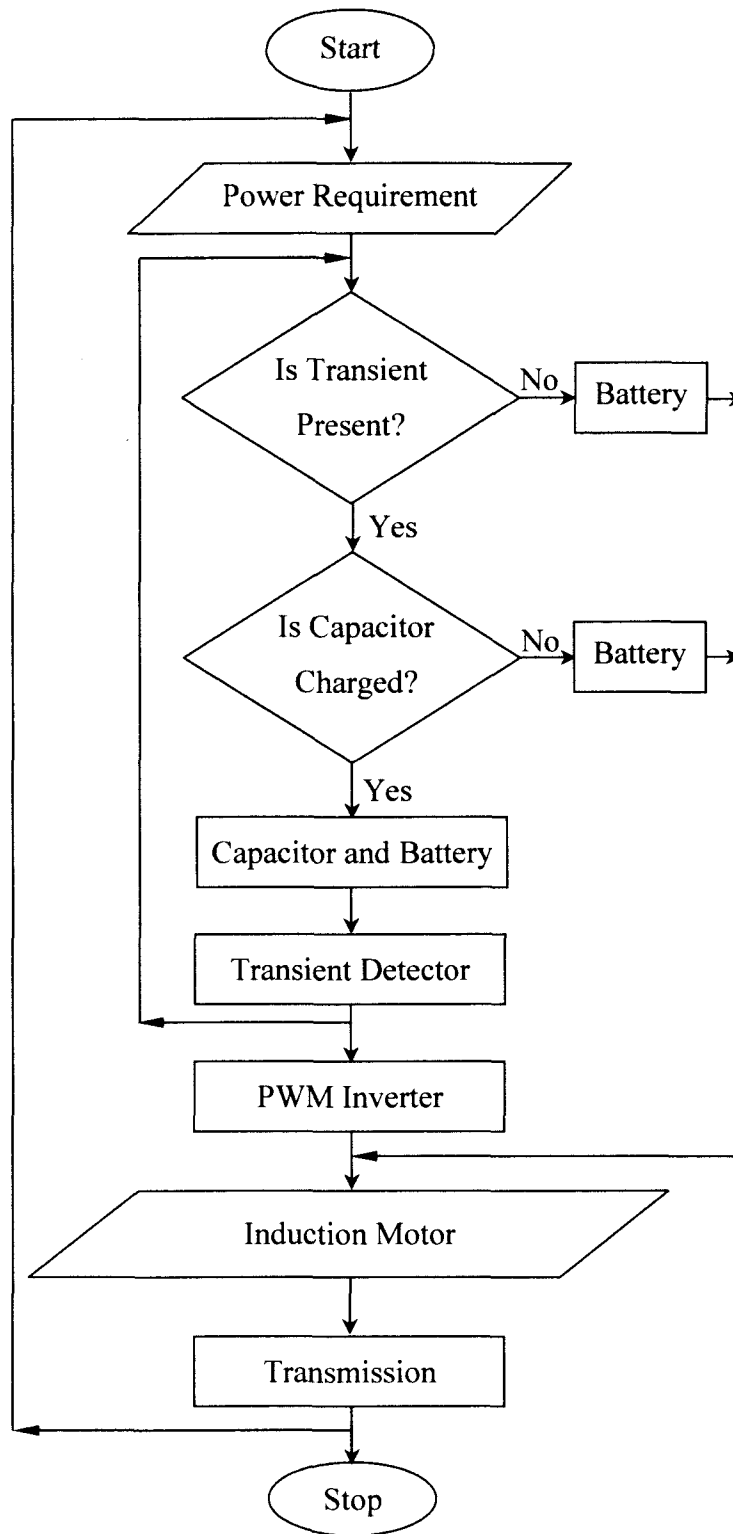


Fig. 5.7: Flowchart of the control scheme.

The initial state of charge of battery and super-capacitor is assumed to be 100%. The power distribution modes are:

1. Battery-Capacitor mode

This mode persists when the super-capacitor is fully charged and a transient is traced. The battery has constant discharge, thus protected against sudden current surges. It also extends the battery cycle time and in turn the life span. During regenerative braking, the ultracapacitors is charged first due to its high charge acceptance rate. This maximizes the brake energy utilization factor, enhancing the vehicular performance.

2. Battery mode

This mode takes place when a steady state is attained or the super-capacitor has no charge to meet the required vehicular power demand. The battery mode is initiated when the transient detector traces stability for 250 consecutive samples.

5.4 Results

The simulation conducted on Matlab/Simulink model is represented in Fig. 5.6 and the control flowchart in Fig. 5.7. The high pass finite impulse response filter coefficients as used in the simulation is mentioned in Table 5.1. The induction motor parameters considered in the simulation are given in Table 5.2.

TABLE 5.1
HIGH PASS FIR COEFFICIENTS

Order	Coefficients
h0	-0.1115407434
h1	0.4946238904
h2	-0.7511339080
h3	0.3152503517
h4	0.2262646940
h5	-0.1297668676
h6	-0.0975016056
h7	0.0275228655
h8	0.0315820393
h9	0.0005538422
h10	-0.0047772575
h11	-0.0010773011

The battery has a nominal voltage of 400V while the individual super-capacitor rating is fixed at 2700 μ F, 100V. A super-capacitor bank, consisting of 20 similar rated capacitors, is considered to power the transient loads.

TABLE 5.2
INDUCTION MOTOR PARAMETERS

Parameters	Value
Rated Power	2,238 W
Rated Speed	1,725 rpm
Rated Voltage	209 V
Mechanical Torque	12 N.m
Stator Resistance	0.435 Ω
Stator Inductance	2.2 mH
Rotor Resistance	0.816 Ω
Rotor Inductance	2 mH
Mutual Inductance	69.31 mH
Total Inertia	0.089 kg.m ²

5.4.1 Transient Detection Using Wavelet Decomposition

The load current profile is shown in Fig. 5.8 which is fed for transient analysis to the Wavelet Decomposition Block. Fig. 5.9 shows high frequency details from the Wavelet Decomposition Block. It can be observed that there exists a considerable amount of transients, due to the use of pulse width modulation to run the induction motor. In order

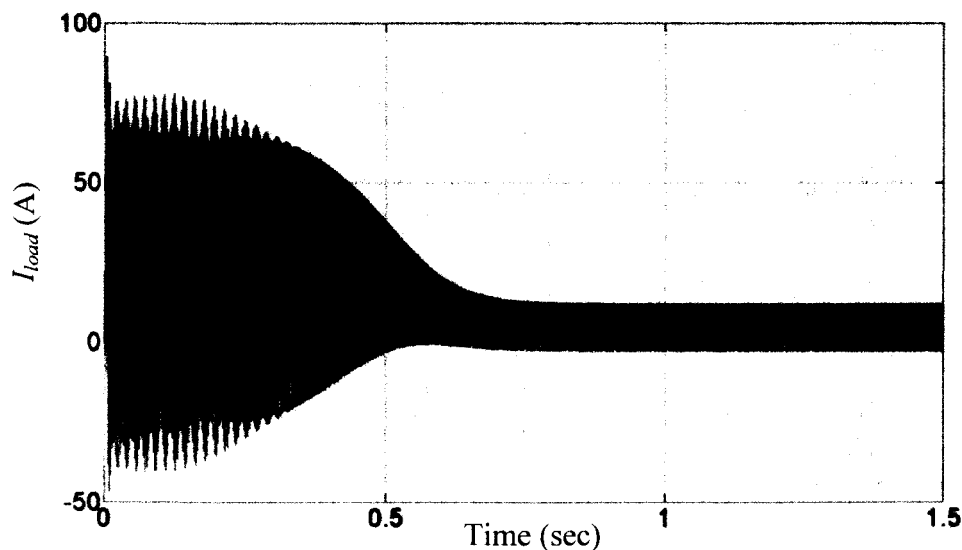


Fig. 5.8: Load current profile.

to extract useful information the signal has to be normalized based on dominant transients. The threshold is specified and a digital signal is obtained by through the Normalization Block, Fig. 5.10 shows the resulting normalized transient details. The resultant signal is passed through another wavelet decomposition block to extract high frequency details as shown in Fig. 5.11. The signal is passed through a transient tracker to generate a digital signal for the Power Optimization Unit. Fig. 5.12 shows the digital control signal from the Transient Detection Unit.

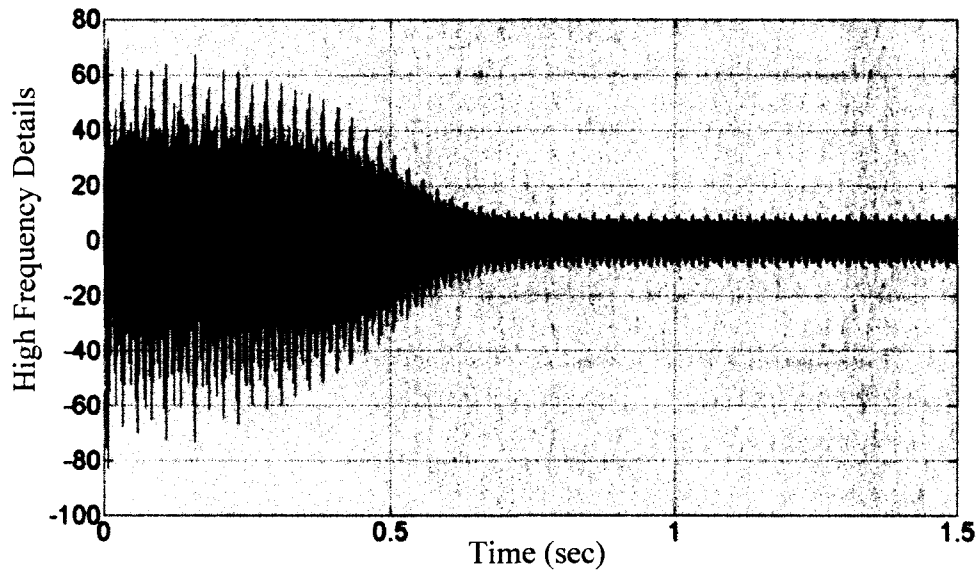


Fig. 5.9: High frequency details-level 1.

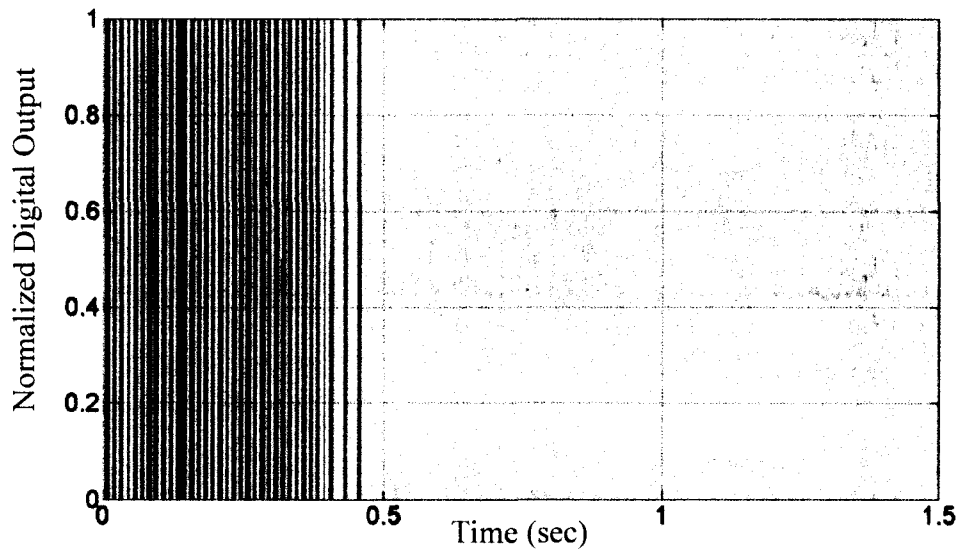


Fig. 5.10: Normalized digital output.

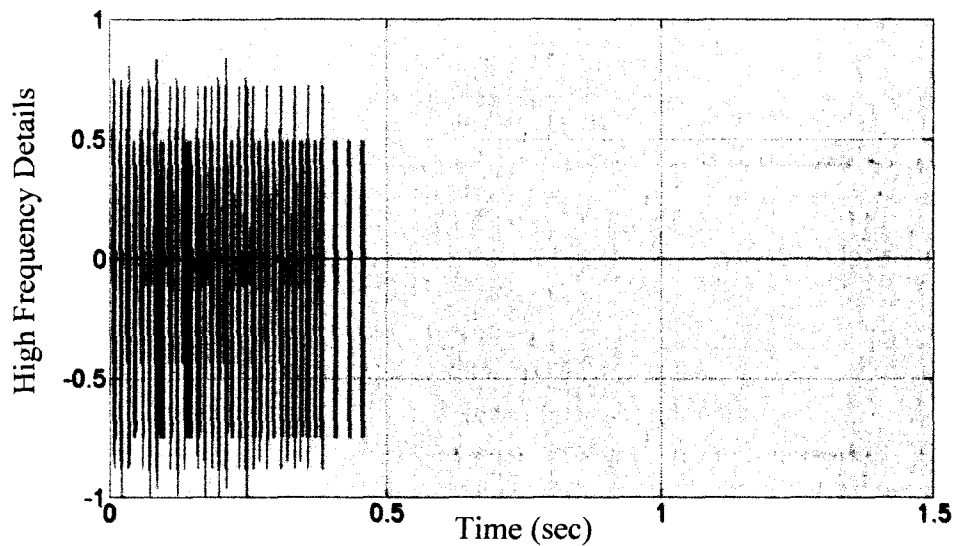


Fig. 5.11: High frequency details-level 2.

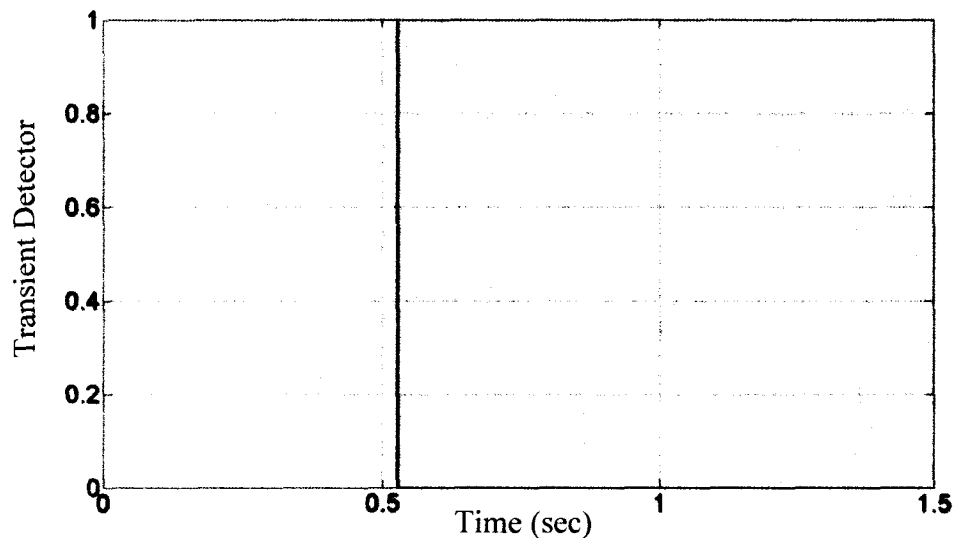


Fig. 5.12: Transient detector output.

5.4.2 Power Optimization

The electromagnetic torque production of induction motor is shown in Fig. 5.13. The current profile is in complete accordance with the torque produced. It is assumed that the IM is operated at constant torque. As the capacitor is assumed to be fully charged, it starts providing the excess current in order to meet the transient. This is battery and capacitor mode. At 0.55 sec, the torque tends to stabilize along with the current to a limit which the battery can withstand without any external stress. The capacitor current profile as shown in Fig. 5.14, corresponds to the transient detectors output. The super-capacitor discharge is shown in Fig. 5.15. The ultracapacitor has a very low energy density, thus discharging

in 0.55 sec, leading to the battery mode. The charge retention of super-capacitor can be extended by operating the battery at a high discharge rate. The discharge rate of the battery is fixed according to the stable operating region.

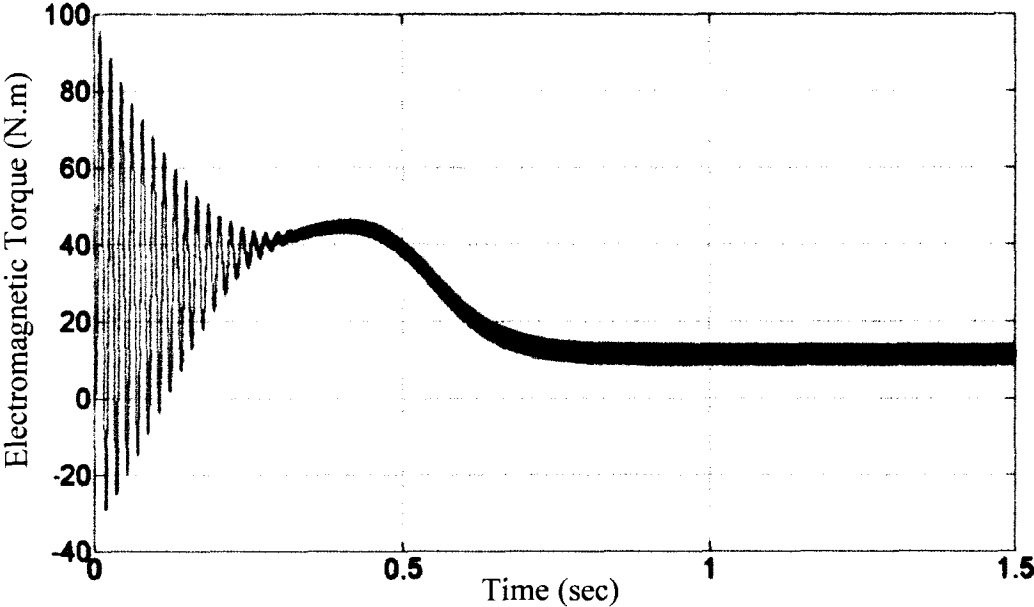


Fig. 5.13: Initial transients of the torque output of IM.

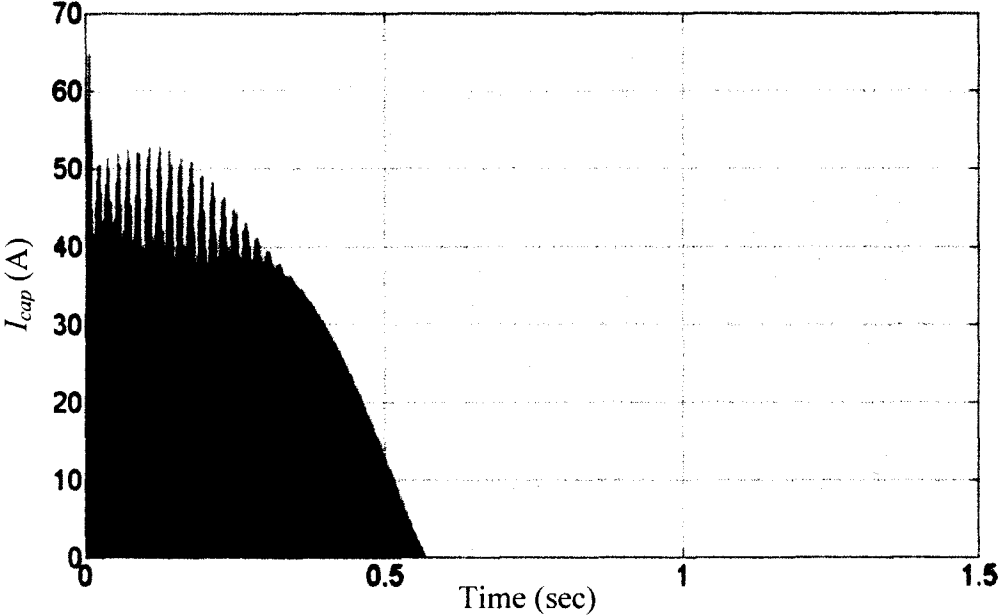


Fig. 5.14: Ultracapacitor current variation in accordance with the torque production.

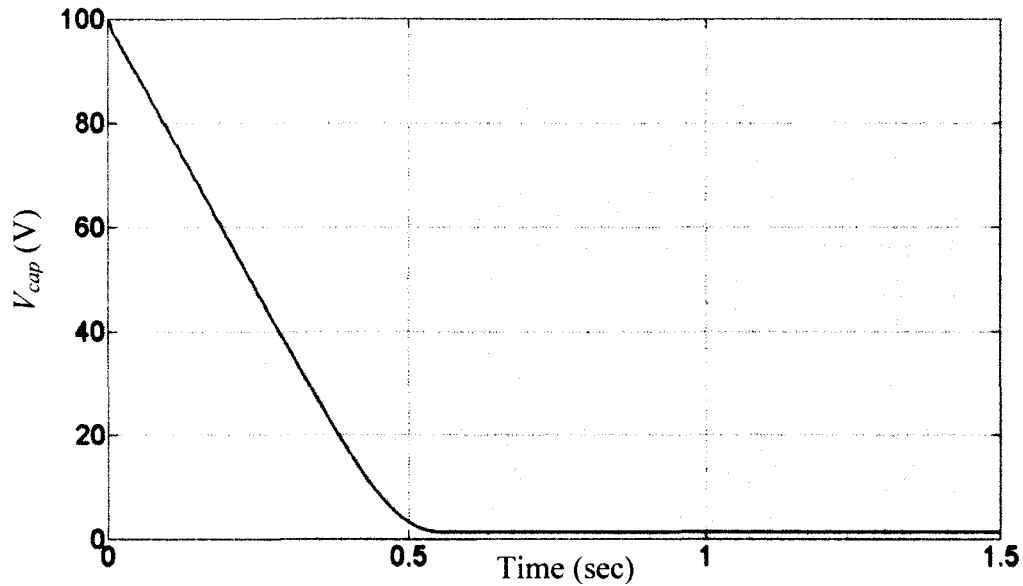


Fig. 5.15: Ultracapacitor voltage profile.

5.5 Summary

The ultra capacitor is used only to meet the initial transient of the motor. The application has been limited to launch mode, while the battery is used in the both launch and electric range operation. The capacitor is discharged within the initial 0.5 sec supplying the extra power during the launch and acceleration mode. In parallel battery-capacitor mode, the ultracapacitors are delivering the peak power as the battery cannot respond as quickly as the capacitor.

5.6 Research Significance

The commercial popularity of electric vehicle is directly dependent on the driving range, charging easiness and operational cost. Unlike a single battery, the usage of multiple sources can enhance the performance and lower the operational cost. The cost to performance ratio makes the ultracapacitor appropriate as the power supplementing device of battery. The use of wavelet transient detection method increases the power distribution accuracy and overall drivetrain efficiency. This application of wavelet theory in the field of vehicular technology has been a unique approach to render improved control mechanism. The power distribution scheme protects the battery from transients, extends the drive range, and the cycle and life time of the battery.

6 CONCLUSIONS AND FUTURE WORK

6.1 Conclusions

The rapid depletion of fossil fuels due to the increasing petroleum demand by on-road transportation has led to the search for alternative means of transport. The concerns over global warming and economic instability have alarmed the governments, resulting in an increased demand for electrification of the conventional vehicular drive train. Hybrid electric vehicles and electric vehicles that offer a suitable solution as an environment-friendly and sustainable transportation have been thus successfully launched commercially by many of the leading automakers. The major constraint that is posing a hindrance to its commercial popularity in terms of cost and performance is the battery.

This thesis analyses the battery operation in complete accordance with the present technological advancements and vehicular requisites from an electrical standpoint. The research findings that have great significance in determining and analyzing the performance of batteries are summarized below:

- The battery is a crucial component of the electric drivetrain that determines the overall vehicular efficiency and fuel reduction. Thus, the battery operation needs to be illustrated accurately in order to optimize and maximize the efficiency. Modeling of the battery is the best solution for this characteristics analysis.
- The electric circuit model proposed takes into consideration the important temperature criterion. It can be successfully applied to analyze the characteristics of different battery chemistries used in the electric drivetrain.
- The electric circuit models developed for battery operations illustration can be used effectively to determine the battery optimization parameters. It can be used to complete the modeling of the electric drivetrain composed of traction motors and power electronic devices.
- The variation in drivetrain components brings a change in the drivetrain performance and the battery optimization parameters. The simulation conducted with different traction motors justified the importance of considering the assisting components while designing the battery management system.

- The battery and ultra capacitor parallel mode operation using the wavelet transient detection had been a novel application in the area of vehicular technology. The initial transients and extra power demand for launch and acceleration of the vehicle was met by the ultracapacitors, thus protecting the battery from any undesired stress.

6.2 Future Work

There are still a lot of challenges in the area of battery technology that needs to be addressed in order to achieve commercial success. The work presented in this thesis can be further progressed as follows:

- The battery models in addition to the electric drivetrain components can be used to determine the loss occurring across every electrical component.
- Mathematical modeling of the electric drivetrain on the basis of the electric models.
- The battery model can be applied across permanent magnet synchronous motors to validate its performance.
- The battery ultracapacitor combination can be used to improve regenerative braking efficiency and improve the drivetrain components performance.

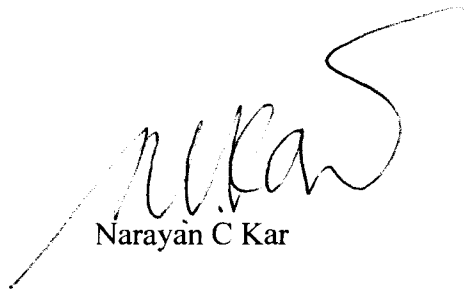
APPENDIX A LIST OF PUBLICATIONS

- [1] C. Sen, Y. Usama and N. C. Kar, "Electric Vehicle Multiple Source Optimization Using Wavelet Theory Transient Detection," *Submitted at the IEEE International Symposium on Industrial Electronics*, June, 2010.
- [2] C. Sen and N. C. Kar, "Analysis of the Battery Performance in Hybrid Electric Vehicle for Different Traction Motors," *IEEE 7th Annual Electrical Power Conference, October, 2009*.
- [3] C. Sen and N. C. Kar, "Battery Pack Modeling for the Analysis of Battery Management System of a Hybrid Electric Vehicle," *IEEE Vehicle Power and Propulsion Conference*, September 2009.
- [4] C. Sen and N. C. Kar, "Analysis of a Novel Battery Model to Illustrate the Instantaneous Voltage for Hybrid Electric Vehicle," *24th International Battery, Hybrid and Fuel Cell Electric Vehicle Symposium and Exposition*, May 2009.

APPENDIX B COPYRIGHT RELEASE

Mr. Chitradeep Sen is authorized to use the following publications in this thesis.

- [1] C. Sen and N. C. Kar, "Analysis of the Battery Performance in Hybrid Electric Vehicle for Different Traction Motors," *IEEE 7th Annual Electrical Power Conference*, October, 2009.
- [2] C. Sen and N. C. Kar, "Battery Pack Modeling for the Analysis of Battery Management System of a Hybrid Electric Vehicle," *IEEE Vehicle Power and Propulsion Conference*, September 2009.
- [3] C. Sen and N. C. Kar, "Analysis of a Novel Battery Model to Illustrate the Instantaneous Voltage for Hybrid Electric Vehicle," *24th International Battery, Hybrid and Fuel Cell Electric Vehicle Symposium and Exposition*, May 2009.



Narayan C Kar

REFERENCES

- [1] B. S. Guru and H. R. Hiziroglu, *Electric Machinery and Transformers*, 3rd Ed., New York: Oxford University Press, 2001.
- [2] C. Chan, "The state of the art of electric, hybrid, and fuel cell vehicles," *Proceedings of the IEEE*, vol. 95, pp. 704-718, April 2007.
- [3] M. Ehsani, Y. Gao, S. E. Gay, and A. Emadi, *Modern Electric, Hybrid Electric, and Fuel Cell Vehicles: Fundamentals, Theory, and Design*, Boca Raton: CRC Press, 2005.
- [4] C. M. Jefferson and R. H. Barnard, *Hybrid Vehicle Propulsion*, Southampton: WIT Press, 2002, pp. 1-27.
- [5] J. M. Miller, *Propulsion Systems for Hybrid Vehicles*, United Kingdom: IEEE, 2004.
- [6] F. Burke, "Batteries and ultracapacitors for electric, hybrid, and fuel cell vehicles," *Proceedings of the IEEE*, vol. 95, pp. 806-820, April 2007.
- [7] D. Linden and T. B. Reddy, *Handbook of Batteries*, New York: McGraw-Hill, 2002.
- [8] W. A. van Schalkwijk and B. Scrosati, *Advances in Lithium-Ion Batteries*, New York: Kluwer Aca./Plenum Publishers, pp.393-402, 2002.
- [9] M. Pedram and Q. Wu, "Design considerations for battery powered electronics," in *Proc. 1999 Design Automation Conference*, pp. 861-866.
- [10] M. Chen and G. A. Rincón-Mora, "Accurate electrical battery model capable of predicting runtime and I-V performance" *IEEE Transactions Energy Conservation*, vol. 22, pp. 504-511, June 2006.
- [11] P. Rong and M. Pedram, "An analytical model for predicting the remaining battery capacity of lithium-ion batteries," in *Proc. 2003 Design, Automation, and Test in Europe Conference and Exhibition*, pp. 1148-1149.
- [12] R. C. Kroeze and P. T. Krein, "Electrical battery model for use in dynamic electric vehicle simulations," in *Proc. 2008 IEEE Power Electronics Specialists Conference*, pp. 1336-1342.
- [13] P. M. Gomadam, J. W. Weidner, R. A. Dougal, and R. E. White, "Mathematical

- modeling of lithium-ion and nickel battery systems,” *Journal of Power Sources*, vol. 110, pp. 267-274, August 2002.
- [14] H. L. Chan and D. Sutanto, “A new battery model for use with battery energy storage systems and electric vehicles power systems,” in *Proc. 2000 IEEE Power Engineering Society Winter Meeting*, pp. 470-475.
- [15] O. Trebmlay, L. Dessaint and A. Dekkiche, “A generic battery model for the dynamic simulations of hybrid electric vehicles,” *IEEE Vehicular Power and Propulsion Conference*, May 2005.
- [16] B. Tsenter, “Battery management for hybrid electric vehicle and telecommunication applications,” *The Seventeenth Annual Battery Conference on Applications and Advances*, pp. 233-237, 2002.
- [17] M. Koot, J. T. B. A. Kessels, B. de Jager, W. P. M. H. Heemels, P. P. J. van den Bosch, and M. Steinbuch, “Energy management strategies for vehicular electric power systems,” *IEEE Trans. on Vehicular Technology*, vol. 54, pp. 771-782, May 2005.
- [18] M. Zeraouia, M. E. H. Benbouzid, and D. Diallo, “Electric motor drive selection issues for HEV propulsion systems: A comparative study,” *IEEE Trans. on Vehicular Technology*, vol. 55, pp. 1756-1764, Nov. 2006.
- [19] M. Krishnamurthy, C. S. Edrington, A. Emadi, P. Asadi, M. Ehsani, and B. Fahimi, “Making the case for applications of switched reluctance motor technology in automotive products,” *IEEE Trans. on Power Electronics*, vol. 21, pp. 659-675, May 2006.
- [20] C. S. Edrington, M. Krishnamurthy, and B. Fahimi, “Bipolar switched reluctance machines: A novel solution for automotive applications,” *IEEE Trans. on Vehicular Technology*, vol. 54, pp. 795-808, May 2005.
- [21] S. Wang, Q. Zhan, Z. Ma, and L. Zhou, “Implementation of a 50-kW four-phase switched reluctance motor drive system for hybrid electric vehicle,” *IEEE Trans. on Magnetics*, vol. 41, part 2, pp. 501-504, Jan. 2005.
- [22] K. M. Rahman, B. Fahimi, G. Suresh, A. V. Rajarathnam, and M. Ehsani, “Advantages of switched reluctance motor applications to EV and HEV: Design and control issues,” *IEEE Trans. on Industry Applications*, vol. 36, pp. 111-121,

Jan. -Feb. 2000.

- [23] E. Meissner and G. Richter, "Battery monitoring and electrical energy management precondition for future vehicle electric power systems," *Journal of Power Sources*, vol. 116, pp. 79-98, 2003.
- [24] G. Landrum, T. A. Stuart and W. Zhu, "Fast equalization for large lithium ion batteries," *OCEANS*, pp. 1-6, 2008.
- [25] H. Dai, X. Wei, and Z. Sun, "Online SOC estimation of high-power lithium-ion batteries used on HEVs," *International Conference on Vehicular Electronics and Safety*, pp. 342-347, 2006.
- [26] A. Jossen, V. Spath, H. Doring, and J. Garche, "Battery management systems (BMS) for increasing battery life," *The 21st International Telecommunications Energy Conference*, pp. 6, 1999.
- [27] B. Pattipati, K. Pattipati, J. P. Christopherson, S. M. Namburu, D. V. Prokhorov, and L. Qiao, "Automotive battery management systems," *AUTOTESTCON*, pp. 581-586, September, 2008.
- [28] A. Asumadu, M. Haque, H. Vogel, and C. Willards, "Precision battery management system," *Instrumentation and Measurement Technology Conference*, vol. 2, pp 1317-1320, May, 2005.
- [29] A. Affanni, A. Bellini, G. Franceschini, P. Guglielmi, and C. Tassoni., "Battery choice and management for new-generation electric vehicles," *IEEE Trans. on Industrial Electronics*, vol 5, pp. 1343-1349, 2005.
- [30] C. Chen, J. Jin, and L. He, "A new battery management system for li-ion battery packs," *Asia Pacific Conference on Circuits and Systems*, pp. 1312-1315, 2008.
- [31] J. Garche and A. Jossen, "Battery management systems (BMS) for increasing battery life time," *The Third International Telecommunications Energy Special Conference*, pp. 85-88, 2000.
- [32] H. Shimizu, J. Harada, C. Bland, K. Kawakami, and L. Chan, "Advanced concepts in electric vehicle design," *IEEE Transactions on Industrial Electronics*, vol. 44, pp. 14-18, 1997.

- [33] T. Dong, X. Wei, and H. Dai, "Research on high-precision data acquisition and SOC calibration method for power battery," *Vehicle Power and Propulsion Conference*, pp. 1-5., 2008.
- [34] P. Famouri and W. L. Cooley, "Design of DC traction motor drives for high efficiency under accelerating conditions," *IEEE Transaction on Industrial Applications*, vol. 30, pp. 1134-1138, 1994.
- [35] M. E. H. Benbouzid et al., "An efficiency-optimization controller for induction motor drives," *IEEE Power Engineering Letters*, vol. 18, no. 5, pp. 43-45, May 1998.
- [36] I. Husain, *Electric and Hybrid Vehicles - Design Fundamentals*, Boca Raton: CRC Press, 2003.
- [37] X. D. Xue, K. Cheng, and N. C. Cheung, "Selection of electric motor drives for electric vehicles," *Universities Power Engineering Conference*, pp. 1-6, December 2008.
- [38] Y. K. Chin and J. Soulard, "A permanent magnet synchronous motor for traction applications of electric vehicles," *IEEE Int. Electric Machines and Drives Conf.* vol. 2, pp-1035-1041, June, 2003.
- [39] S. Henneberger, U. Pahner, K. Hameyer, and R. Belmans, "Computation of a highly saturated permanent magnet synchronous motor for a hybrid electric vehicle," *IEEE Trans. on Magnetics*, vol. 33, part 2, pp. 4086-4088, Sept. 1997.
- [40] Y. Gao, L. Chen, and M. Ehsani, "Investigation of the effectiveness of regenerative braking for EV and HEV," *Society of Automotive Engineer Journal*, SP-1466, paper No. 1999-01-2901, 1999.
- [41] T. Kanno, "Flat type super high voltage power capacitors for hybrid air-conditioner," *EVS23*, December 2007.
- [42] L. Zubieta, and R. Boner, "Characterization of double-layer capacitors for power electronics applications," *IEEE Trans on Industry Applications*, vol. 36, no. 1, Jan./Feb. 2000, pp.199-205.
- [43] J. N. Marie-Francoise, H. Gualous and A. Berthon, "Supercapacitor thermal and electrical behavior modeling using ANN," *IEE Proc. Electric Power*

Application, Vol. 153, No. 2, March 2006, pp. 255-261.

- [44] S. Atcitty, "Electrochemical capacitor characterization for electric utility applications," *Dissertation*, Virginia Tech University, 2006.
- [45] K. Ohta, "Development of power capacitors for inverter-driven battery forklift," *EVS20*, Aug. 2003.
- [46] I. Daubechies, *Ten Lectures on Wavelets*, Philadelphia, SIAM, 1992.
- [47] J. Shen and G. Strang, "Asymptotics of Daubechies filters, scaling functions, and wavelets," *Applied and Computational Harmonic Analysis*, vol. 5, pp. 312-331, July, 1998.
- [48] G. Strang and T. Nguyen, *Wavelets and Filter Banks*, Wellesley, MA Wellesley–Cambridge Press, 1996.
- [49] J. Upendar, C. P. Gupta, and G. K. Singh, "Discrete wavelet transform and genetic algorithm based fault classification of transmission systems," *Fifteenth National Power Systems Conference (NPSC)*, IIT Bombay, December 2008.
- [50] A. S. Youssef, "Fault classification based on wavelet transform," *IEEE T&D Conference*, 2001, USA.

VITA AUCTORIS

Name	Chitradeep Sen
Place of Birth	West Bengal, India
Year of Birth	1985
Education	<i>University of Windsor, Windsor, Ontario</i> September 2008 - January 2010 M.A.Sc. <i>West Bengal University of Technology, India</i> August 2003 - July 2007 Bachelor of Technology